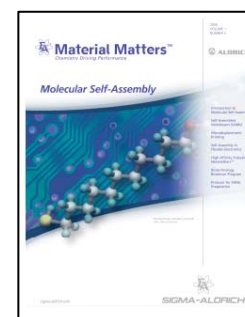
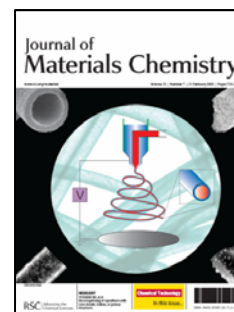
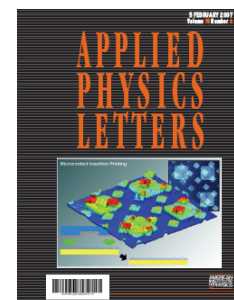
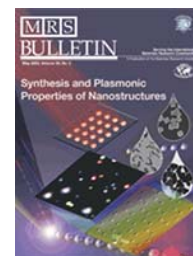
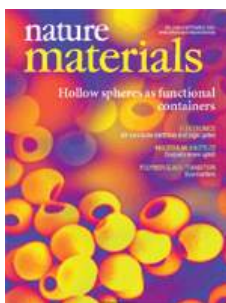
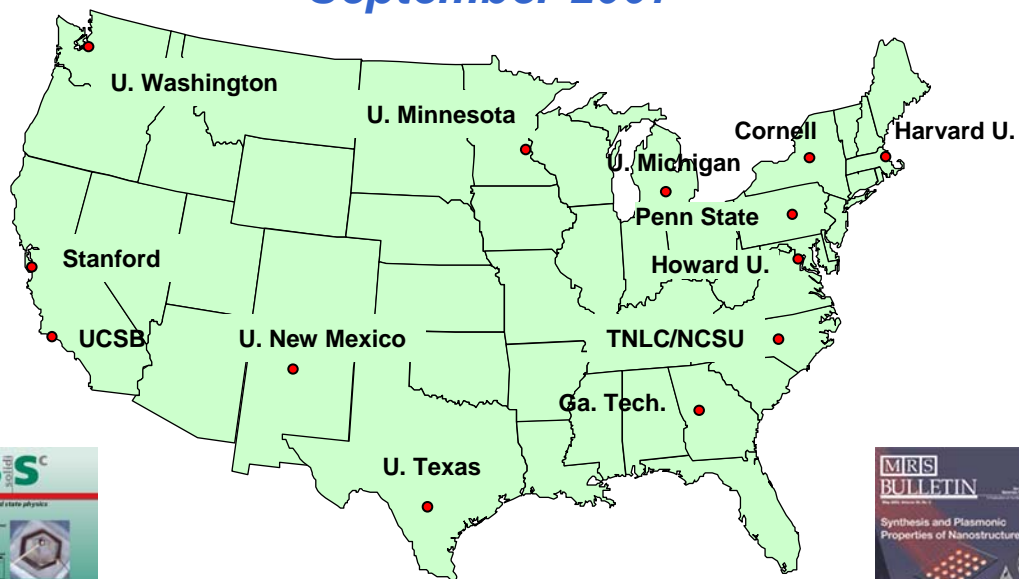


National Nanotechnology Infrastructure Network

Research Highlights September 2007



Life Sciences

Nanoscale Biological Physics: Evolution and Adaptation in Microfabricated Habitat Patches

This project aims at testing the foundations of our understanding of evolution and adaptation in the microbiological world. The premise is that by designing micro environments using nanofabrication to control resource flow and by limiting the movement of organisms between islands of communities, complex environments, even, if you will, a collection of countries with time can be simulated. Figure 1 shows a schematic of a microhabitat patch fabricated at CNF. These experiments have shown the rapid adaptation that bacteria can achieve under stress, as opposed to non-stress conditions

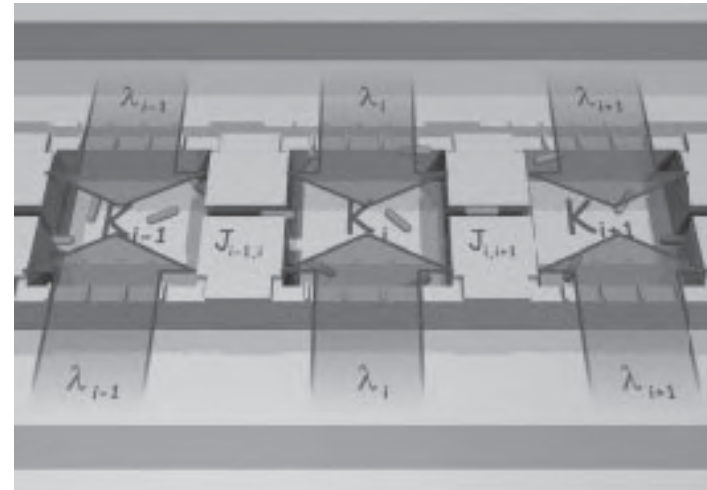
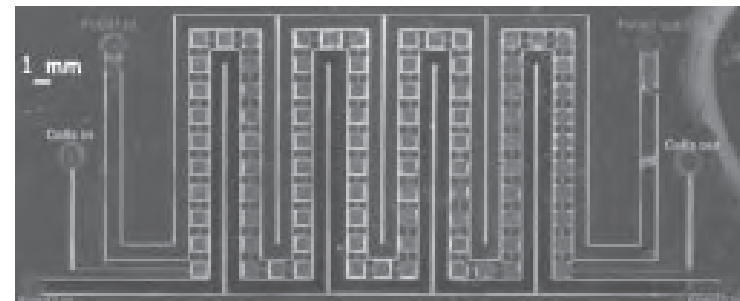


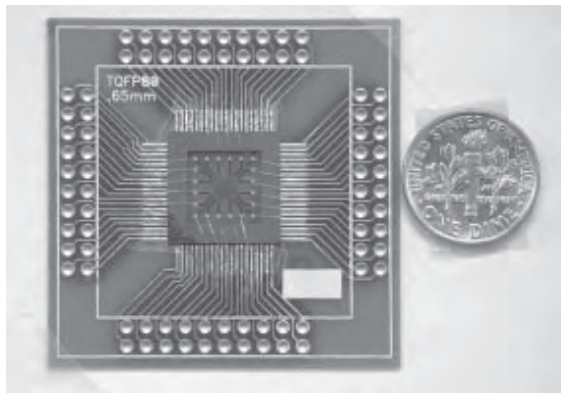
Fig.1 One Dimensional Array of Microhabitat Patches



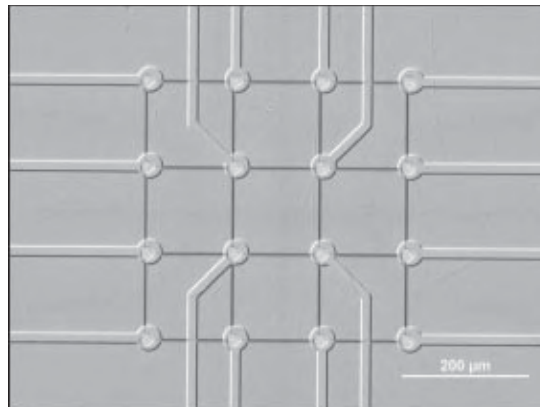
Well Coupled MicroHabitat Array

Multi-Electrode Array for Patterned Neuronal Network

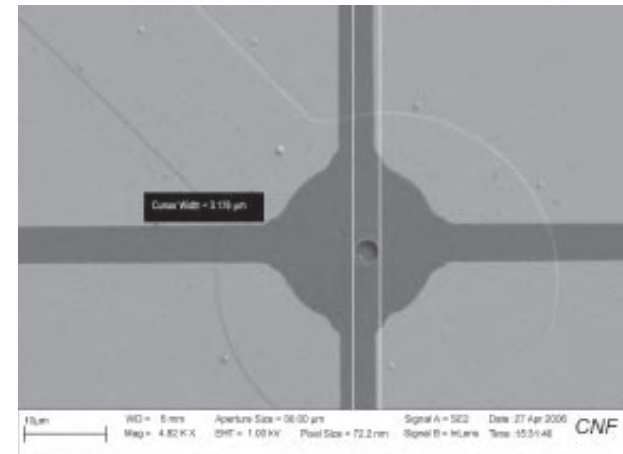
Multi-electrode arrays (MEA) have been widely used as a non-invasive in vitro recording method to study excitable cells and tissues, such as peripheral neurons, stem cells, or sliced brain tissue. The limitation for a conventional MEA system is the accuracy of the response of an individual-cell-based neuronal network. This research develops a novel MEA system with the capability to culture neuron cells in predefined patterns on top of electrodes which can record the signals of excited neuron cells.



A single MEA die wire bonded on a board.



Fabricated Multi Electrode Array for Guided Neural Growth

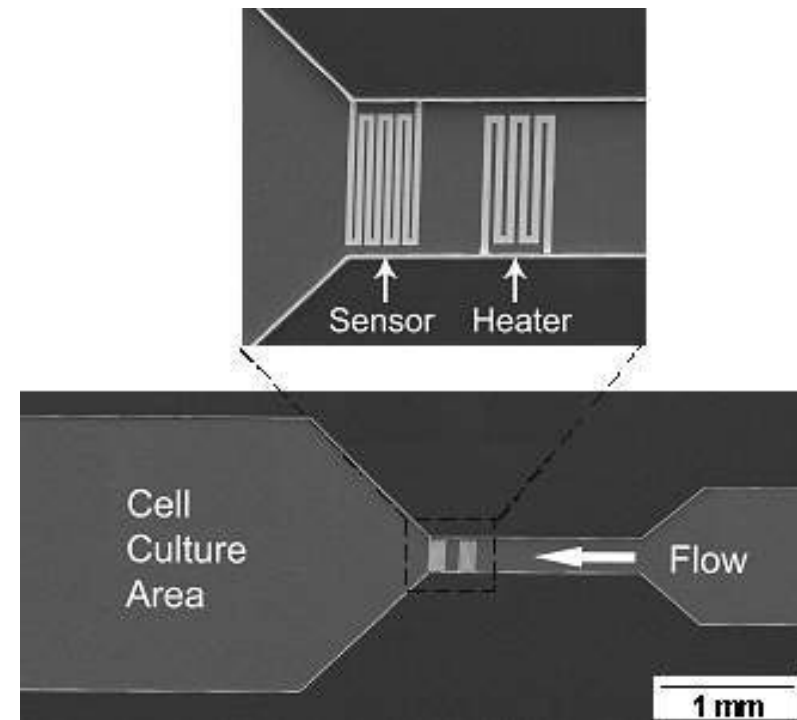


SEM of a single probe in the MEA

Microfluidic High Speed Thermal Stimulator

This microfluidic thermal chip provides rapid temperature changes in the solution combined with accurate temperature control. The thermal chip was designed to facilitate the patch-clamp to study temperature dependent activities of ion channels. The device consists of a fluid channel for perfusing solution connected to an accessible reservoir for making patch-clamp measurements on individual cells.

The chip is capable of changing the temperature ranging from a bath temperature of 200°C to 800°C at an optimum heating rate of 0.50C/ms. On-chip patch clamp recordings of temperature sensitive ion channels (TRPV1) transfected into HEK293 cells. The heat-stimulated currents were observed using whole-cell and cell-attached patch configurations.

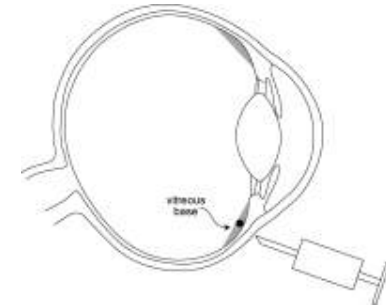
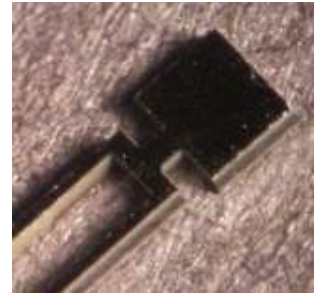


Microfluidic Thermal Activation Chip

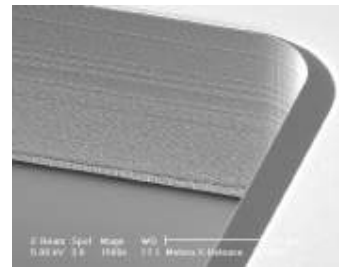
Wireless Silicon Micro Pressure Sensor

Micro scale wireless pressure sensor technology provides the ability to accurately measure pressure inside the human body without the infection risk and mobility constraints of “wired” systems. The small size will allow the sensors to be injected with a syringe in the future. Silicon wafer batch fabrication provides a low cost, high reliability, and controllable method of medical device production.

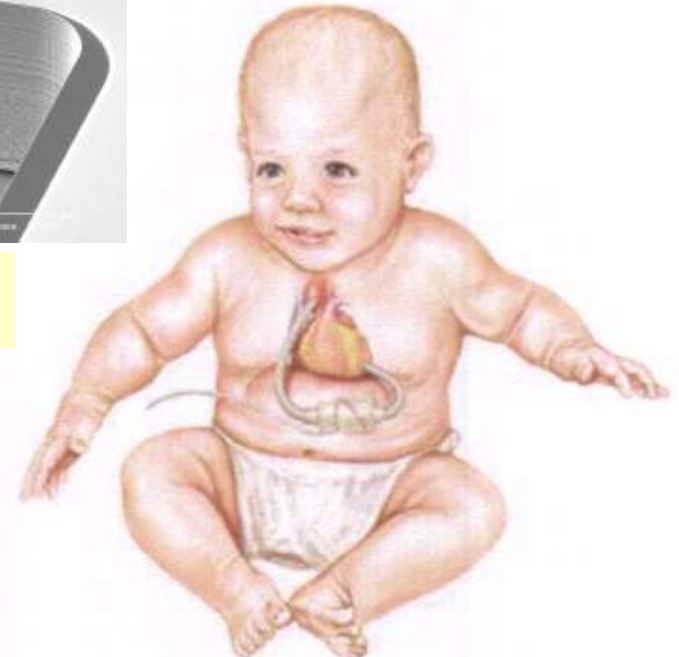
The research performed to date at the UCSB National Nanotechnology Infrastructure Network Laboratory validates the ability to produce the sensor element with excellent dimensional accuracy. The prototypes produced are being tested for sensing accuracy and signal-to-noise ratio.



Intraocular Pressure Sensor



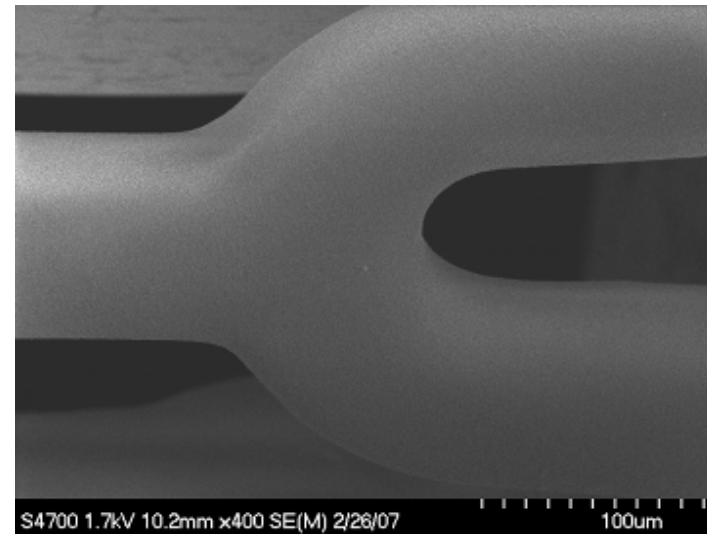
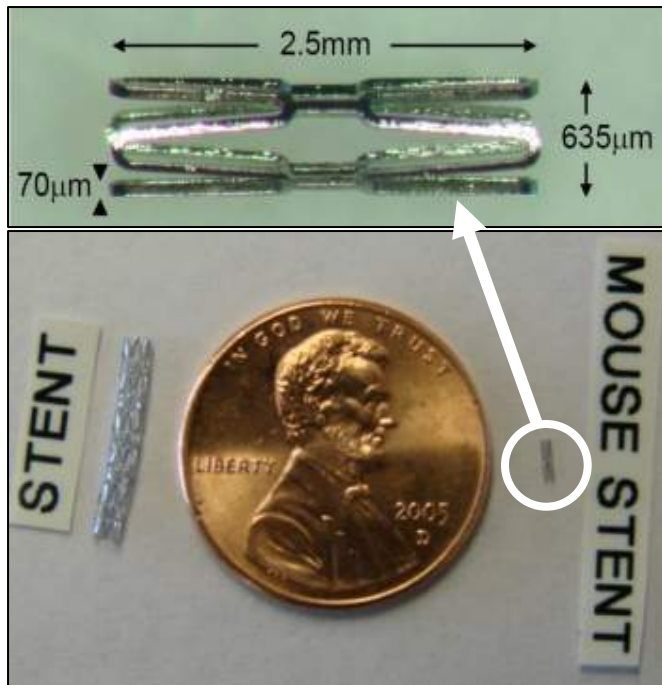
MEMS Processing



Pediatric VAD Blood Pressure Sensor

B. Norling, LaunchPoint Inc.
Work performed at UCSB

Mouse Stent for Testing Coronary Artery Therapies Utilizing ElectroNanospray™



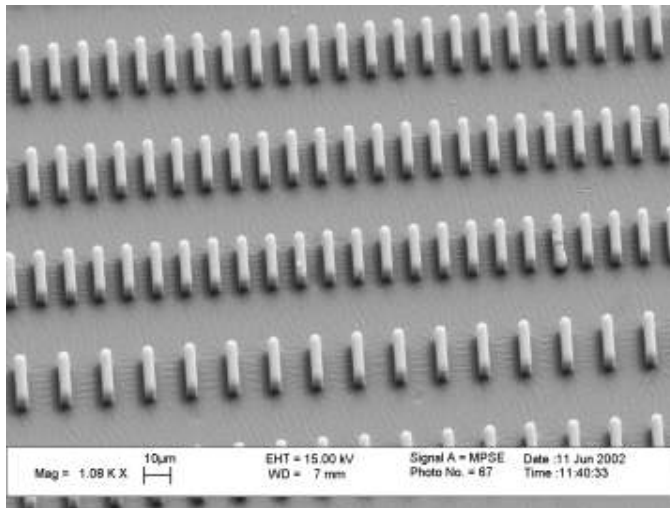
R. A. Hoerr, Nanocopoeia, Inc.
Work performed at U. of Minnesota

- Nanocopoeia is helping to develop a miniature stent for testing new coronary artery therapies in atherosclerotic mice.
- The tiny stent is coated with a novel ElectroNanospray process that deposits nanoparticles on the surface and then implanted into the mice.
- University of Minnesota's Characterization Facility has helped develop methods for evaluating the surface features of the coatings using scanning electron microscopy and atomic force microscopy.

Microfabricated Devices for Sparse Cell Isolation

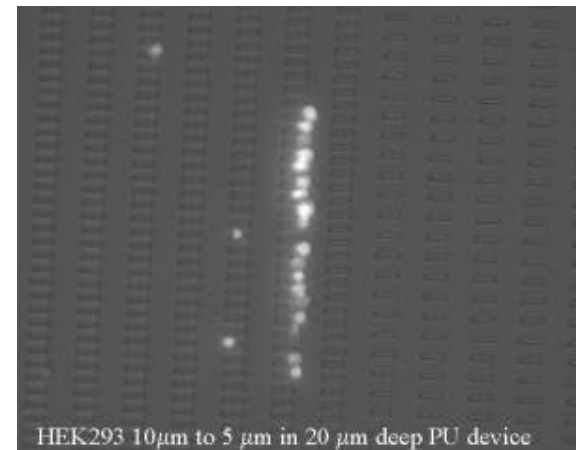
DESCRIPTION OF WORK

- ◆ Goal: To isolate rare cell types from peripheral blood.
- ◆ Method: Exploit the difference in size and deformability between regular cells and rare cells using a micromachined device.
- ◆ Results: Separate fetal red cells from adult white blood cells in cord blood, and separate cultured cancer cells from whole blood.



MAJOR OBSERVATIONS

- ◆ We demonstrated proof of concept using 8 cancer cell lines and cord blood.
- ◆ Future work will improve the device's sensitivity.



Publications

- ◆ **H. Mohamed**, J. N. Turner, and M. Caggana, "A Micromachined Sparse Cell Isolation Device: Application in Prenatal Diagnostics," *Proceedings of the 2006 NSTI Bio Nano Conference*, vol2, pp. 641-644, 2006.

M. Caggana*, H. Mohamed*, J. N. Turner*,**

*Wadsworth Center, New York State Department of Health

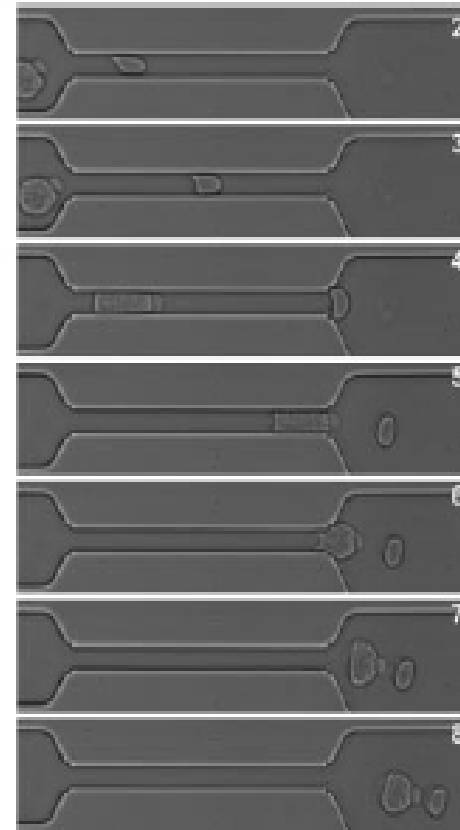
**The University at Albany

Work performed at U. of Minnesota

NNIN_Nuggets.ppt – Oct., 2007

High-Speed Microfluidic Differential Manometer for Cellular-Scale Hydrodynamics

We show a high-speed microfluidic approach for measuring dynamical pressure-drop variations along a micrometer-sized channel and illustrate the potential of the technique by presenting measurements of the additional pressure drop produced at the scale of individual flowing cells.



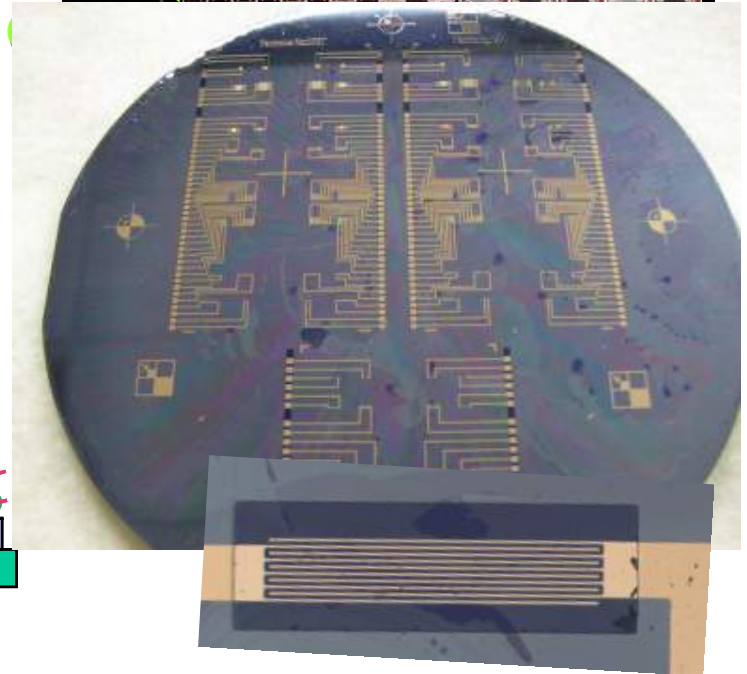
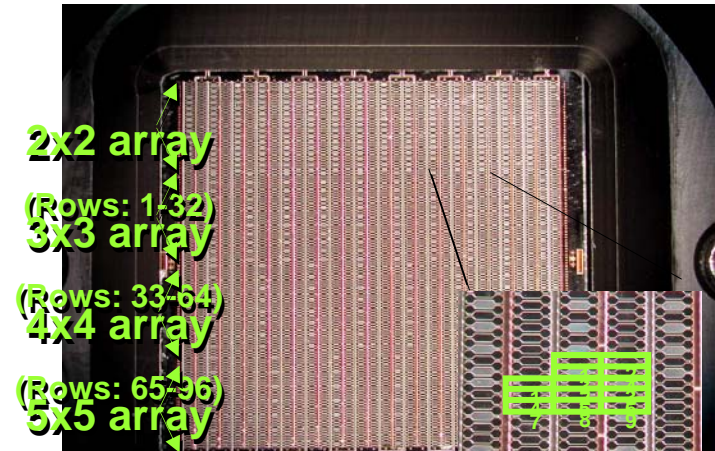
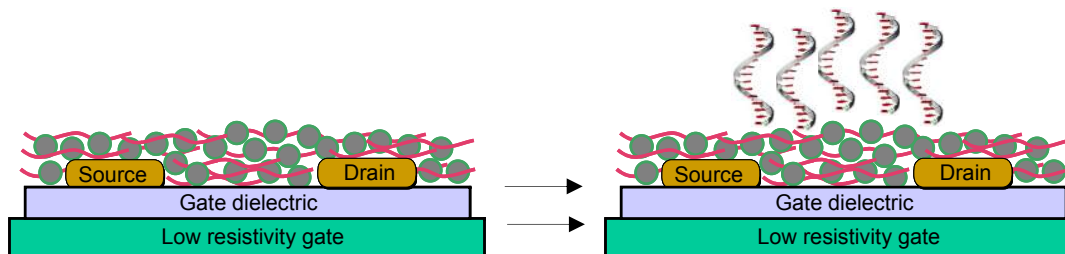
Blood cells in microfluidic channels.

H. A. Stone, Harvard University
Work performed at Harvard University

Biomolecular Field Effect Transistor Arrays

Direct electronic sensors reduce diagnostic protocol complexity and add sensitivity to biomolecular detection array based platforms.

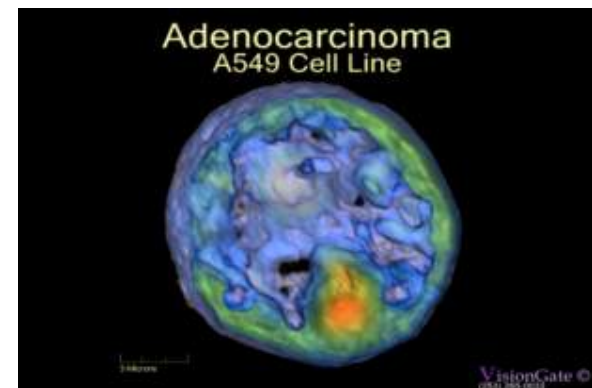
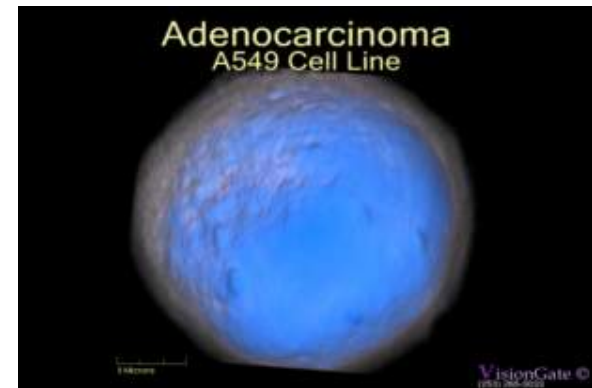
In this study, Nanohmics is lithographically patterning FET array devices to be used as direct biomolecular detection devices. The custom formulated active layer provides a surface for coupling probe molecules and facilitating the direct transduction of hybridization into a change in the source-drain current of the FET device



Cancer Screening with the Cell-CT

Lung cancer is responsible for the largest number of cancer-related deaths in the world and the WHO estimates that there are 1 million new cases worldwide per year. Most lung cancers are diagnosed late, which minimizes chances of survival. VisionGate is developing a screening test to detect lung cancer at an early, curable, stage. The basis of this test is an entirely new imaging system (Cell-CT™) that allows visualization of cells in high definition and in 3D. Cells shed from the inner surface of the lung into the mucus (sputum) exhibit characteristic changes during cancerous transformation. When analyzed in 3D, these changes can be detected with higher sensitivity and specificity compared to 2D-based approaches.

VisionGate uses confocal microscopy at the UW Nanotech User Facility for evaluating various aspects of specimen processing, and for demonstrating the expression of cell-surface markers used for immunobased cell enrichment.

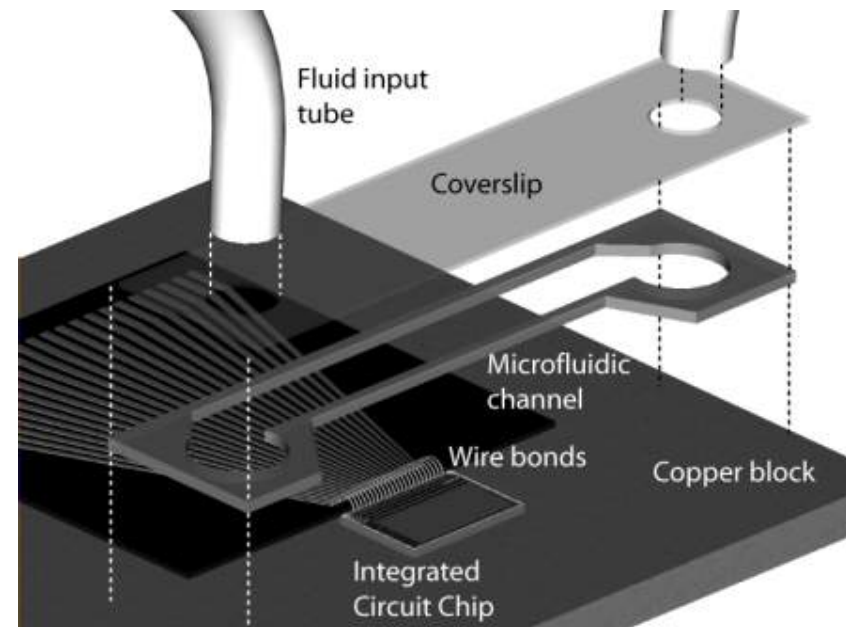


3D views of a lung cancer cell imaged with the Cell-CT™. The upper image shows the cell surface, the lower image is a slice through the same cell.

VisionGate, Inc.
Work performed at UW Nanotech User Facility

Hybrid CMOS / Microfluidic Systems for Cell Manipulation with Dielectrophoresis

A hybrid CMOS/microfluidic chip combines the biocompatibility of microfluidics with the built-in logic, programmability, and sensitivity of CMOS integrated circuits (ICs). We have designed a CMOS IC for moving individual cells using dielectrophoresis (DEP). The IC was built in a commercial foundry and we subsequently fabricated a microfluidic chamber on the top surface.



An RF can be applied to each pixel with respect to the conductive lid of the microfluidic chamber, producing a localized electric field that can trap a cell.

Phyllotaxis as a Dynamical System

Background

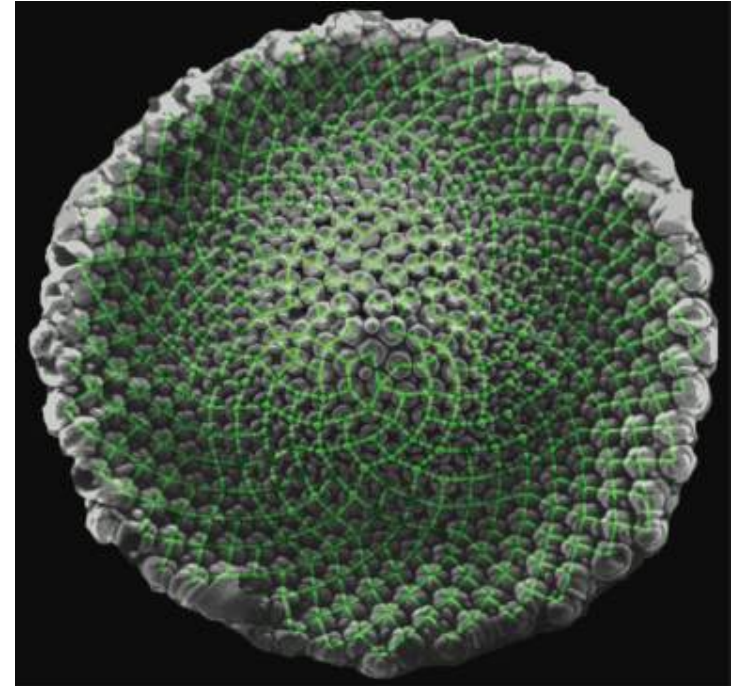
The crystal-like symmetries found in many biological structures reflect the simple geometrical constraints imposed by the close packing of equivalent subunits.

Objective

Determine empirically and formally why some phyllotactic configurations are more common than others in plants.

Experiment

Develop a databank of plant patterns that will be used in this project and will be made available to the scientific community. Now developing a close-packing model which can reproduce patterns such as the one illustrated here with greater accuracy than the classical models based on spiral lattices.

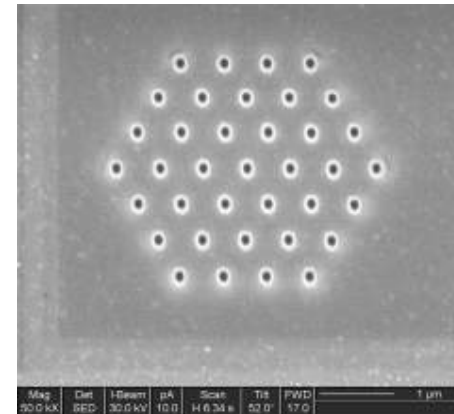


Phyllotactic pattern in an artichoke.

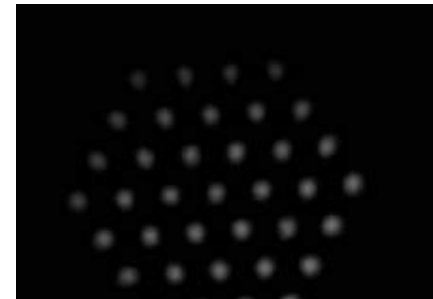
Flower primordia are packed onto the apex of the plant and form a characteristic pattern. Green lines highlight the sequence of contacts that led to the final pattern.

Surface Plasmon-based Biosensors Nanofabricated by Focused Ion Beam

Appropriately patterned surfaces allow the resonant coupling of photons to higher momentum surface plasmons via grating momentum. The DB 235 FIB is used for this patterning. Light transmission through holes in this patterning is strongly enhanced through the SP collection. This effect is used for ultra-resolution microscopy and bio-sensing.

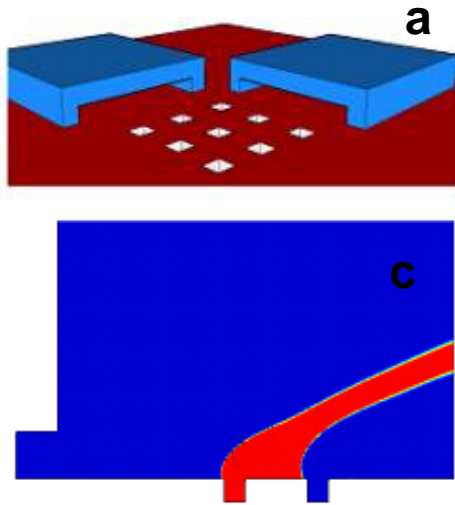


Array of 150nm holes in Au film. Transmission through holes smaller than should be close to zero and evanescent.

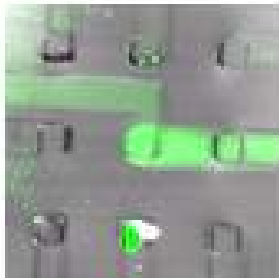
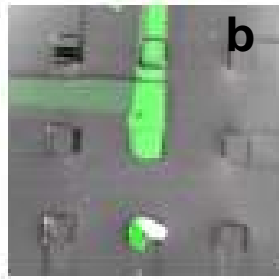


Far field image of light ($\lambda=550\text{nm}$) transmission through subwavelength ($\lambda/4$) array (more than 100% of the light incident on the hole is transmitted through the hole).

Microfluidics for Cellular Bioassays



(a) Diagram of the device. In future studies, cells will be patterned in between the nine outlet holes. (b) Fluorescence images showing control of fluid flow direction. (c) Simulation showing the control of fluid stream height.



Microfluidic devices have emerged as popular platforms for performing assays on biological cells. These devices offer several advantages over conventional cellular assays including the ability to control fluid flow and automation. Here we are developing a microfluidic device for studying cell-to-cell communication in a patterned neural network. The device has been designed such that the direction and height of fluid flow can be accurately controlled. This will allow specific regions of the network to be exposed to various pharmacological agents so changes in the network communication pathways can be monitored.

A. Ewing, Penn State University
Work performed at Penn State

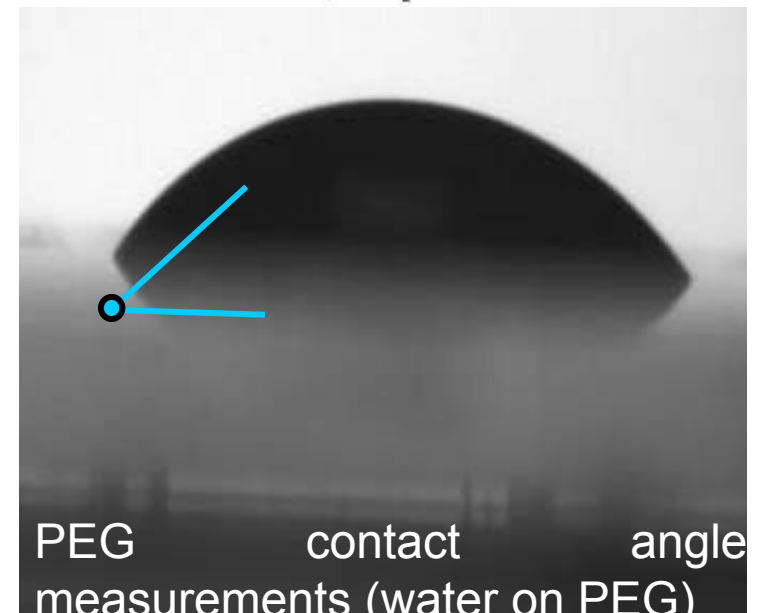
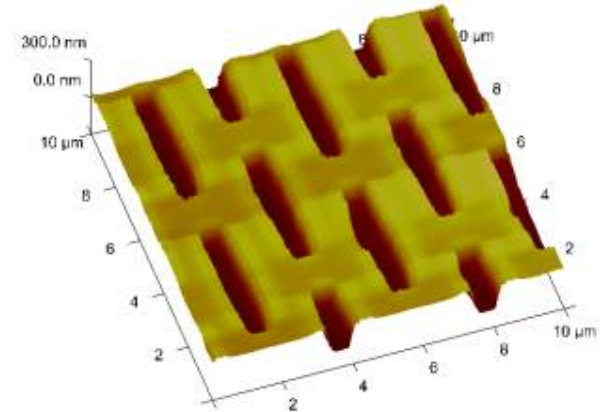
Microfluidic devices enable fundamental studies involving cell-to-cell communication in a patterned neural network

Nanoscale Engineering of Tissue Scaffolds

The PI are investigating adipogenic cell-substrate interactions at the nanometer scale to create advanced, clinically translatable biomimetic scaffolds for reparative adipogenesis. The research team hypothesize that polyethylene glycol (PEG) scaffolds appropriately patterned at the nanometer scale and functionalized with cell adhesion molecules will promote adipogenic processes in preadipocytes (PAs, *a.k.a.* adipocyte precursor cells).

Immediate Aims:

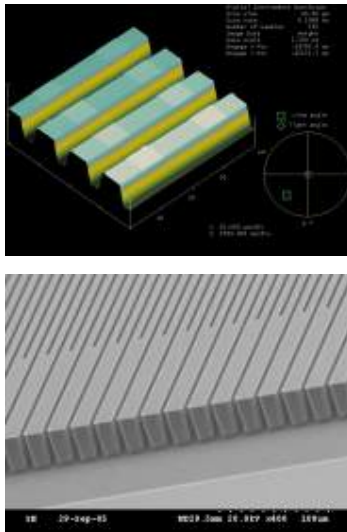
1. To design and fabricate a portfolio of functionalized 2D PEG surfaces with defined nanotopographies down to 20 nm resolution (approaching the molecular level) using advanced UV lithography techniques. The PEG is derivatized with synthetic YIGSR peptide sequences to render it cell adhesive.
2. To seed PAs onto the nanopatterned surfaces and quantitatively assess the effect of nanotopology on processes of adipogenesis. PA adhesion, morphology, motility, proliferation, and differentiation will be quantified. The particular nanotextures that optimize PA functions will be selected for investigation in SA3.
3. To fabricate and characterize 3D PEG scaffolds possessing micron length-scale architectures with nanotextured surface topographies to study 3D topographical effects on adipogenesis.



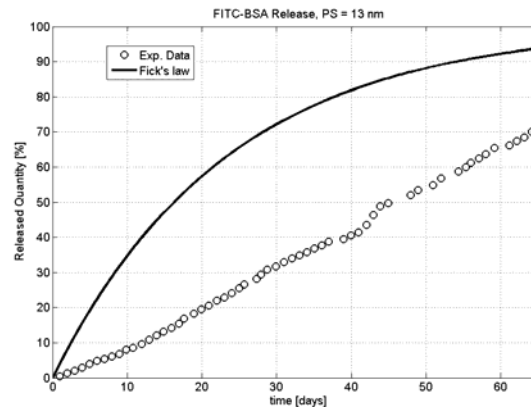
Patrick's research group, U. Texas
Work performed at U Texas

A Silicon Implant for Controlled Drug Delivery

Top-down microfabrication techniques were used to create silicon-based membranes consisting of arrays of uniform channels having a width as small as 7 nm. The measurement of diffusion kinetics of solutes across these membranes under sink conditions reveals non-Fickian behavior as the nanopore width approaches the hydrodynamic diameter of the solute. Zero-order diffusion of interferon is observed at channel width of 20 nm, and the same phenomenon occurs with albumin and 13-nm-wide channels, whereas Fickian diffusion kinetics is seen at 26 nm and larger pore sizes. Such a nonmechanical device offers important advantages in drug delivery applications, including zero-order release and high loading capacity.



Device fabrication in NNIN /MRC facility



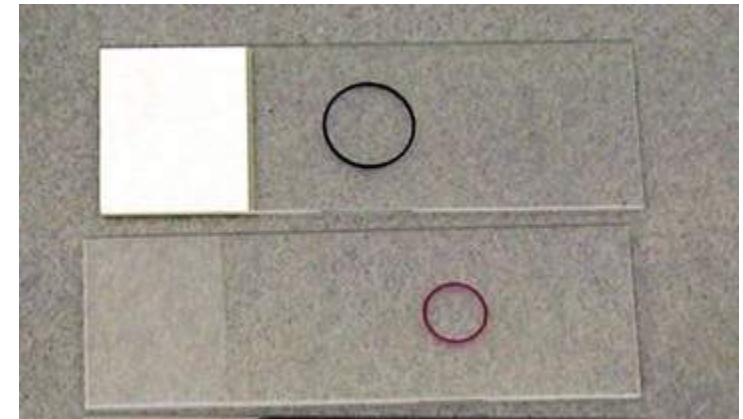
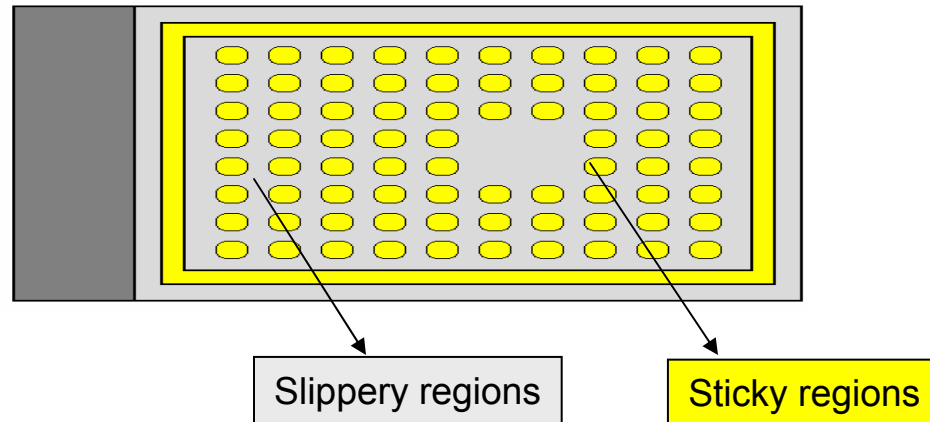
In-vitro diffusion characterization



In-vivo animal test in Texas Medical Center

Cancer Cells Immobilization and Detection

S. Nie, Ga Tech
Work performed at Ga Tech



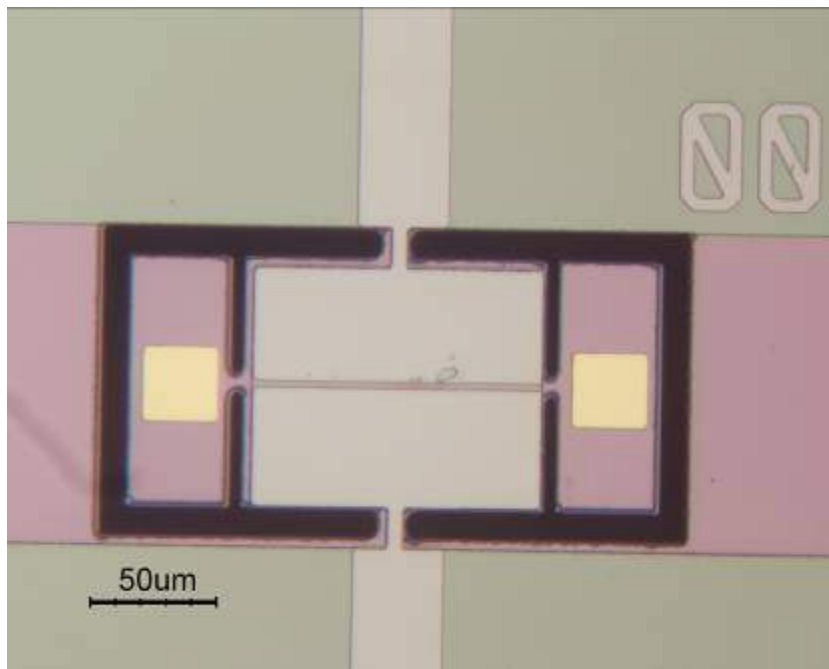
Sticky regions - For protein/antigens for cells to attach (20x20 μ m wells, 5 μ m depth, 10 μ m apart; EpCAM for cell adhesion). Slippery regions - For cell to spread out (PEG DA – repels proteins and cells; SU-8 polymer – Hydrophobic properties)

Circulating Tumor Cells (CTC) very rare in blood. Only a few in 7.5 mL blood. Therefore it is important to immobilize them and cannot afford to lose any during processing steps for imaging. Goal is to fabricate “Sticky & Slippery” (SS) surfaces on slides. The surfaces were accordingly modified to be able to immobilize the cells.

This work is important because it provides a way to detect cancer at an early stage by modified surfaces

Piezo-Resonator based Immunoassay for the Detection of Proteins Expressed in Cancer Cells

J. Meindl, and S. Nie, Ga Tech
Work performed at Ga Tech



Before AB coating



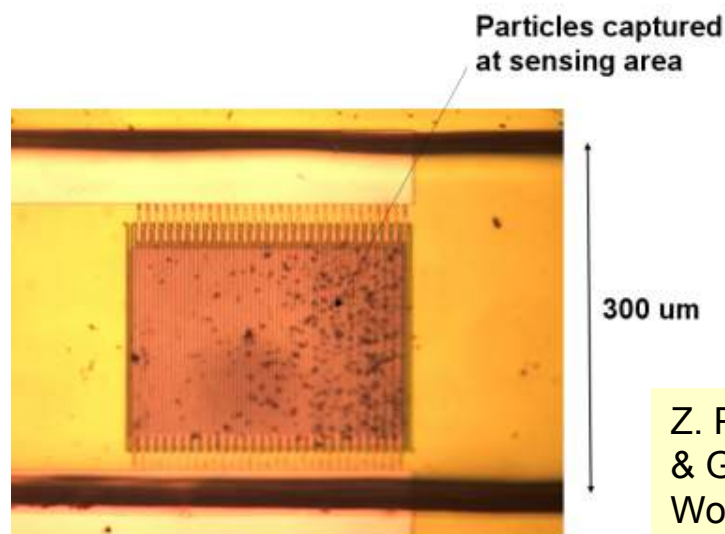
After AB coating

Change of resonant frequency is 33.6kHz

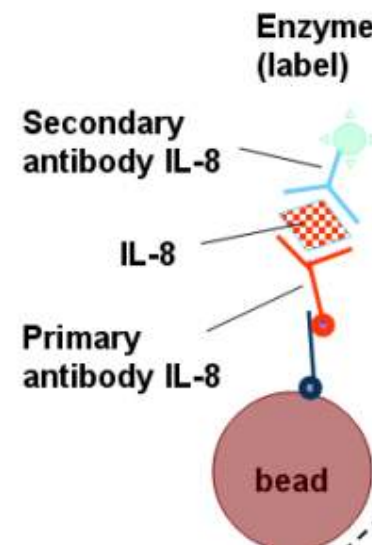
- The Surface of Si/SiO₂ successfully modified to study the antigen-antibody interactions.
- The electrical integration was achieved by the metallization Piezoelectric-resonators was fabricated
- The attachment of anti-TNF-alpha antibodies were successfully attached to the sensing platforms.
- The attachment of antibodies were verified by the shift in the resonance frequency shift to the lower side

This work is important because it provides a way to detect proteins that are highly expressed in cancer cells there by helping in diagnosing cancer .

Nanoparticle / Microfluidic based Electrochemical Biosensors

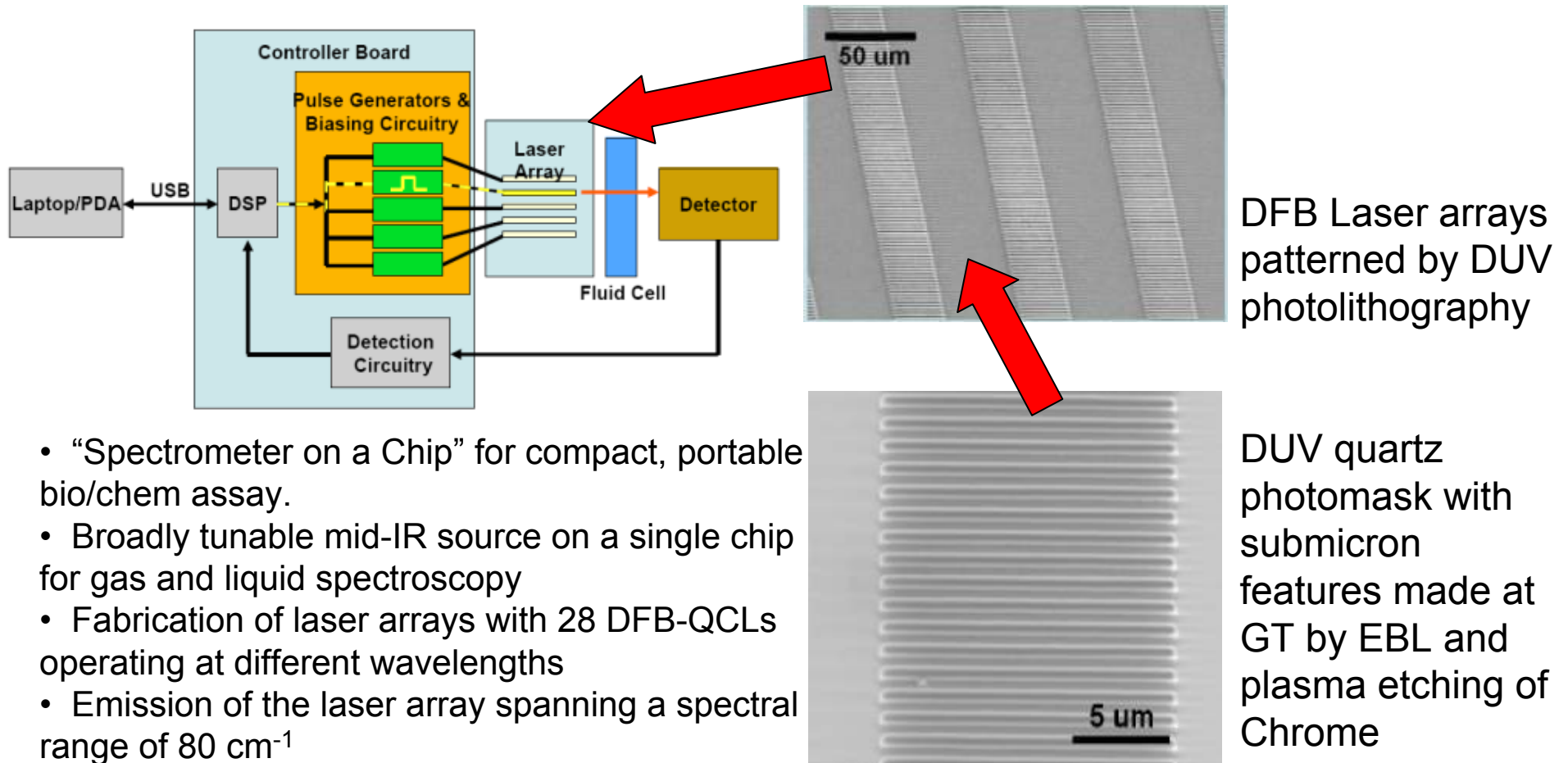


Z. Peng, P. J. Hesketh, K. Kellar, CDC & Ga Tech
Work performed at Ga Tech



There has been a remarkable trend towards the use of microfluidic devices for biochemical assays. Immobilization of biospecific molecules onto micro/nanoparticle surfaces increase the available binding surface area per unit volume. Furthermore, using a particle-immobilized reagent allows localization of the biomolecular interaction to a specific point in the analysis system. The role of the enzyme is to produce the electroactive species for electrochemical detection of the proteins. Figure above (left) shows paramagnetic particles located over an array of 2.4 micron sized interdigitated Pt electrodes along with small counter and reference electrodes fabricated of silicon chip and integrated with PDMS microchannel to form a miniaturized electrochemical cell. Figure above (right) shows IL-8 conjugation of antibody-antigen-antibody-enzyme complex.

Broadband Infrared Spectrometer for Microfluidic Lab-on-a-chip Integration

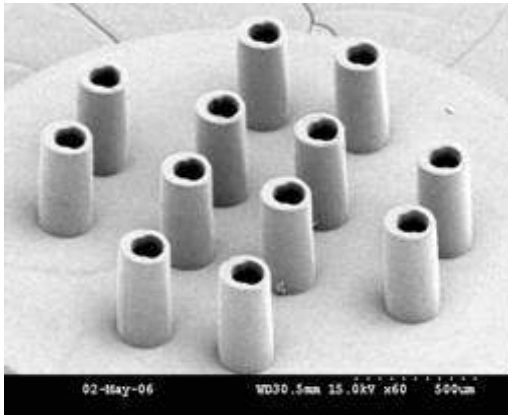


- “Spectrometer on a Chip” for compact, portable bio/chem assay.
- Broadly tunable mid-IR source on a single chip for gas and liquid spectroscopy
- Fabrication of laser arrays with 28 DFB-QCLs operating at different wavelengths
- Emission of the laser array spanning a spectral range of 80 cm^{-1}

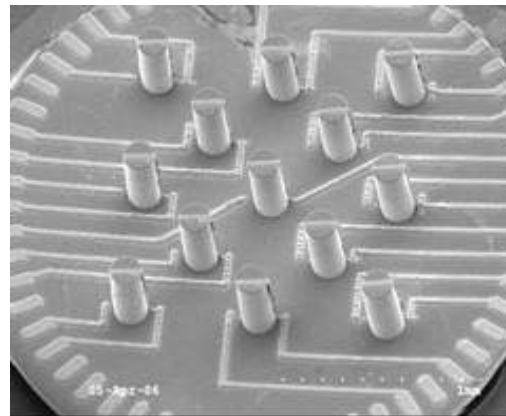
B. Lee, F. Capasso, Harvard University
D. Brown, Ga Tech
Work performed at Ga Tech

3-D Microelectrode Arrays (MEAs) with Microfluidic Ports

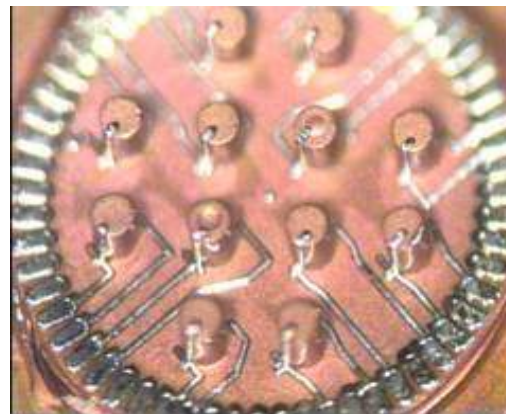
M. Allen, Georgia Tech
Work performed at Ga Tech



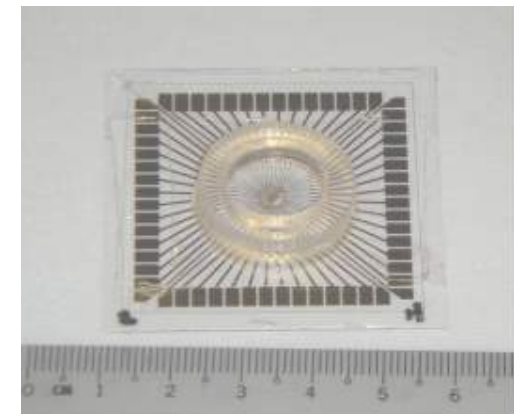
SEM images of fabricated tower arrays for Microfluidic capability



Fabricated and packaged 3-D MEA



Microelectrodes defined on tower arrays for recording electrophysiological data from cell networks and tissues in culture

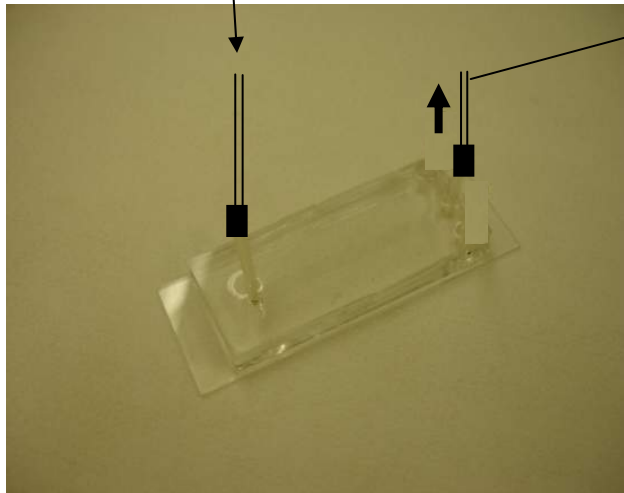


Micro-fluidic Assay for the Detection of Protein Toxins

S. Zkuklinyck, J. Barr, P. Joseph, CDC & Ga Tech
Work performed at Georgia Tech

Protein Toxins, Botulinum and Antrax lethal factor and lethal toxin are likely agents for Bioterrorism. Development of a rapid screening assay is critical

1. Injecting micro-beads with toxins
2. Injecting Substrate to release products



Proposed Micro-fabricated Module for Protein Toxins Detection



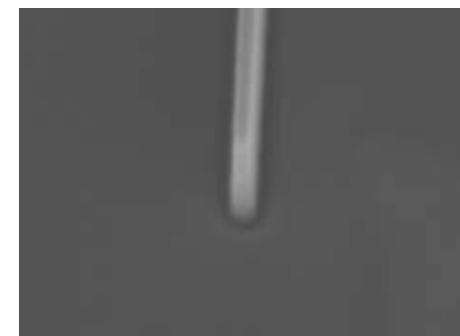
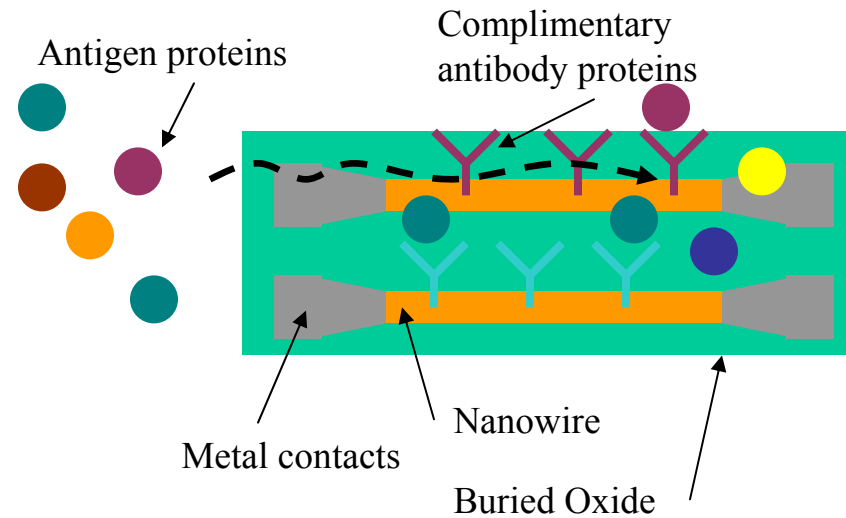
Products confirming the presence of the toxins withdrawn and analyzed using MS

Advantages:

- Portable Diagnostics
- Inexpensive
- Disposable
- Large Scale production
- Au base for electrical integration

Silicon Nanowire Protein Sensor

- Si nanowires are used for the detection of unlabeled proteins
 - ◆ The charge of the target protein changes the conductivity of the wire
- Devices are top-down fabricated with lithography and dry etching
- Array configurations planned for simultaneous detection of multiple proteins

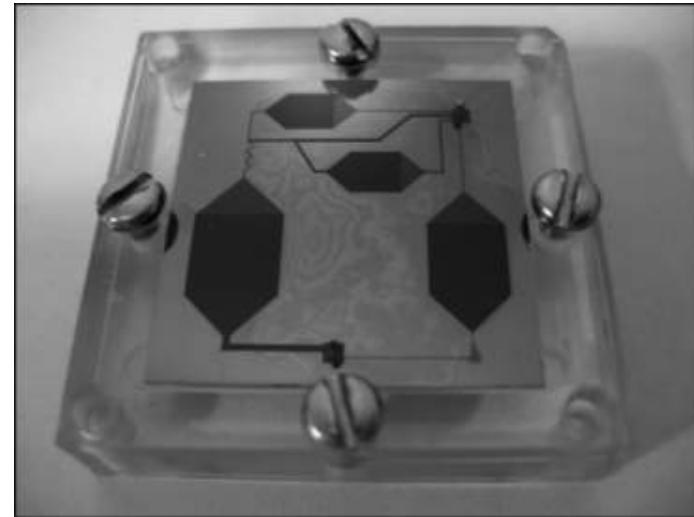


30 nm wide Si wire

J. D. Meindl, Ga Tech
Work Performed at Ga Tech

Microfluidic Cell Culture Analogs for Toxin and Drug Studies

Microfluidic *in vitro* devices were developed to mimic the response of humans or animals to drugs, toxins, or nanoparticles. Each device, or cell culture analog (CCA), contains an array of pseudo tissues that are interconnected by microfluidic channels. The recirculation of blood surrogate through the microchannels allows us to study tissue-tissue interactions, such as the breakdown of a parent compound in the liver and subsequent transport and reaction in the lung. Combining these *in vitro* device experiments with physiologically-based pharmacokinetic model simulations to predict toxin and drug dynamics in humans.

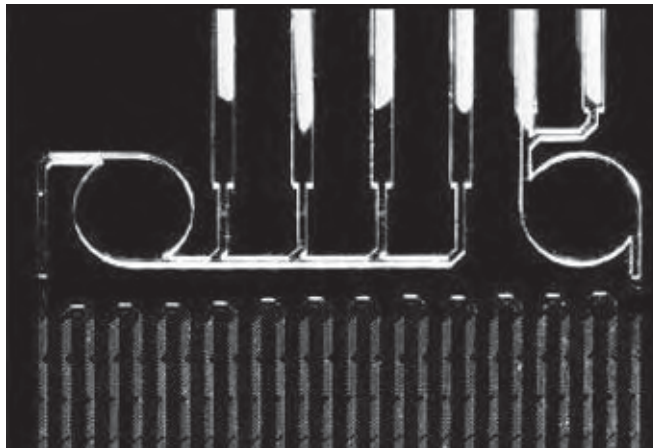


A microfabricated Cell Culturing Analog (CCA) to test for colon cancer treatments.

Magnetic Bead-Based

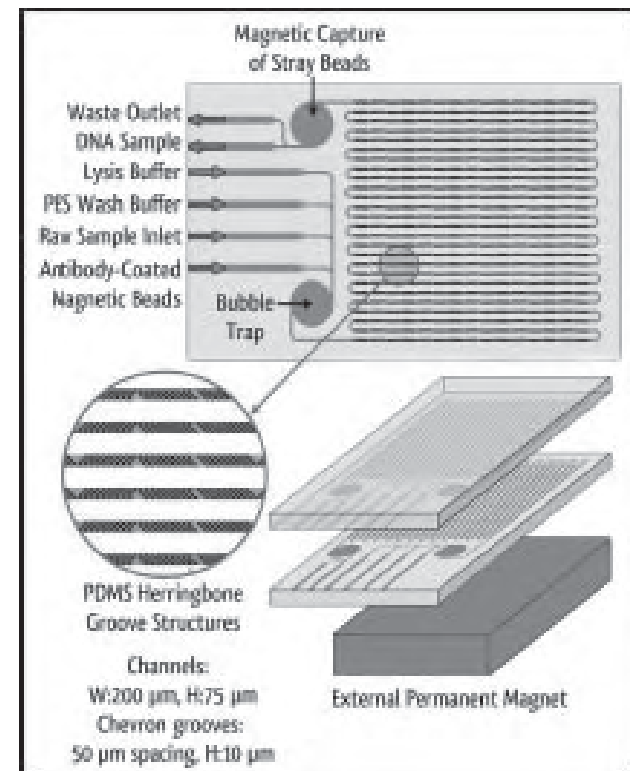
For the purposes of rapid detection of bacterial pathogens and forensic deoxyribonucleic acid (DNA) analysis, a portable, fully-automated, polymerase chain reaction (PCR)-based detection system has been developed. Microfabricated DNA purification and real-time PCR microchips were fabricated and tested for their ability to purify and detect DNA sequences from a variety of bacteria.

Current work has focused on the development of a magnetic bead-based microfluidic sample preparation system for the isolation and purification of target cells from a raw sample using antibody-coated magnetic beads.



Microfluidics Desktop automated PCR System

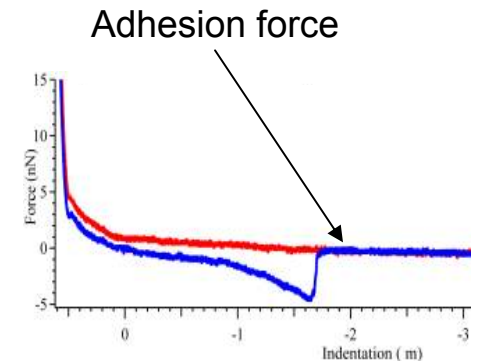
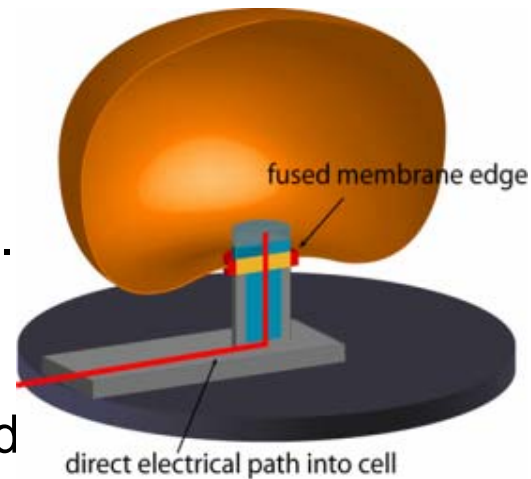
Microfluidic mixer schematic.



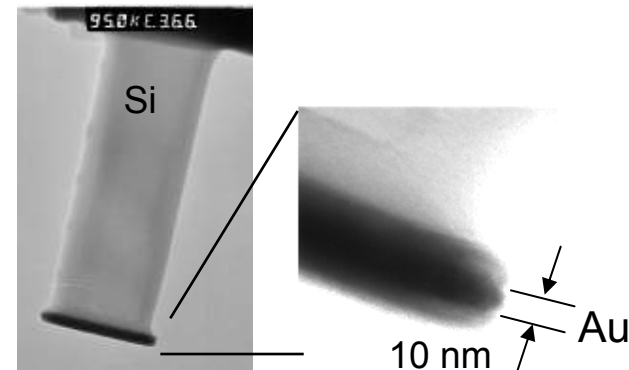
C. A. Batt, Cornell University
Work performed at Cornell NanoScale Facility

Integration of Electronics into Cells

- Nanoscale-functionalized probes at the end of AFM cantilever tips that can directly integrate into a cell membrane.
- “Stealth electrodes” do not cause membrane damage, and specifically attach to the core of the lipid bilayer.
- Future work will involve fabrication of planar arrays of the devices for on-chip electrophysiological measurements.



AFM force measurements of the tip interaction with the bilayer.

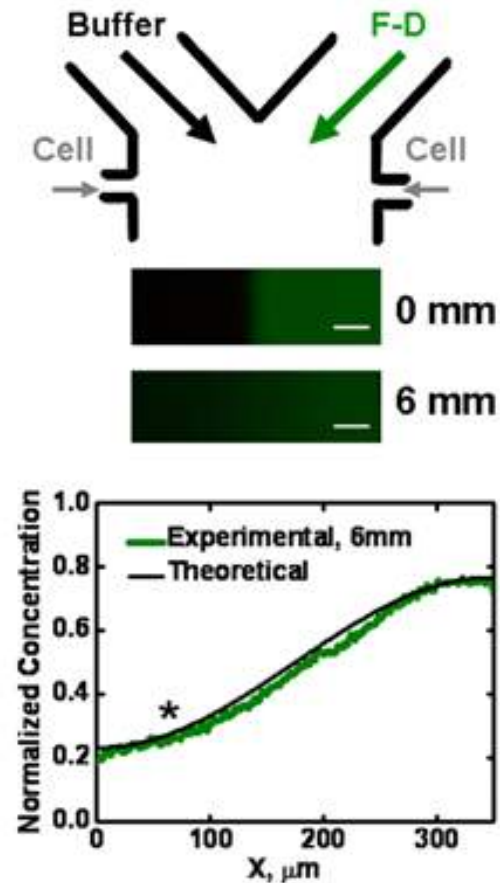


A nanoprobe tip.

N. Melosh, Stanford University
Work performed at SNF

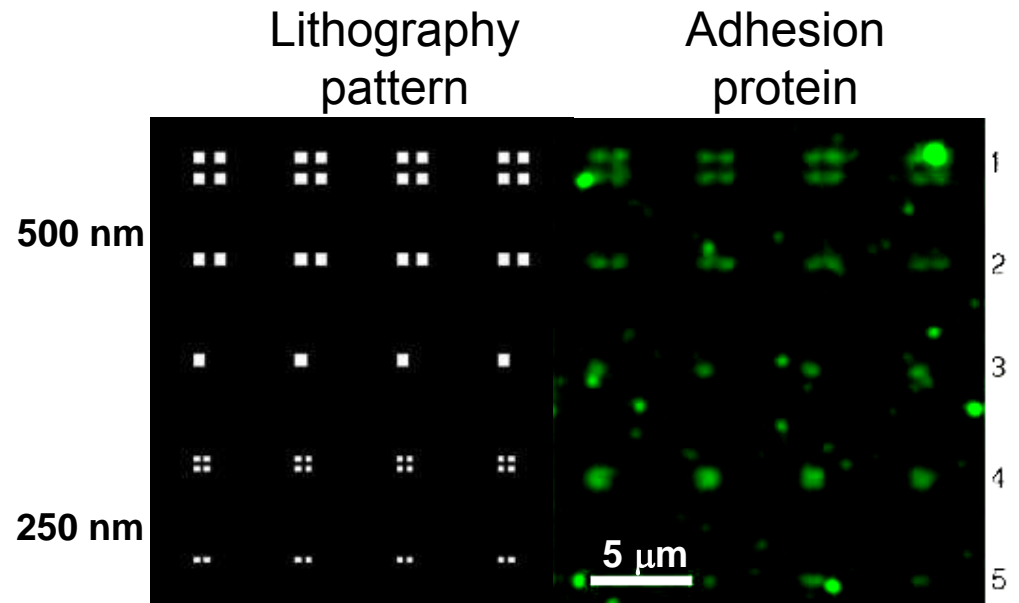
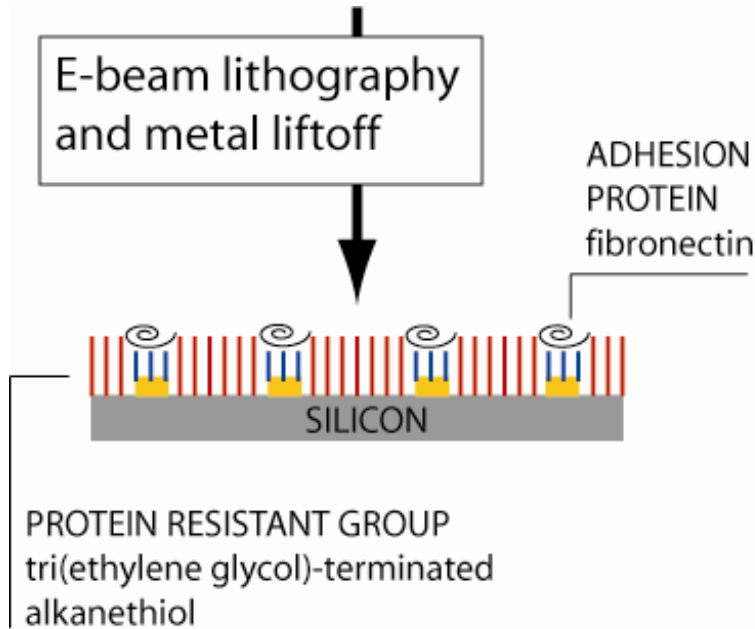
Microfabricated Devices for Studying Immune Cell Chemotaxis

- A simple microfluidic device for studying T cell chemotaxis.
- Device is fabricated in PDMS using soft-lithography and consists of a “Y” type fluidic channel.
- Using the device, robust chemotaxis of human T cells in response to chemokine gradients has been demonstrated.

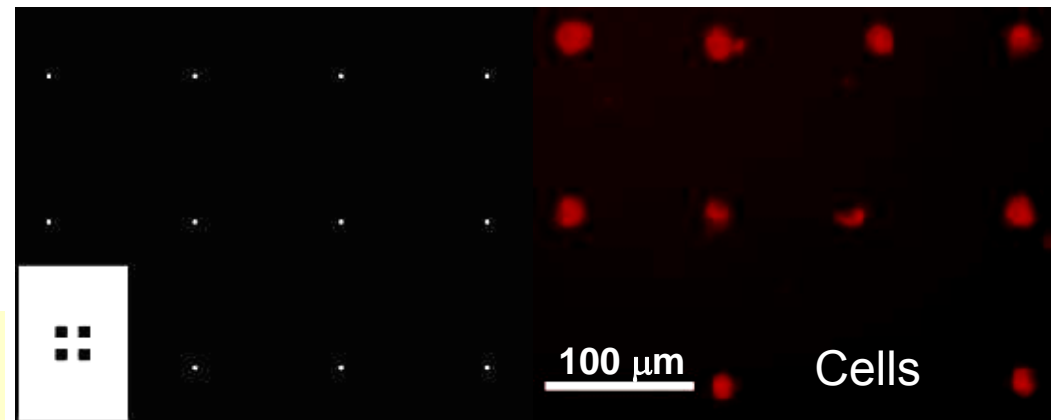


E. Butcher and Dr. F. Lin, Pathology, Stanford University
Work performed at SNF

Nanopatterned Protein Arrays



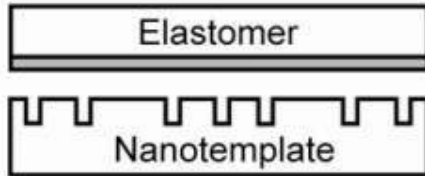
Patterned arrays presenting adhesive protein islands within a non-fouling background for analysis of cell adhesion



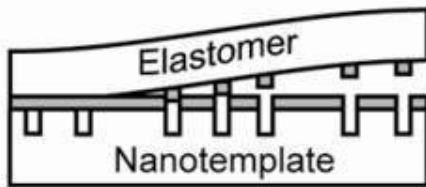
A. J. García, Ga. Tech
Work performed at Ga Tech

Subtractive Patterning Technique

a) planar elastomer inked with proteins

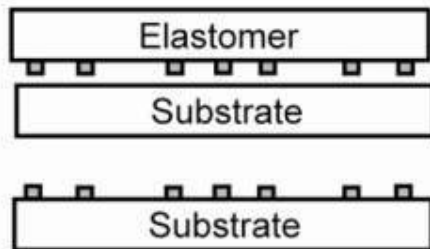


b) contact and release generates pattern by subtraction



clean and reuse nanotemplate

c) contact and release prints protein pattern to substrate



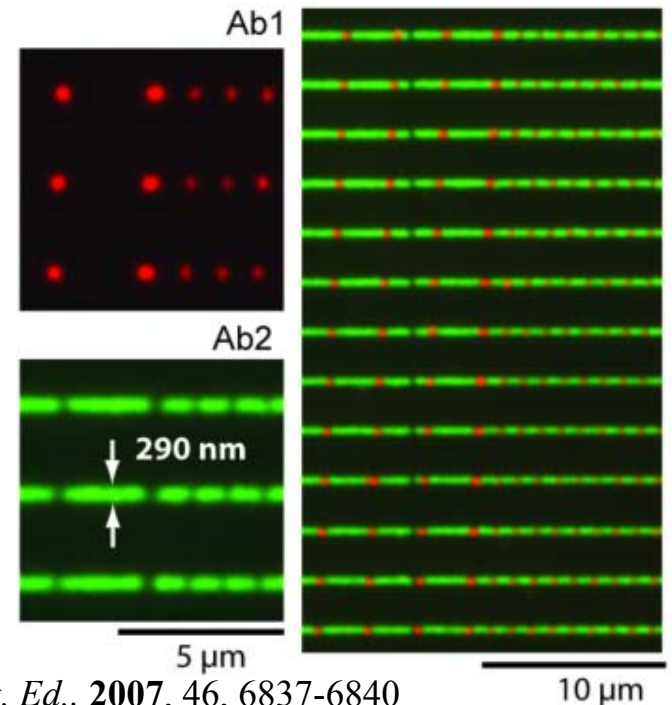
Benefits of technique:

- High Resolution antibody patterns
- High-throughput method
- Multiple types of antibodies patterned simultaneously with self-alignment

Andrés J. García, Ga. Tech
Work performed at Ga Tech

Fluorescent antibody

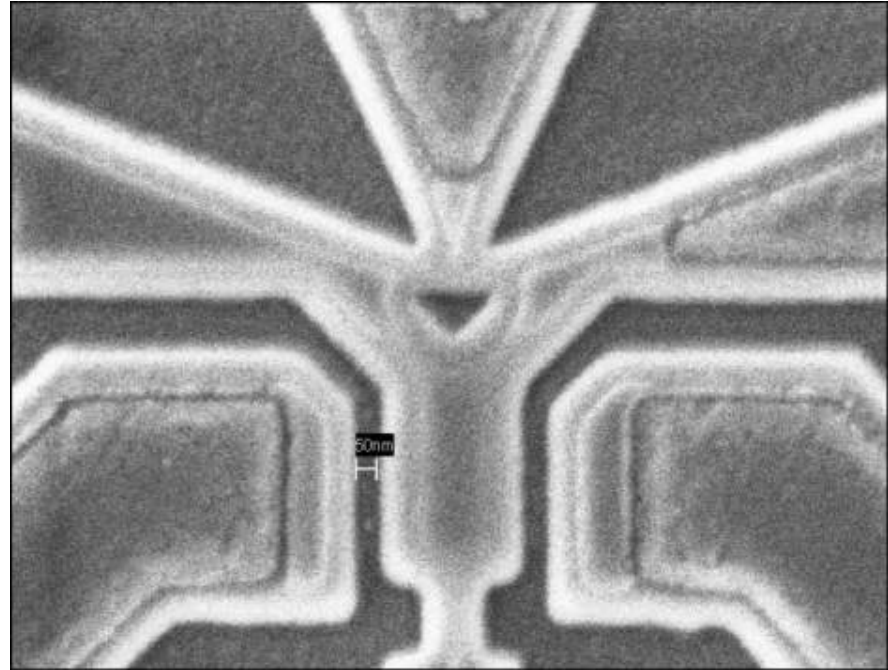
Silicon substrate



Electronics

Ballistic Deflection Transistor

This work investigates the properties of non-linear ballistic transport and optimizing the design of a novel device, the ballistic deflection transistor (BDT). The electron steering effect required for an operational BDT is understood as a shift in energy created by a scattering mechanism rather than a PN junction. The steering effect has been demonstrated in InGaAs-InAlAs heterostructures in which electric gates steer electrons toward an artificial scatterer.



SEM of the ballistic deflection transistor. The triangle at the center is the artificial scatterer

M. Margala & M. Feldman, University of Rochester
Work performed at Cornell NanoScale Facility

Silicon SET for Electrical Metrology and Electrometry

This work centers on fabrication of silicon (Si) nanotransistors with multiple levels of gates, for two purposes: 1) Silicon single-electron tunneling (SET) devices at low temperatures, and 2) Electrostatic sensing of charge reconfigurations in fluids at room temperature.

The SET devices are based on Coulomb Blockage physics and when fabricated in silicon can have much reduced charge offset drift. Those shown here are fabricated on silicon on insulator (SOI) wafers; with back gate, the active layer, two layers of poly-Si gates, and metallization, the process flow has about 60 steps.

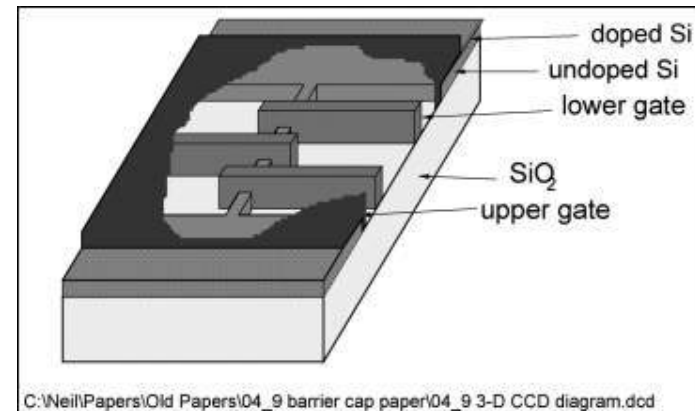


Figure 1: Schematic of single-electron

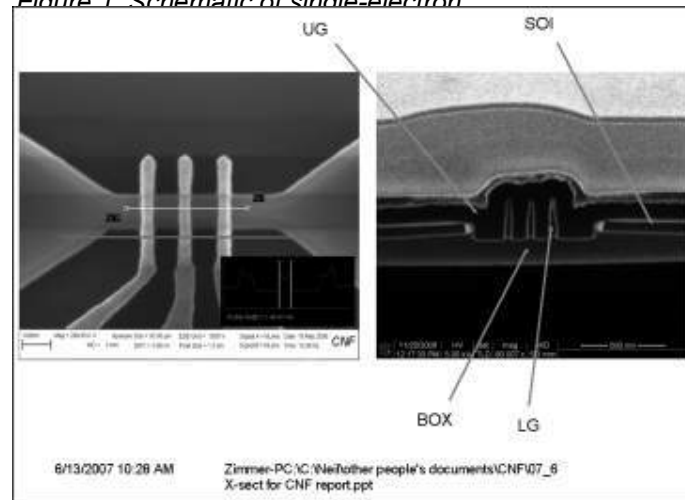
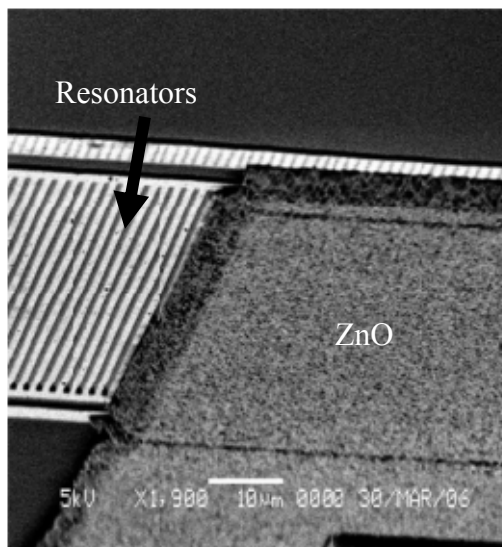
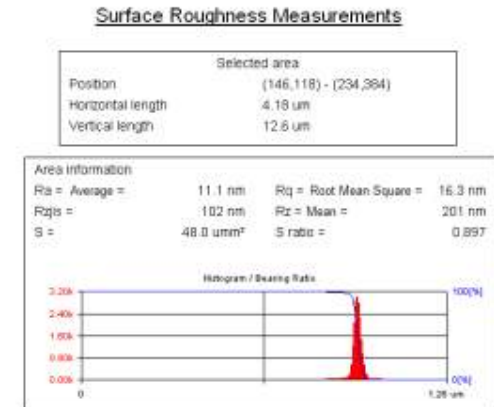
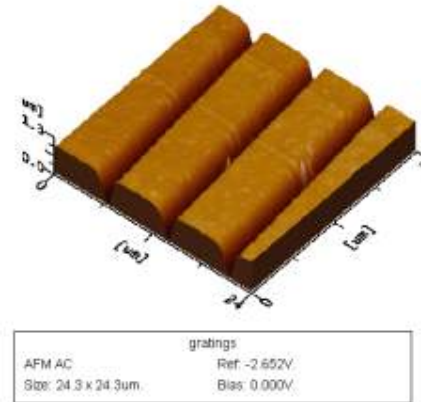


Figure 2: Left; top-down view before upper gate fabrication. Right; cross-sectional view after complete fabrication process.

N. Zimmerman, NIST
Work performed at Cornell NanoScale Facility

CMOS Surface Acoustic Wave (SAW) Resonators

- Project:
 - ◆ Integration of Surface Acoustic Wave resonators in standard CMOS
- Objective:
 - ◆ Deposition of high quality piezoelectric Zinc Oxide layer.



AFM & SEM measurements done at Howard Nanoscale Science and Engineering Facility

- Results
 - ◆ High quality ZnO layer with XRD peaks at 34.2° indicating crystal orientation in the (002) plane
 - ◆ Surface roughness : 201 nm
 - ◆ Successful deposition done on CMOS 1.6 mm, 0.6 mm, and 0.18 mm standard and RF CMOS technology
- Recent Publications
 - ◆ A.N. Nordin, M.Zaghloul, "Modeling and Fabrication of CMOS Surface Acoustic Wave Resonators" IEEE Trans. on Microwave Theory and Tech. May 2007.
 - ◆ A.N. Nordin, M.Zaghloul, "Design and Implementation of a 1GHz CMOS Resonator Utilizing Surface Acoustic Wave", ISCAS 2006.

M Zaghloul, George Washington University
Work performed at Ga Tech & Howard University

Capacitive Micro-machined Ultrasonic Transducer Array

- The capacitive Micro-machined Ultrasonic Transducer (cMUT) technology provides an easy fabrication approach for large number of element ultrasound arrays and the potential to integrate with supporting electronic circuits.
- The cMUT multi-directional imager on 3D hexagonal silicon prism was developed as shown in Fig1. It can be used as the transducer in the Intravascular Ultrasonic Imaging system for medical diagnosis.
- The cMUT characterization and imaging measurement were conducted using one of the CMUT arrays on the prism as the receiving transducer. The results are shown in Fig 2 and Fig 3 respectively.

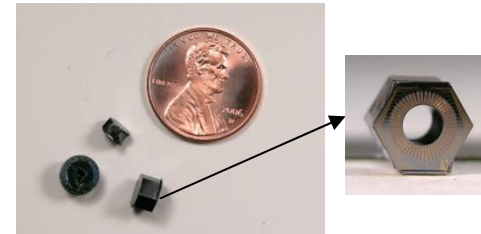


Fig 1 The assembled hexagonal imager

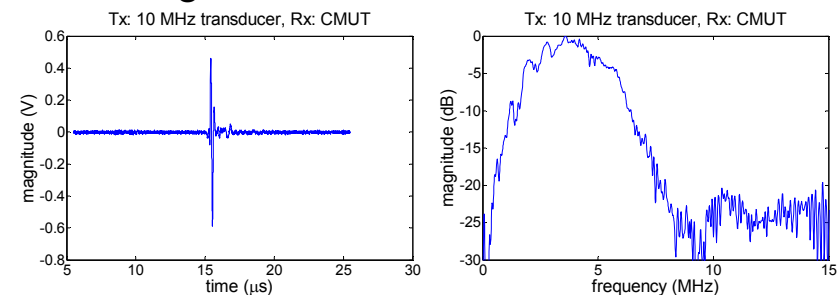


Fig 2 The received signal and its frequency spectrum

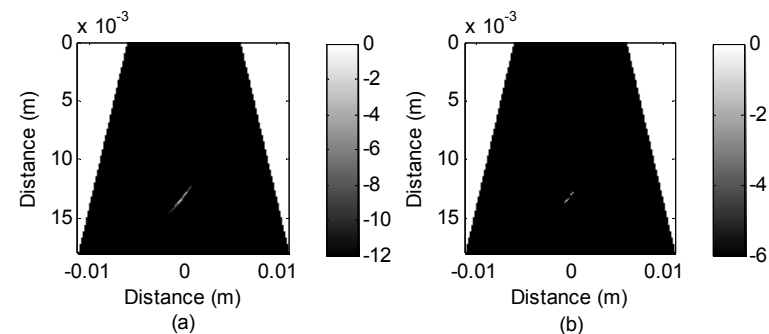
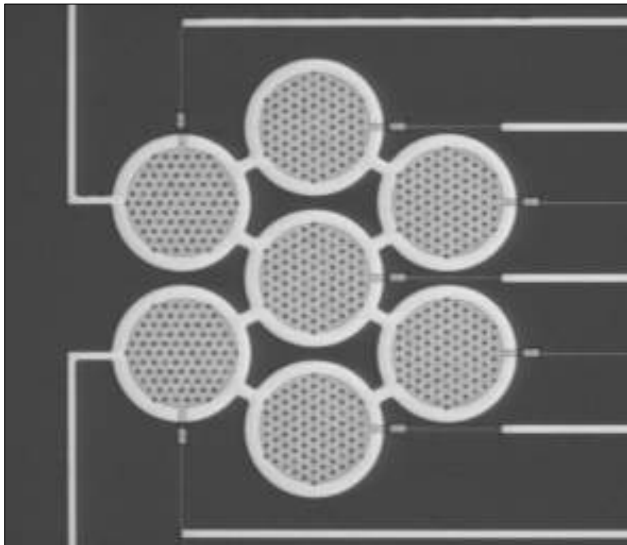


Fig 3 The reconstructed B mode image of metal wire tip

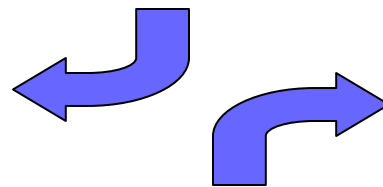
X. Cheng & J. Chen, University of New Mexico
Work performed at Michigan Nanofabrication Facility

Micromachined Transducer Arrays for 3D Imaging

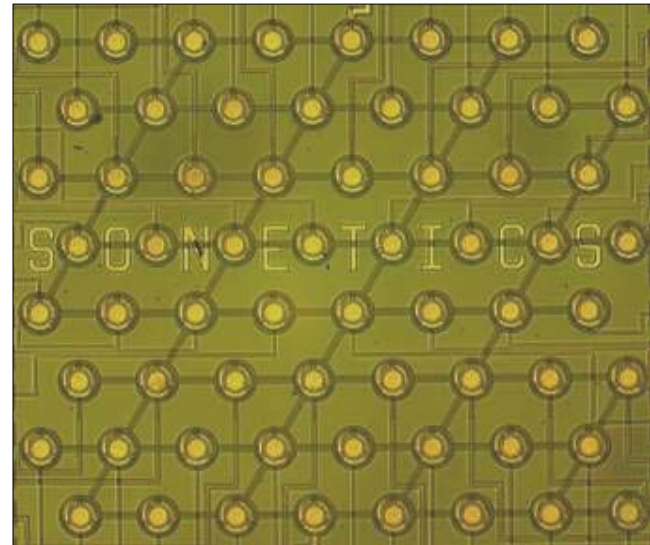
Sonetics Ultrasound, Inc. is developing large-scale transducer arrays intended for real-time 3D ultrasound imaging. Sonetics' patent-pending technology uses standard integrated circuit fabrication steps to build thousands of micromachined electrostatic membrane transducers on a chip. These transducers produce short pulses of acoustic energy and detect echoes returning from features in tissue. When combined with low-noise front-end circuits and sophisticated signal processing hardware, high-quality 3D medical images can be acquired. Because the arrays are batch fabricated on silicon wafers, they promise to provide significant cost-savings and performance improvements over traditional manually-assembled piezoelectric transducer technology.



Prototype elements for membrane transducers. (Fabricated at the MNF).

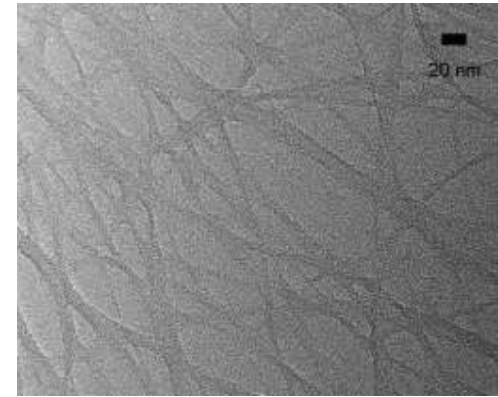


Early generation Sonetics array. (Also processed at the MNF).

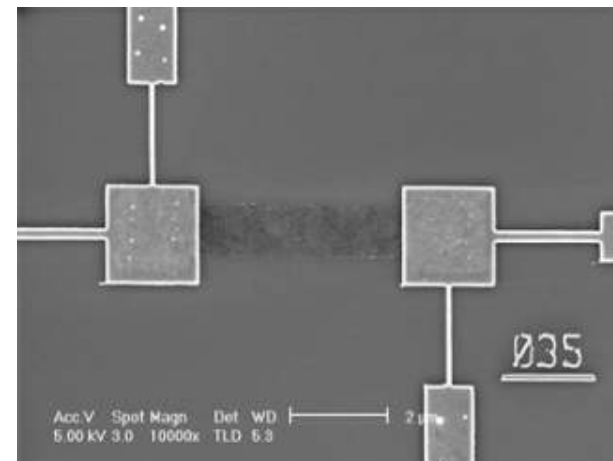


CMOS Compatible Nanotubes

Nantero has developed methods and processes that allow carbon nanotubes to be used for the first time in any production CMOS fab. The nanotubes themselves can now meet the specifications required for new materials in a semiconductor fab, and Nantero's proprietary methods for creating nanotube films and patterning them allow high-volume manufacture of a wide variety of devices.



Nanotube fabric



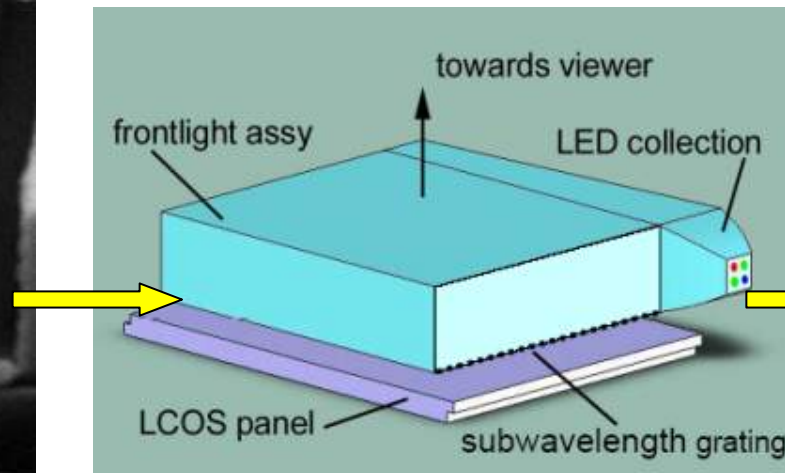
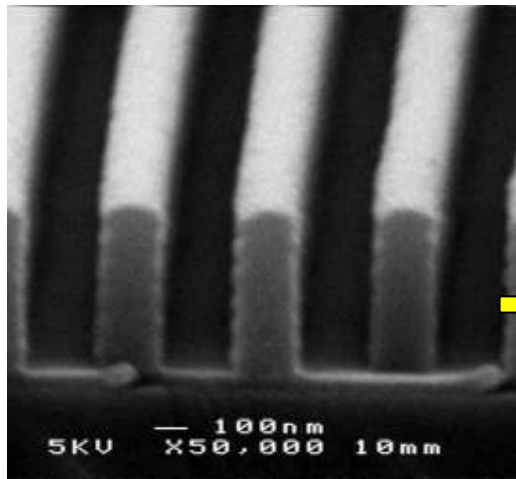
Patterned nanotube fabric
with metal contacts

B. Segal, Nantero
Work performed at Harvard University

Novel Illumination for Ultra-Miniature Projectors

Ultra-miniature projection displays promise on-the-go users big images from pocket-sized products. Projectors could be embedded inside mobile phones to utilize down-loaded imagery, and standalone designs could display images from memory sticks or memory cards. These projectors will utilize high-power LED's or lasers to illuminate liquid crystal on silicon (LCOS) panels to generate fine-resolution images.

Critical to obtaining a high quality image is the choice of illumination technology used in the projector. The technique must provide efficient, uniform illumination of the LCOS panel, and it must be compact and light-weight. A technique being explored by Displaytech, Inc. utilizes sub-wavelength gratings to out-couple light from a waveguide. The unique IFL facility in UNM's CHTM provided the lithography and characterization required to process the waveguides and gratings.

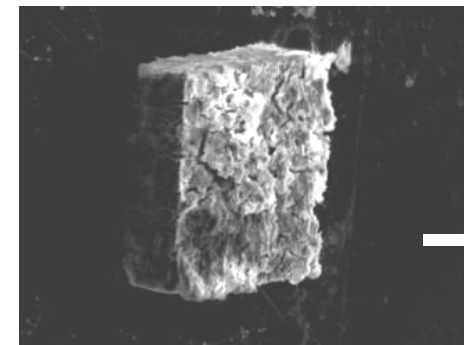
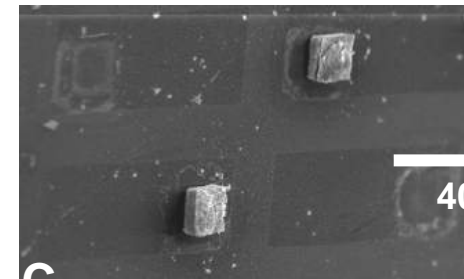
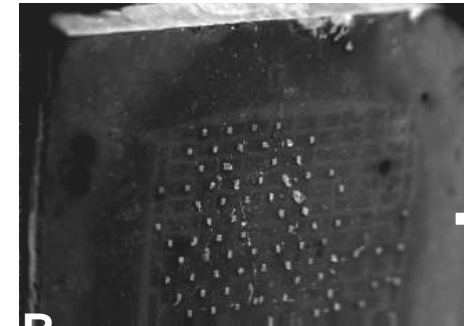
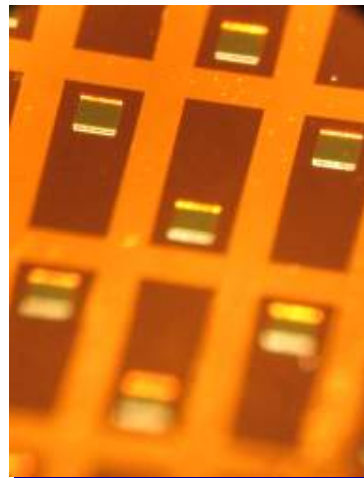
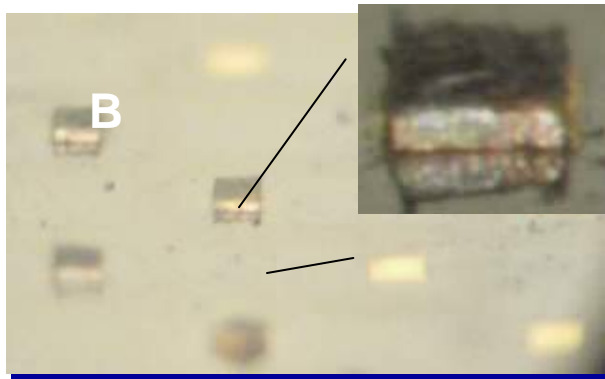


Displaytech, Inc.
Work performed at UNM

Microthermoelectric devices

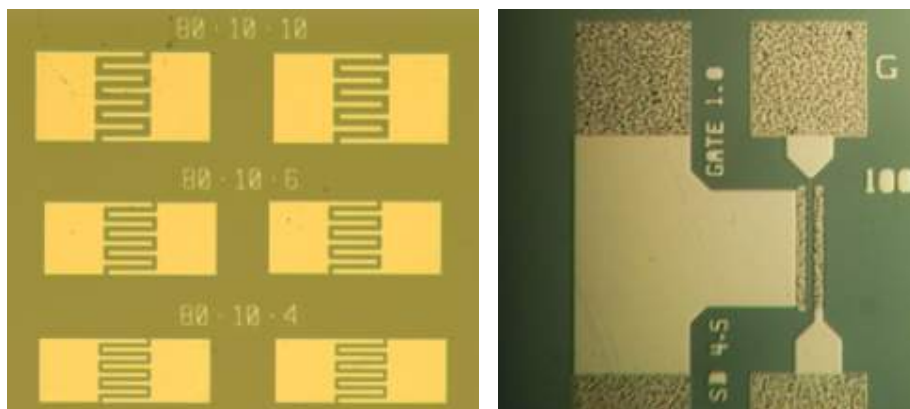
Solid state heating or cooling devices that can be made more efficient by virtue of increasing the thermoelectric Figure of Merit hold promise in small device heat dissipation (detectors, microchips) as well as larger scale heat recovery process (thermoelectric generators)

For this program, Nanohmics is using photolithography to fabricate the mold for preparing a flexible thermoelectric cooler devices composed of consolidated PbTe nanoparticle microdice



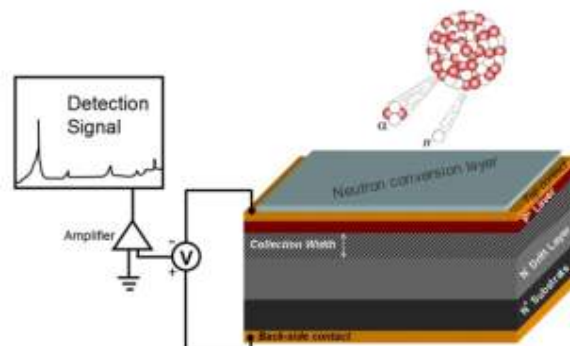
S, Savoy, Nanohmics Inc
Work performed at U Texas

Wide-bandgap Tunable RF and Detection Devices



Integration of complex oxide interdigitated capacitors and GaN/AlGaN HEMT

Tunable RF Devices:
Integrating capacitively-tunable complex oxide materials and nitride-based electronic devices on the same chip for reduced package size, improved performance, and longer operation time in applications such as steerable radar arrays.



Neutron Detectors:
SiC detectors are being used to reduce noise at elevated operating temperatures to fabricate devices with zero cooling requirements.

J. Robinson, M. Fanton, and D. Snyder, Electro-Optics Center
Work performed at Penn State

Wide-bandgap device fabrication allows new applications in high-performance tunable RF electronic and detection devices

60 mV/decade Switching of Carbon Nanotube Transistors with Ultra-thin ALD High-k HfO₂ Dielectric

- 60 mV/decade switching of carbon nanotube transistors with an ultra-thin HfO₂ dielectric has been demonstrated.
- Single wall nanotubes were functionalized with a coating of DNA necessary to achieve a uniform dielectric thickness of 2 to 3 nanometers.

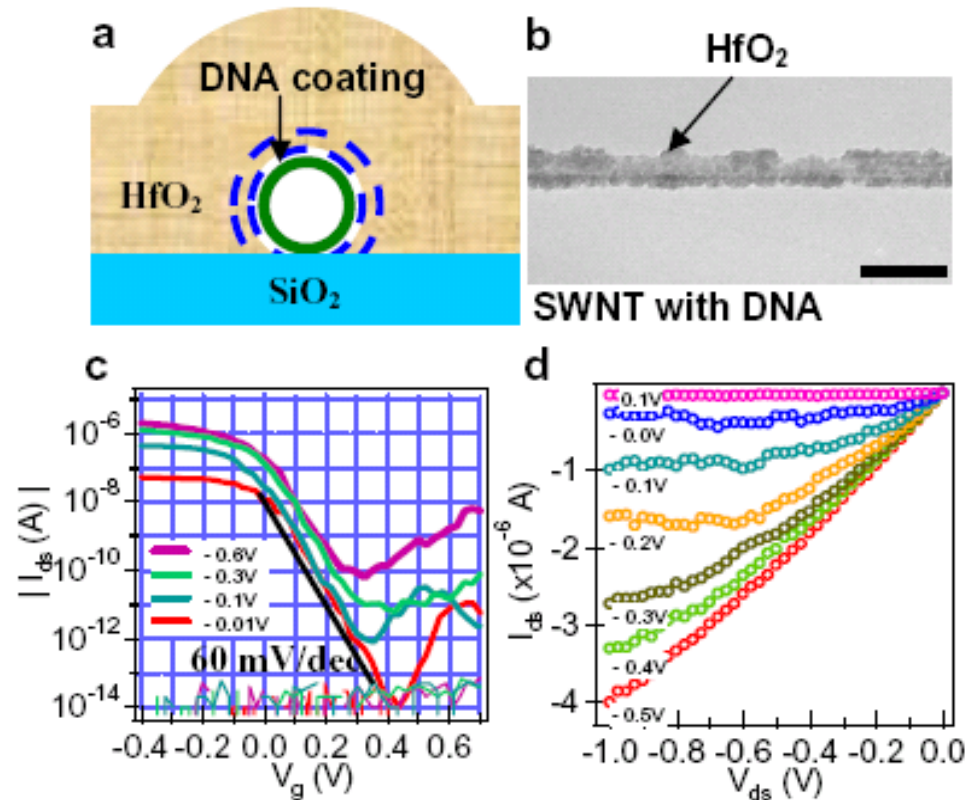
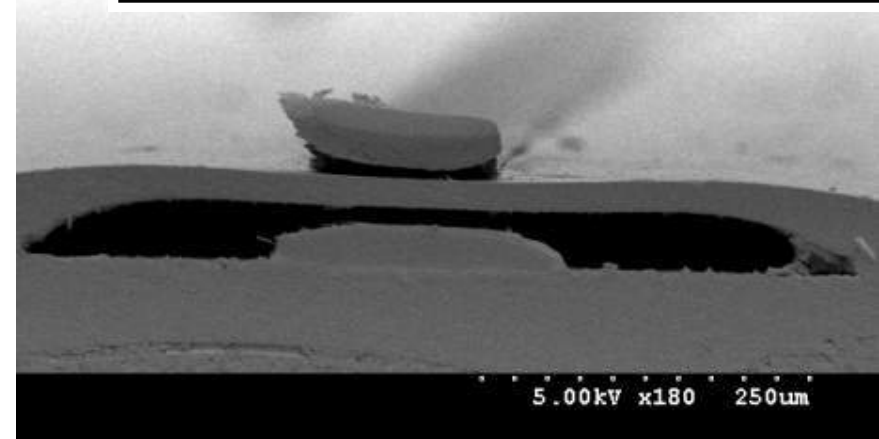
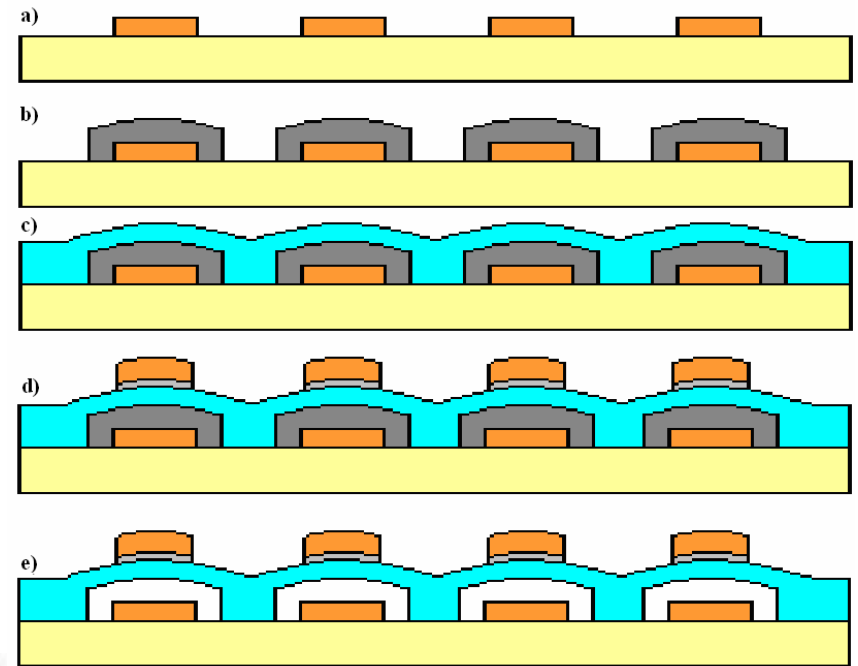


Figure 1. (a) A schematic of conformal HfO₂ coating on a DNA functionalized SWNT. (b) A TEM image. (c) Transfer characteristics of a SWNT FET (MOSFET-like, with contact regions P-doped by back-gating) with 2-3nm HfO₂ gate oxide. (d) I-V characteristic.

Y. Nishi, H.J. Dai and Y. Lu, Stanford University
Work performed at SNF

Air-Clad Transmission Lines on Organic Substrates for Chip-to-Chip Interconnects

- Sacrificial polymer is used to create air gap
 - ◆ Photosensitive polycarbonate (Unity) with a low decomposition temperature (180°C)
 - ◆ Decomposition products permeate overcoat polymer (Avatrel) to create air gap
- Parallel plate and suspended ground microstrip lines fabricated
 - ◆ Capacitance reduced by more than 30% in fabricated structures
 - ◆ Loss tangent reduced by more than 85%
 - ◆ Reduces conductor loss and drastically reduces effects dielectric loss

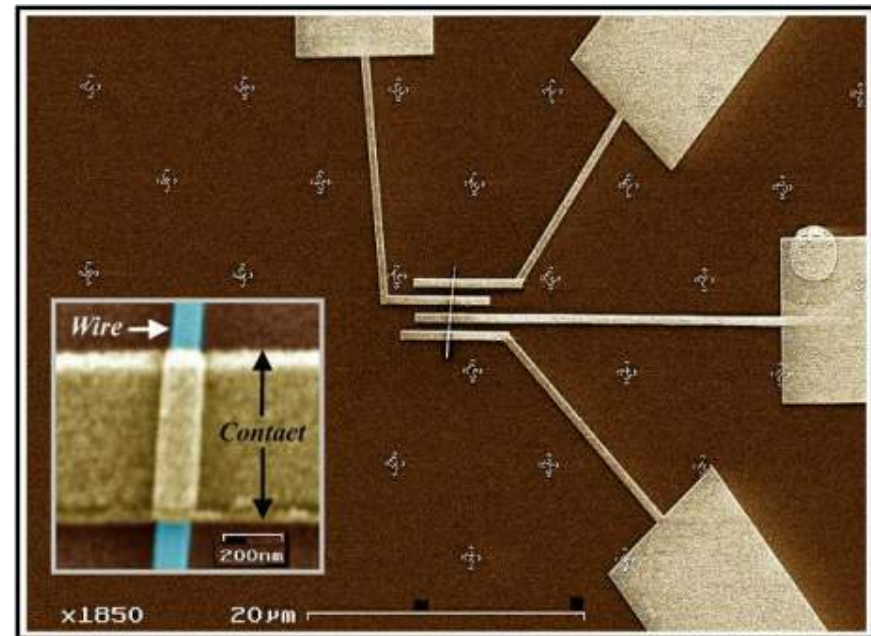


P. Kohl, Ga Tech
Work Performed at Ga Tech

Unity and Avatrel provided by Promerus, LLC Brecksville, OH

GaN Nanowire Channel Transistor

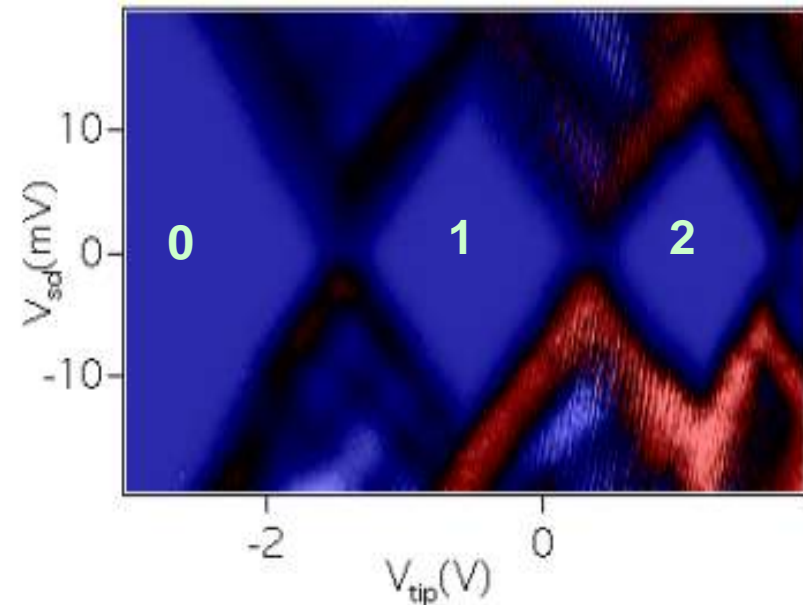
Understanding certain nanowire properties requires the preparation of a single nanowire device. For example, it is currently not feasible to use Hall effect to measure carrier mobility in nanowire, and therefore the only way is to create a field effect transistor and measure field-effect mobility.



V. Narayanamurthi, Harvard University
Work performed at Harvard University

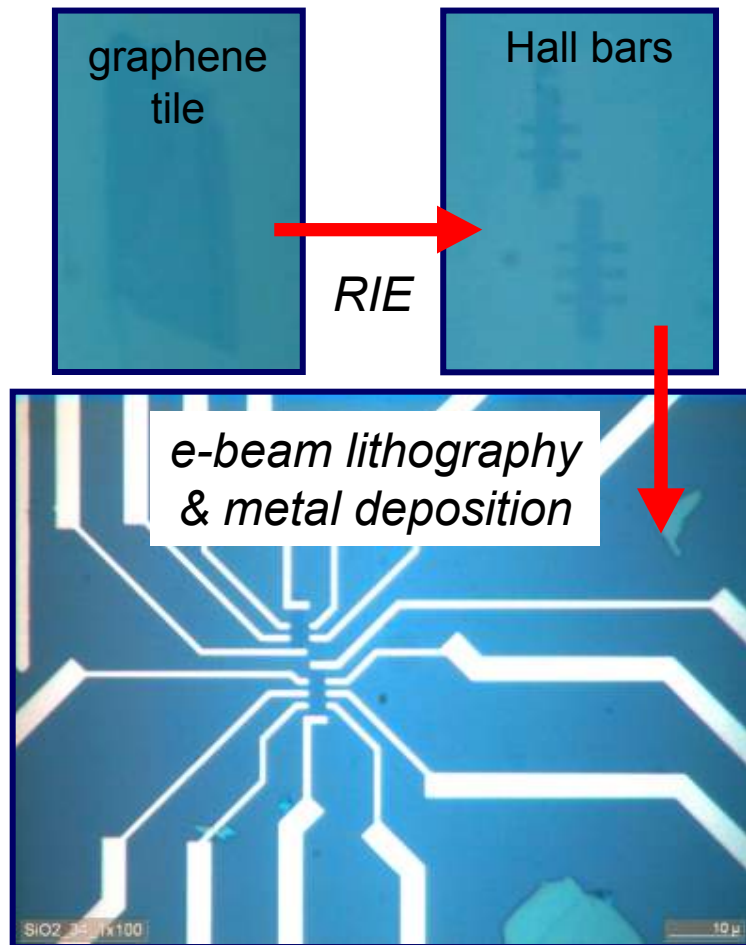
Image of a One-electron InAs Quantum Dot inside an InAs/InP Nanowire

An InAs quantum dot was formed inside an InAs/InP nanowire heterostructure by two InP barriers. The dot has the shape of a hockey puck, and it can be very small. Coulomb blockade diamonds above show that the number of electrons can be reduced to 1, then 0. Conductance through the InAs dot was imaged at liquid He temperatures by using a scanning probe microscope (SPM) tip as a moveable gate. The image above shows a Coulomb blockade ring separating 2 and 1 electrons on the dot. By changing the tip voltage the number can be reduced to 0. SPM imaging will be a powerful tool to manipulate one-electron dots inside InAs/InP nanowires.



Coulomb blockade diamonds for
0, 1, and 2 electrons on the dot.

Graphene Field Effect Transistors



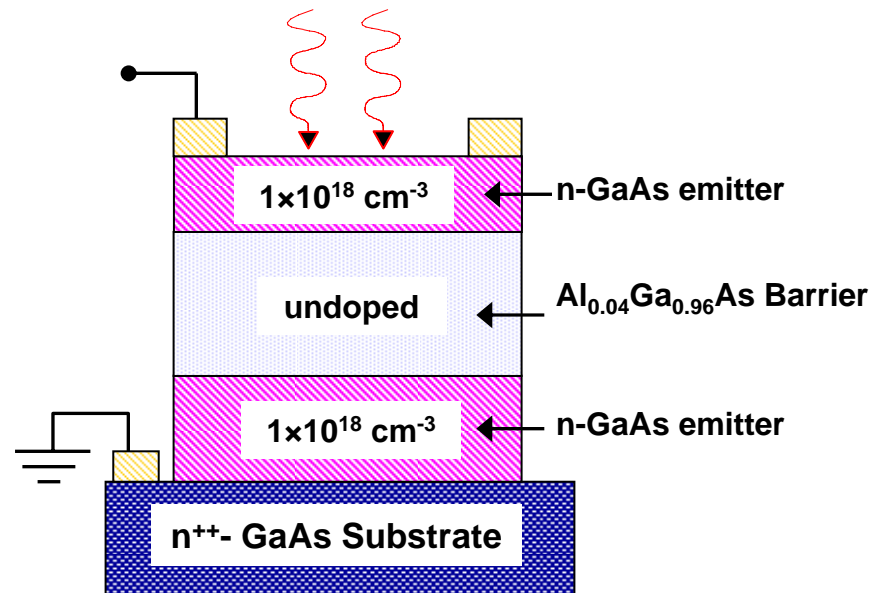
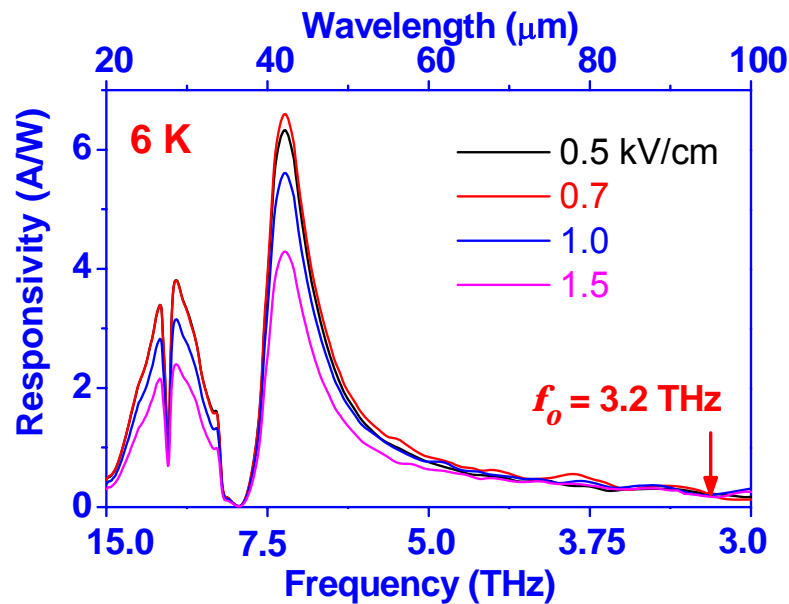
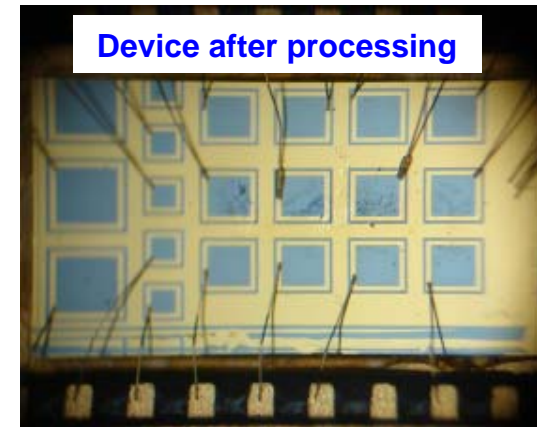
X. Hong and J. Zhu, Penn State University
Work performed at PSU

Graphene, one atomic layer of sp²-bonded carbon atoms arranged in a honeycomb lattice, is the latest member of a family of material systems that can host a 2-D electron/hole gas. 2-D carriers can be injected into graphene via field effect with mobilities as high as 20,000cm²/Vs, comparable to the best Ga(In, Al)As-based HEMTs from the III-V semiconductor group. Graphene has a linear band dispersion and have exhibited unusual physical properties such as anomalous integer quantum hall effect and Klein tunneling. In this study, we design and fabricate graphene field effect transistors in Hall bar geometry on mechanically cleaved graphene tiles using RIE and e-beam lithography.

2-DEG transport studies facilitated by graphene field effect transistors fabricated in Hall bar structure

n-GaAs/*Al*_{*x*}*Ga*_{1-*x*}As Structures for Terahertz Detection

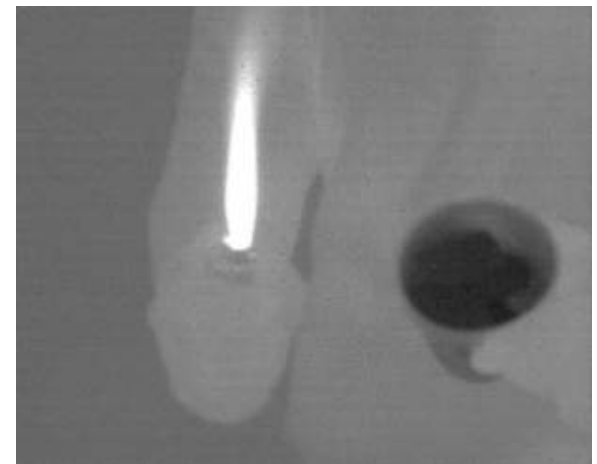
- Smaller workfunction using *n*-GaAs/*Al*_{*x*}*Ga*_{1-*x*}As
- Photo detectors for detect terahertz detection
- Single emitter detector shows photoresponse up to $f_0 = 3.2$ THz (94 μm) at 6 K
- Photoresponses beyond 3 THz (100 μm) is possible



A. G. U. Perera, U. New Mexico
Work performed in part at UNM

Novel Two-Color Infrared Quantum Dot Camera Using InAs/InGaAs Quantum Dots in a Well (DWELL) Focal Plane Array FPA)

- The IR camera system consists of:
- 320x256 Quantum Dots in a Well (DWELL) FPA
 - Material grown and array processed at the Center for High Technology Materials at UNM
 - Array hybridized to a commercially available read out integrated circuit (ROIC) by QMagiq, LLC.
- Two-Color Response
 - Janos Technology MWIR (3-5 μ m) and LWIR (8-12 μ m) lenses
- FPA voltage bias, electronic timing control, and data acquisition provided by the commercially available CamIRa™ system from SE-IR Corporation

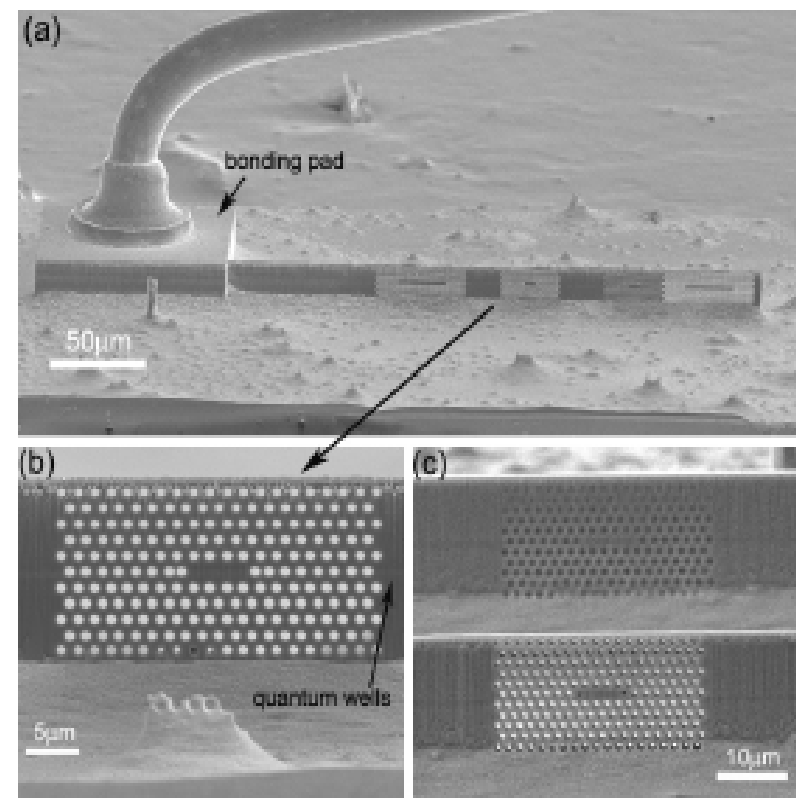


Optics and Photonics

Design and fabrication of photonic crystal quantum cascade lasers for optofluidics

We present novel designs and demonstrate a fabrication platform for electrically driven lasers based on high quality-factor photonic crystal cavities realized in mid-infrared quantum cascade laser material. The structures are based on deep-etched ridges with their sides perforated with photonic crystal lattice, using focused ion beam milling. Porous photonic crystal quantum cascade lasers have potential for on-chip, intracavity chemical and biological sensing in fluids using mid infrared spectroscopy.

M. Loncar, Harvard University
Work performed at Harvard University

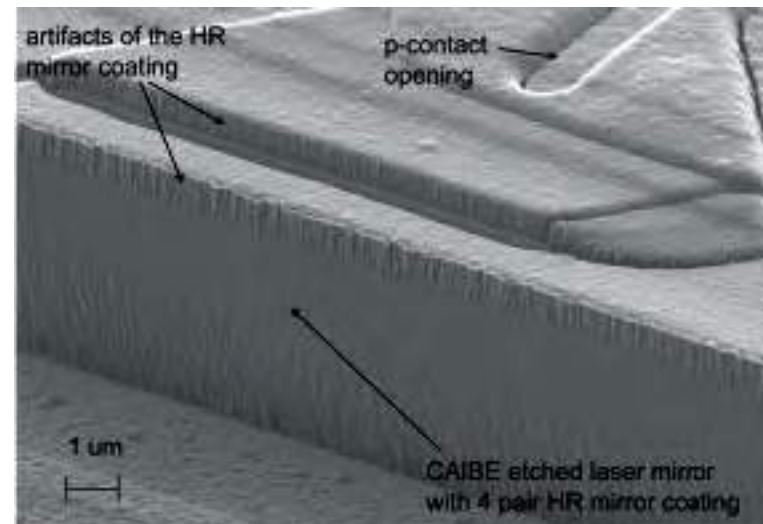


Fabricated PhC cavities. The quantum well active region can be seen as a light-gray stripe, indicated by an arrow.

Etched Facet Technology for Blue-Violet Lasers

A continuous wave (cw) blue-violet (405 nm) emitting laser was fabricated using etched facet technology on blue laser epitaxy on free-standing GaN substrate. A 100 μm cavity laser with cw laser performance had a threshold current as low as 10 mA.

The motivation behind this work is to fabricate blue lasers using BinOptics' etched facet technology (EFT). EFT has been shown to drastically reduce the cost of processing and testing InP-based lasers, and is anticipated to have similar benefits for GaN-based lasers. In addition, EFT allows the formation of shorter cavities than conventional facet cleaving—making possible a much larger number of laser devices from each wafer- as many as three to six times as many devices per wafer. This advance is expected to significantly contribute to lower production costs for blue lasers.

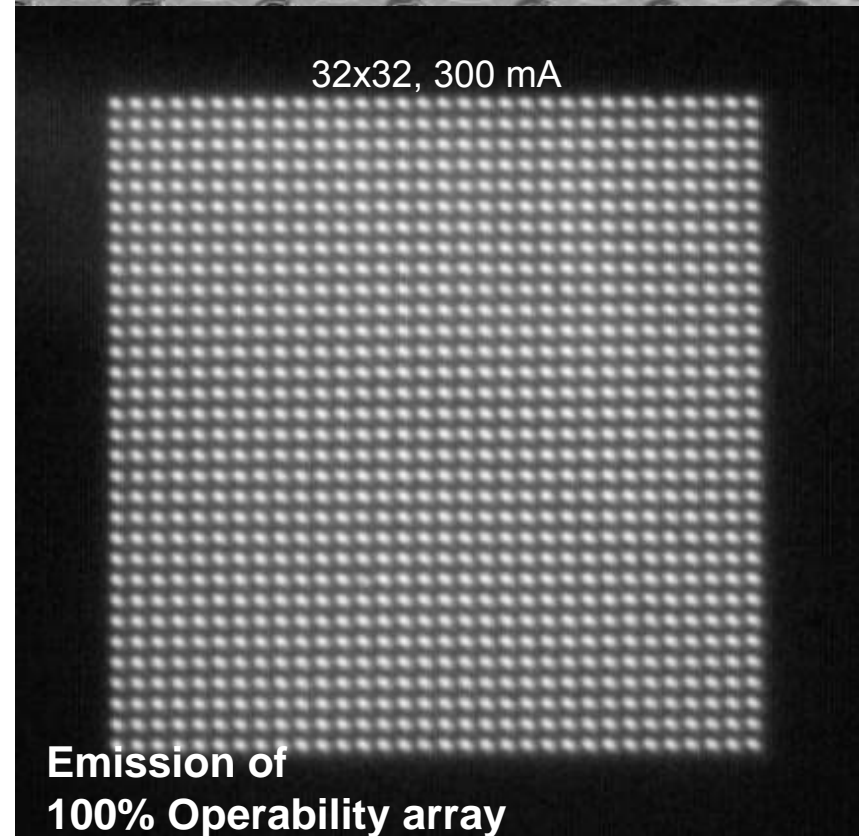
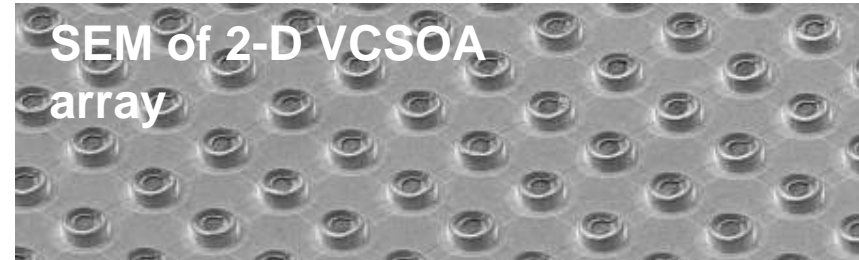


SEM image of a CAIBE etched laser mirror after deposition of a 4-pair high reflectivity (HR) mirror

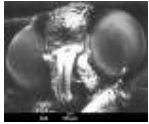
Vertical Cavity Semiconductor Optical Amplifiers

Aerius Photonics has been conducting research toward the development of large format 2-D arrays of Vertical Cavity Semiconductor Optical Amplifiers (VCISOAs). These devices operate in transmission mode, and amplify narrowband light by a resonant stimulated emission process.

Aerius has used the UCSB Nanofabrication facility to develop advanced wafer-scale processes and designs and has achieved 100% operability with excellent device performance properties

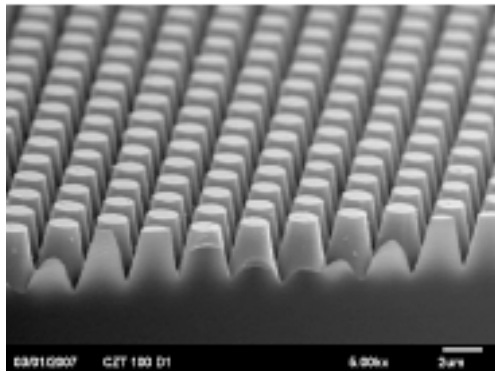


P155-Y, 2144, 300 mA, 20°C

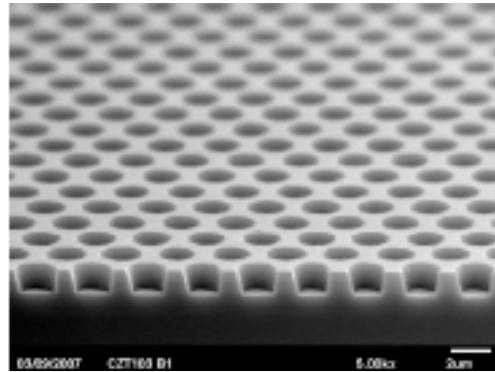


Antireflective Surface Structures

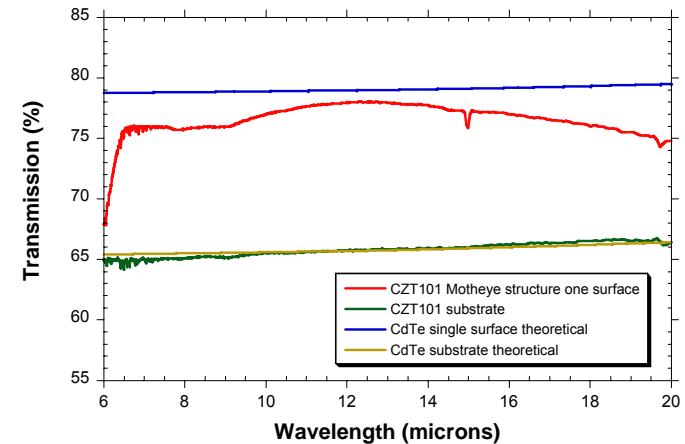
TelAztec is currently developing Radiation Hard Antireflective Surface Structures for space based applications. Antireflection surface structures have been designed and fabricated in CdZnTe substrates for backside illuminated HgCdTe LWIR detectors. These structures replace traditional thin film AR coatings, and eliminate problems such as limited performance, delamination, stress, poor off-axis performance, and susceptibility to radiation damage. Reactive Ion Etching at the UCSB nanofabrication facility has aided in development of AR microstructures in several infrared transmitting materials, including CdZnTe, ZnSe, Ge, sapphire, and silicon.



Motheye Graded Index Antireflection Structure etched into CdZnTe substrate for radiation hard LWIR applications



Effective Index Antireflection Structure etched into CdZnTe substrate for radiation hard LWIR applications

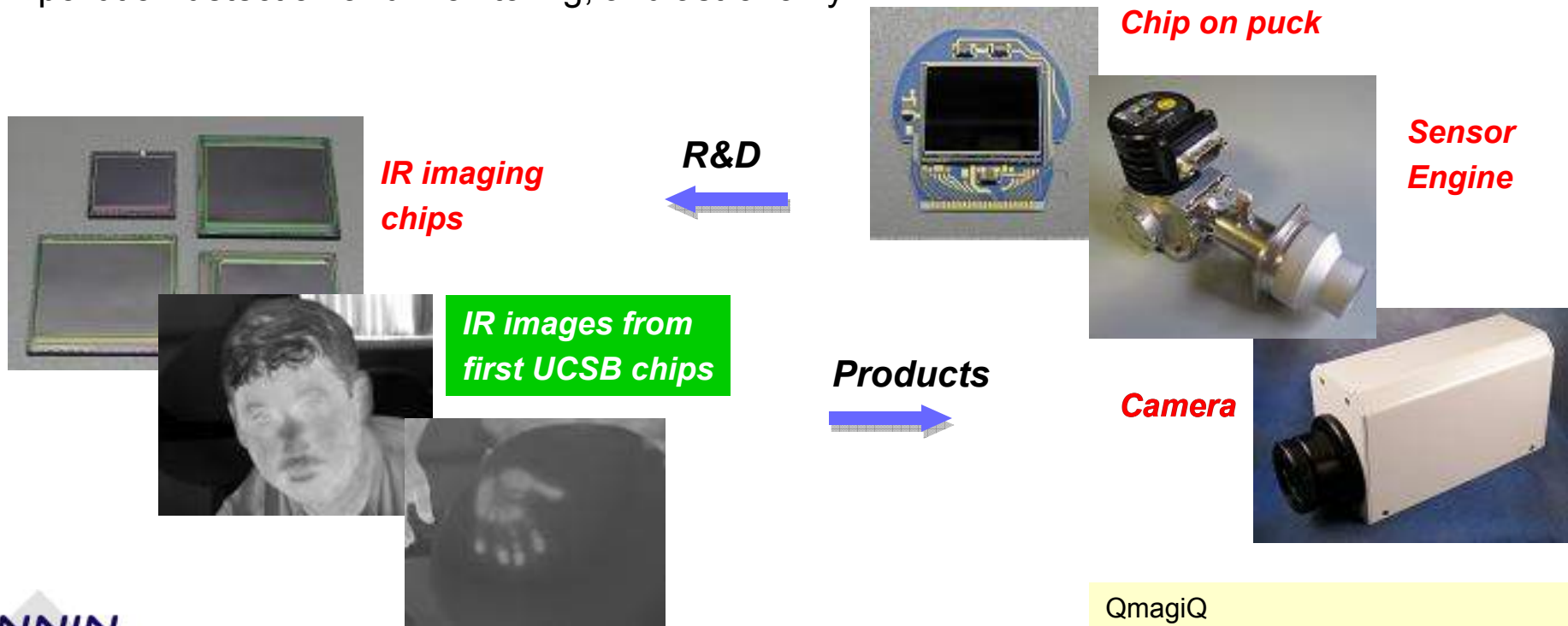


Typical AR performance of Motheye structure in CZT, from 7-20 microns

Infrared Imaging Sensors

QmagiQ develops infrared imaging chips based on quantum wells. Part of the process development is carried out at the UCSB node of the NNIN. The processing at the UCSB facility resulted in performance good enough to lay the groundwork for chips with multi-million pixel formats, imaging simultaneously in multiple infrared spectral bands.

Cameras containing such chips find uses in security and surveillance, missile defense, pollution detection and monitoring, and astronomy.



2D Photonic Crystal Resonator for Electro-Optical Switching

By forming a lattice of macroscopic dielectric media, an optical analogy of a crystal can be fabricated, called a photonic crystal. This investigation uses silicon fabrication techniques to construct photonic bandgap structures with the capability of manipulating light for potential all-optical silicon based optoelectronic circuits.

By carefully tuning the local lattice constant in the center region of a 2D photonic crystal, a resonators with a measured Q factor of the order of 10,000 have been fabricated. If the refractive index of part of the materials is changed—for example, fill the air holes with EO materials like liquid crystal or EO polymer—and change its refractive index by thermal effect or electric field, it is possible to have very high on/off extinction ratio transmission signal for some particular wavelengths. Figure 1 shows an SEM image of the device. A second type of 2D photonic crystal resonator was also made, this time with aluminum electrodes fabricated near the resonator. By filling the photonic crystal with liquid crystals, we were able to red- or blue-shift the resonance by applying an electric field across the electrodes, as seen in Figure 2.

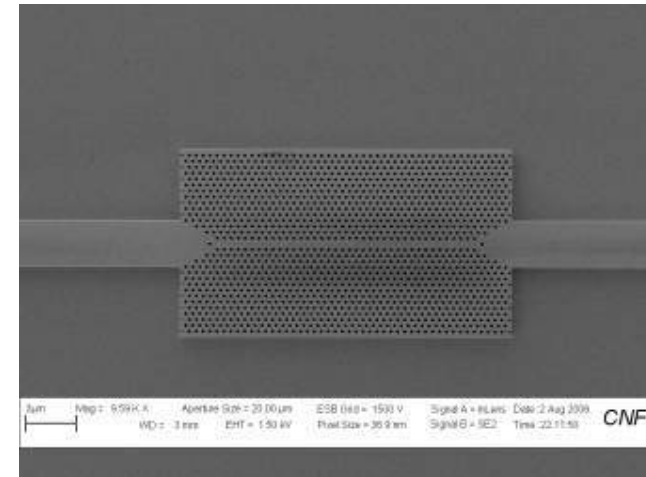


Figure 1: SEM image of the 2D photonic crystal resonator with Q value on the order of 10,000.

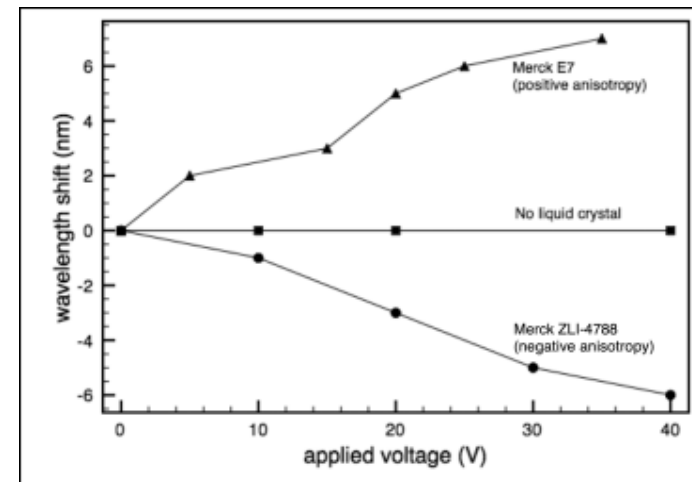
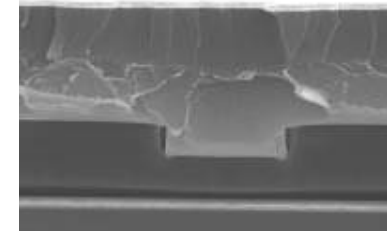
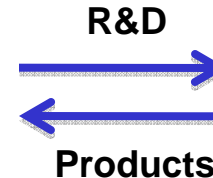
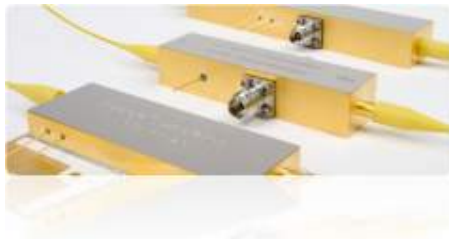


Figure 2: Graph showing the redshift and blueshift of the resonance upon the application of a voltage to the liquid-crystal-containing photonic crystal resonator.

Electro Optical Polymer Modulators

As digital data rates increase, so does the need for high bandwidth, linear response devices. In common crystalline materials, power consumption and bandwidth become compromised as data rates approach 50Gbps.

Polymer-based devices are key to keeping up with demand, as they offer vast improvements in bandwidth, distance, and power consumption. Lumera's polymeric materials are designed and synthesized at the molecular level to exhibit the properties needed for optimum electro-optic functionality. This enables our electro-optic polymer modulators to combine the fastest switching speeds with the lowest drive voltages and optical losses in the industry. We use the tools available in the UW Nanotech User Facility for characterizing and improving our materials and devices.



Electro-optic polymer modulators

Lumera Corp.
Work performed at UW Nanotech User Facility

Voltage-tunable Dual-band Quantum-dot Infrared Photodetectors

Objective:

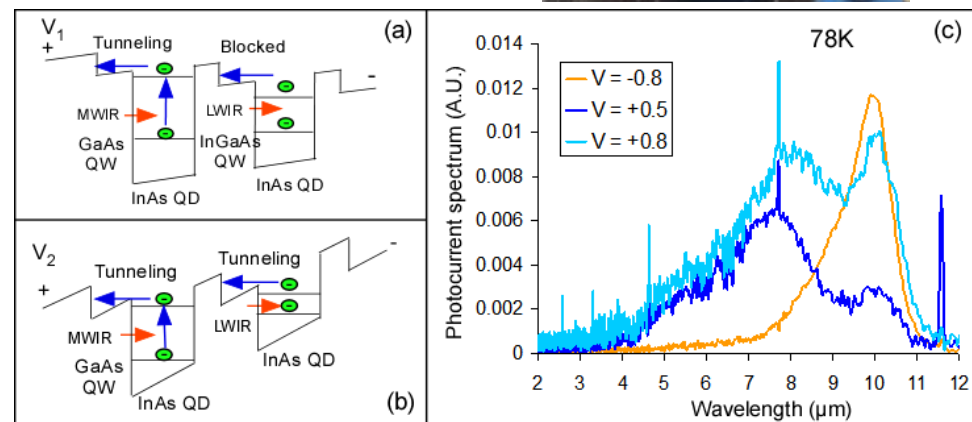
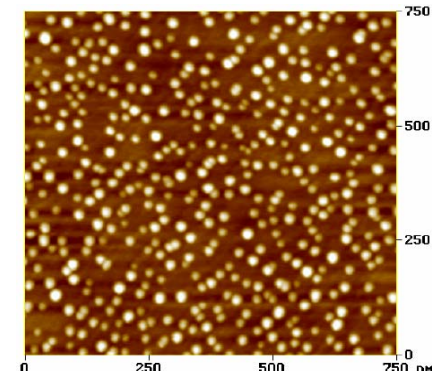
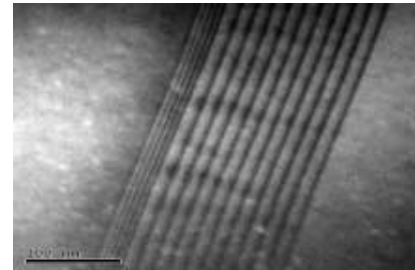
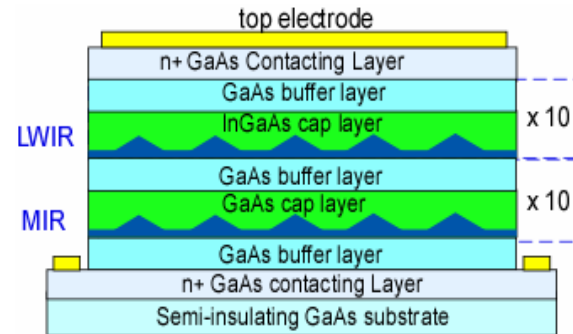
Develop voltage-tunable dual-band QDIP working at MIR and LWIR regions

Approach

Vertically-stacked QDs with InGaAs and GaAs cap layers for MIR and LWIR response, respectively.

Results:

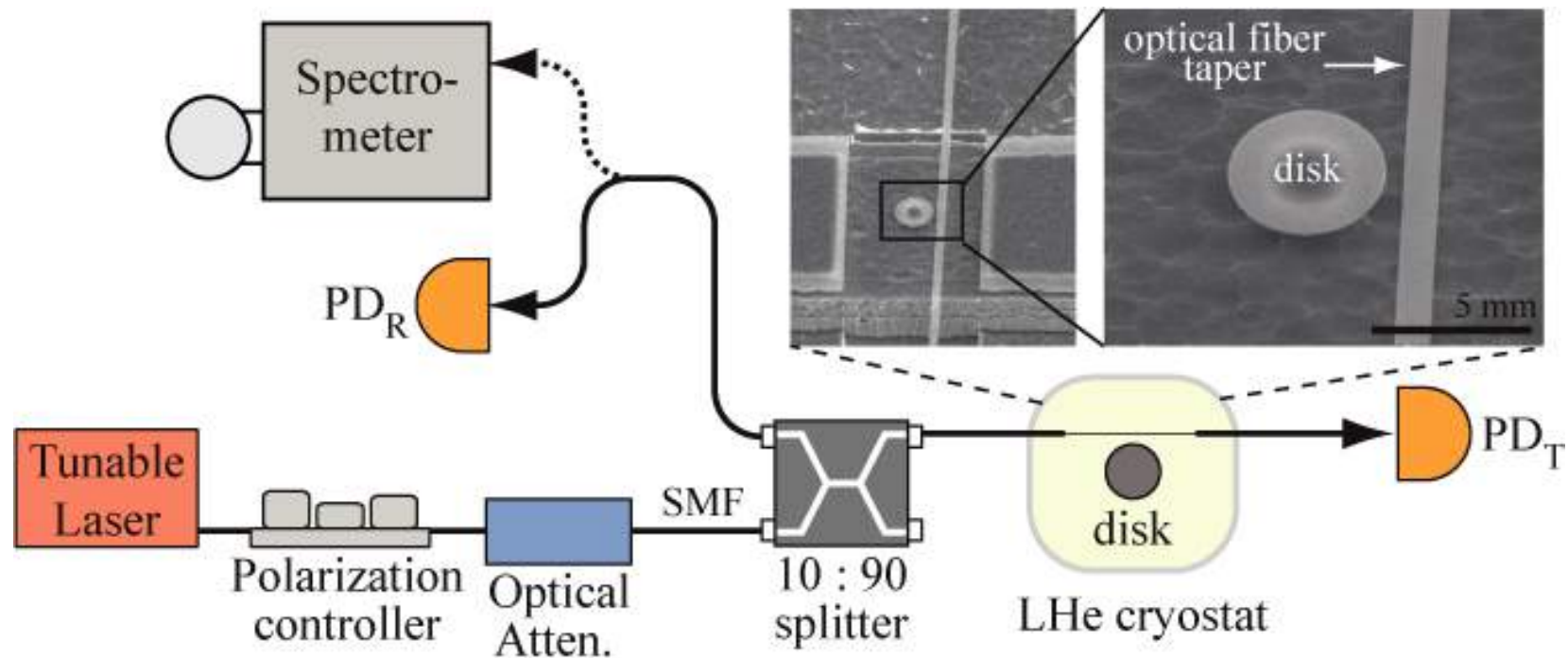
- Voltage-tunable single- or dual-band operations demonstrated.
- Over ten times photoreponsivity and photodetectivity D^* differentiation achieved.
- High photoreponsivity of $> 1 \text{ A/W}$ and photodetectivity $> 10^9 \text{ cmHz}^{1/2}/\text{W}$ obtained at device temperature 78K.



X. Lu, U. Massachusetts at Lowell
Work performed in part at UNM

Fiber-Coupled Cavity-QD System

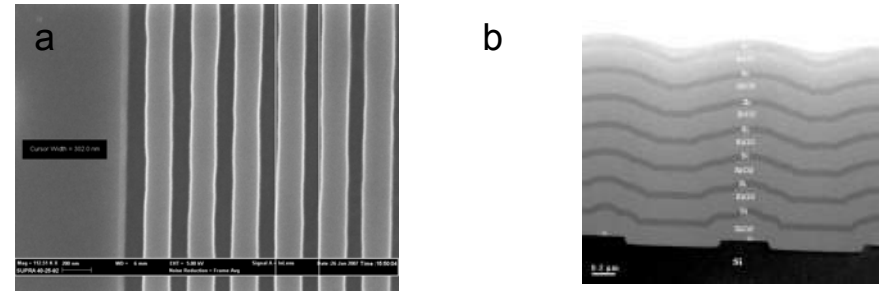
We have developed a series of tools and techniques to allow for *coherent* probing of the quantum system using a simple fiber-optic interface



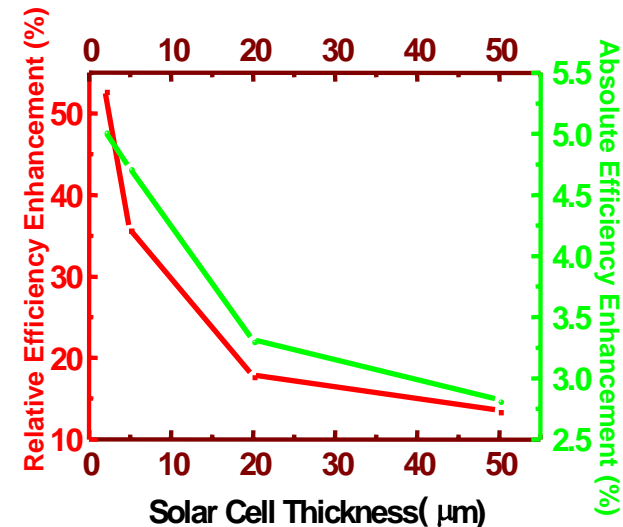
High Efficiency Thin Film Si Solar Cells by Novel Light Trapping

Thin Film Silicon Solar Cells are widely considered the best candidate for next generation solar electricity applications due to their potential low cost, ease of fabrication and low use of Si feedstock. In order to achieve high efficiency, effective light trapping is essential to increase the absorption path length in the thin film.

In this study, a novel, photonic crystal backside reflector is employed to increase the optical path length by more than 10^4 times the film thickness for almost complete light absorption. The design combines a diffraction grating and a distributed Bragg reflector. The grating fabrication requires a period of around 300 nm, and it cannot be fabricated in MIT cleanrooms. Using the interference lithography tool at the UNM node of NNIN, the design was fabricated with an interference process that is capable of low cost scale-up. This optimized, back reflector can increase thin film Si solar cell efficiency significantly. For a 2 μm thick Si thin film solar cell, the relative efficiency enhancement by the back reflector is expected to be as high as 53%.



a) SEM image of a grating with 302 nm period patterned with interference lithography tool at UNM-NNIN; b) XTEM image of a textured photonic crystal backside reflector

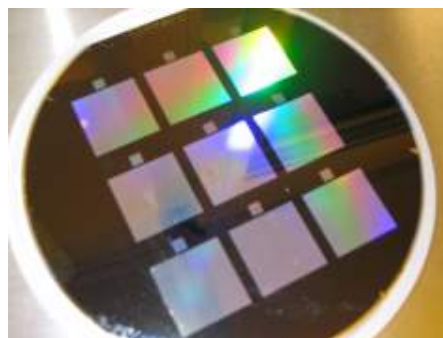
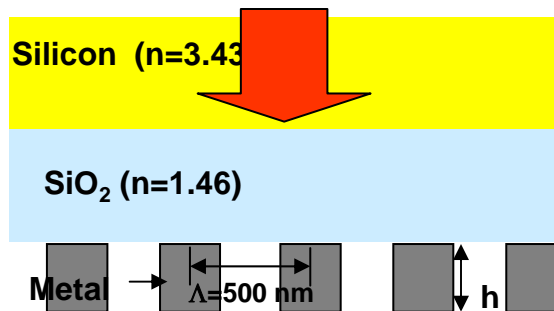


Simulated solar cell efficiency enhancement by textured photonic crystal backside reflector

Silicon Micro-Polarizer Devices for Infrared Imaging: A Mid-Wave Infrared Focal Plane Array Camera

High resolution imaging requires large arrays of focal plane array (FPA) detectors. One of the greatest challenges to developing polarimetric infrared imaging is the development of a good broadband, large-area nano-grid wire polarizer.

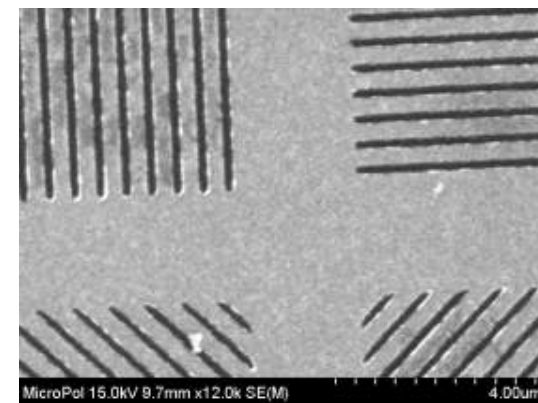
In this study, grid wire polarizer arrays were first modeled using rigorous coupled-wave analysis and then fabricated using the high-resolution, large area patterning capability of the 193 nm scanner, which proved the only viable technology to achieve the required linewidth. The fabricated grid-wire polarizer met the design criteria and achieved an extinction ratio of at least 1000 with transmission that exceeds 80% over a wide spectral range.



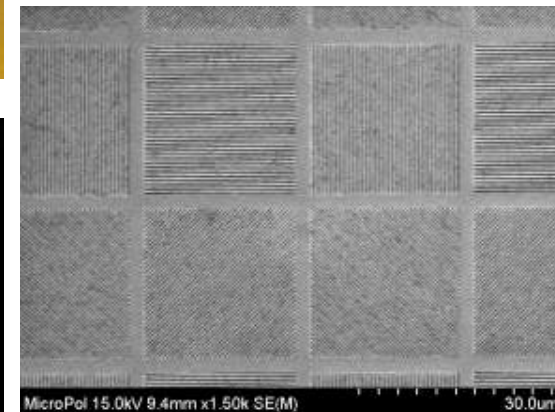
9 arrays on 150 mm wafer



Polarizer as seen by microscope



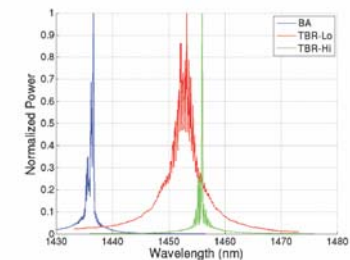
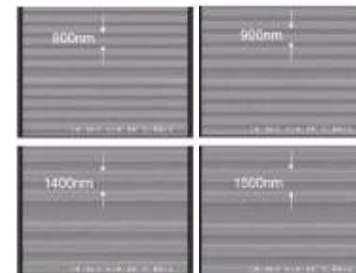
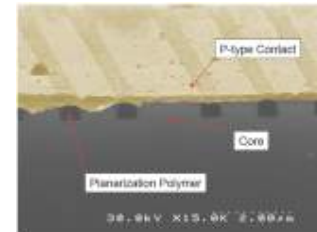
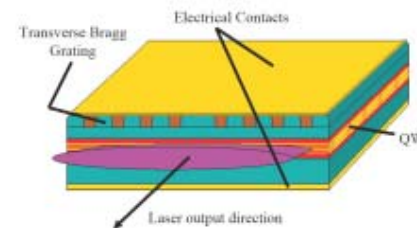
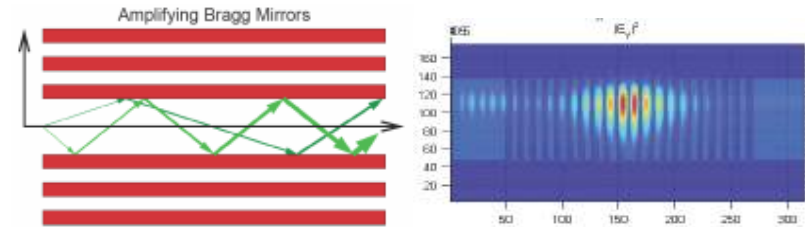
193 nm lithography for 200 nm metal lines (only technology capable of delivering this performance)



Original 1024 X 1024 pixel array reduced to 4- 256 X 256 polarized independent arrays

Transverse Bragg Resonance Laser

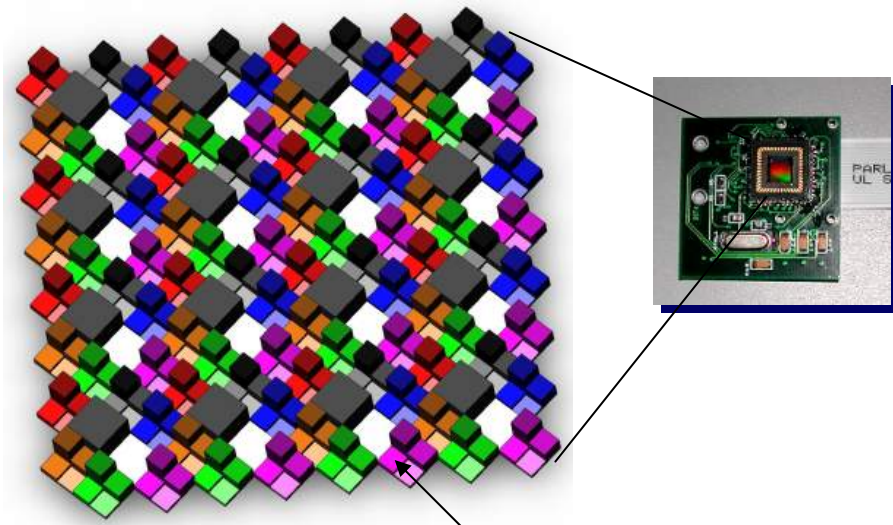
- Traditional index confinement with Bragg reflection in the transverse direction has been replaced.
- Single mode operation in large modal volumes has been achieved.
- Semiconductor transverse Bragg resonance lasers in an InP/InGaAsP/InGaAs material system were designed, fabricated and characterized.



A. Yariv and J. Choi, CalTech
Work performed at SNF

Laser Threat - Compact Alert Module (LT-CAM)

Laser threat detectors for screening threat radiation from non-threat radiation need to be much less costly to be widely adopted in commercial aviation. One method to lower the cost is to integrate expanded spectral capabilities directly onto low cost CMOS image sensors. Expanded mosaic filter array will provide the means to detect wider threat spectral range and enhance background rejection



Expanded color filter mosaic array

In this study, Nanohmics is using lithography to prepare an expanded color filter mosaic consisting of dye impregnated photoresist formulations. This also includes custom formulations for near-IR phosphor nanoparticles as one of the color filter elements

S. Savoy, Nanohmics Inc
Work performed at U Texas

Sub-100-nm Light Confinement in Transparent Photonic Wires

Recently it was theoretically shown that a nanoscale slot in a silicon waveguide could, in principle, achieve loss-less light confinement of less than $\lambda/15$ in air by utilizing the electric field discontinuities at the boundaries of high-index-contrast waveguides. An example of such a structure with an 85 nm slot is shown in Figure 1a. Figure 1b plots the fundamental TE mode showing clear confinement of light to the slot region.

We have employed a novel transmission-based near field scanning optical microscopy (TraNSOM) technique which is based on changes in transmission through a photonic structure induced by near field perturbation by a nm-scale atomic force microscope (AFM) probe to directly measure the light emission from materials embedded in the slot. This TraNSOM measurement represents, to our knowledge, the strongest light confinement measured in dielectric photonic structures. Devices based on this strong light confinement will benefit greatly by the increased light-matter interaction in the slot region.

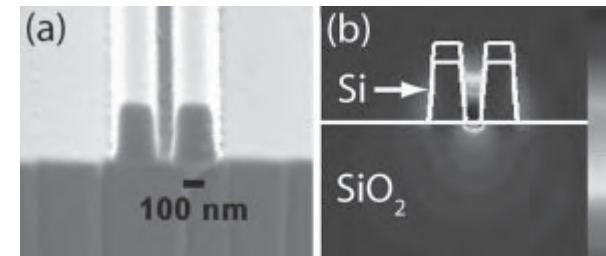


Figure 1: (a) SEM of a slot waveguide;
(b) calculated fundamental TE optical mode.

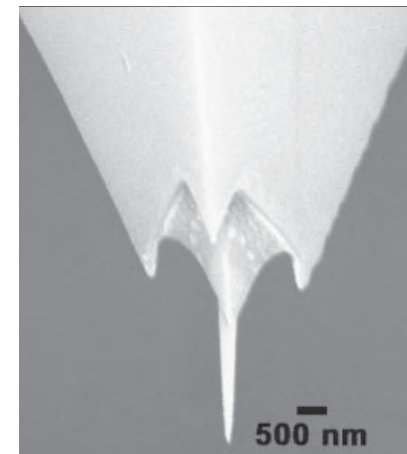


Figure 2: High aspect ratio Si AFM probe used to map the optical field.

M. Lipson, Cornell University
Work performed at CNF

Compact Bandwidth Tunable Micro-Ring Resonators

Optical resonators have vast applications in optical systems. One important characteristic of an optical resonator is its bandwidth. For some applications, such as dynamically configurable filters and optical storage devices, a resonator of tunable bandwidth is desired. Here we demonstrate a compact micro-ring resonator where the bandwidth can be tuned over a broad range using the thermo-optical effect.

The devices were fabricated on a Unibond silicon-on-insulator (SOI) substrate. The waveguide and micro-ring are 520 nm wide and are defined by electron-beam lithography. Subsequently, thermal heaters are then patterned on top of the bus waveguides with electron-beam lithography, evaporation and lift-off process.

The devices were tested with a TE-like polarized light from a wavelength tunable laser. The bandwidth and extinction ratio can be tuned as we drive the micro-heaters to tune the effective coupling as shown in figure 3.

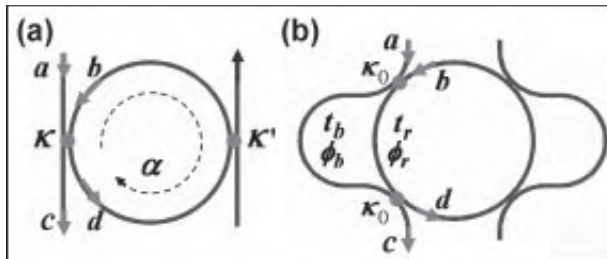


Figure 1. Schematics of micro-ring resonators with (a) simple coupling and (b) interferometric couplers.

M. Lipson, Cornell University
Work performed at CNF

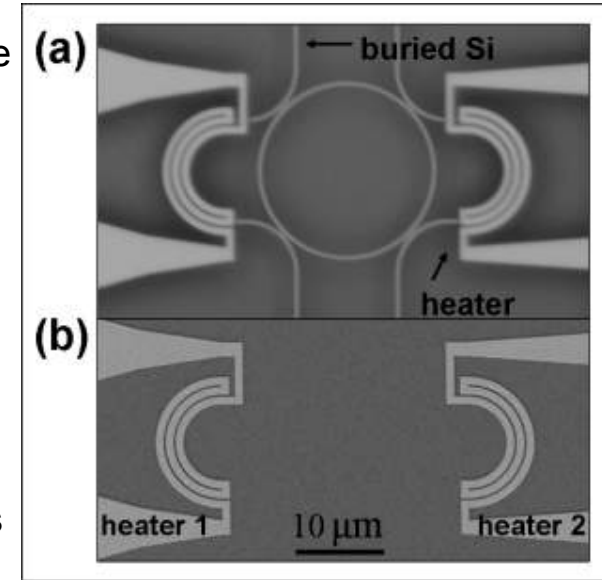


Figure 2a and 2b show light-microscopy and SEM image of the fabricated device.

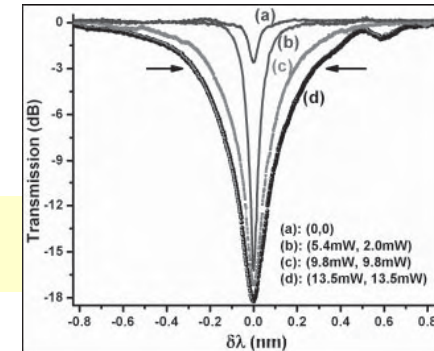
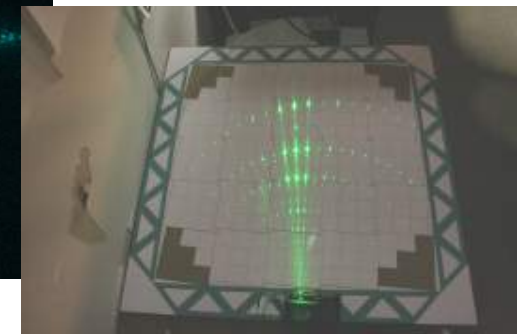
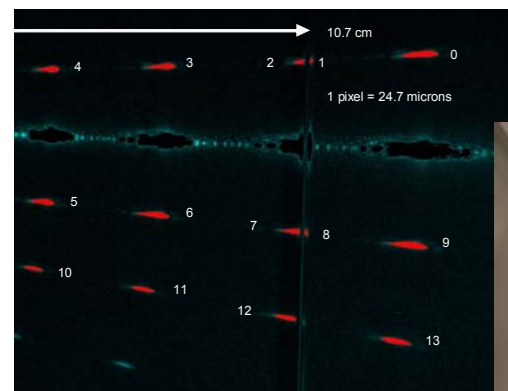
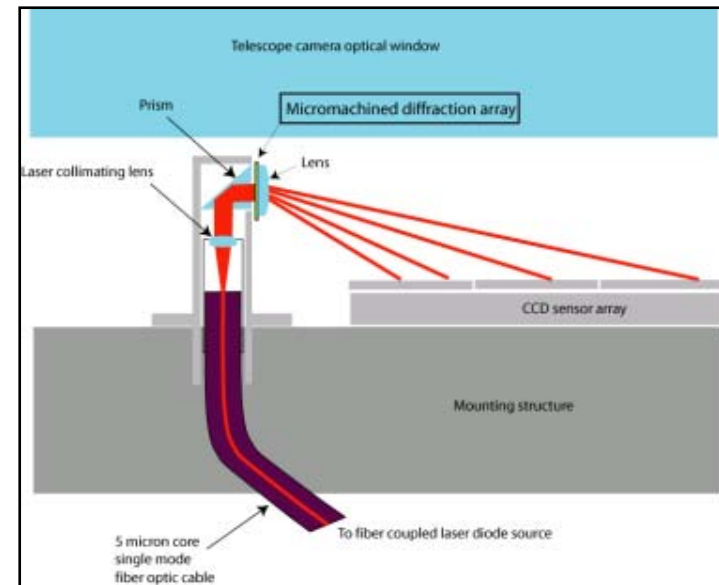


Figure 3: Tuning of resonance bandwidth at 1557 nm with different heater powers.

Micromachined Diffractive Optical Element for the Large Synoptic Survey Telescope

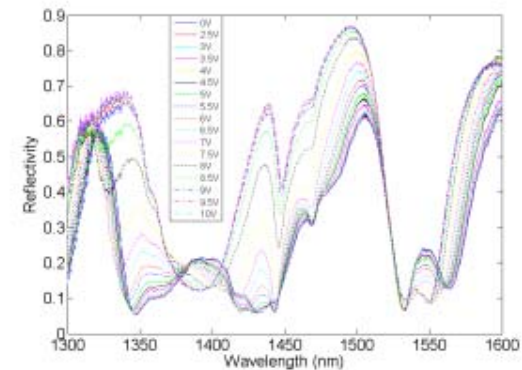
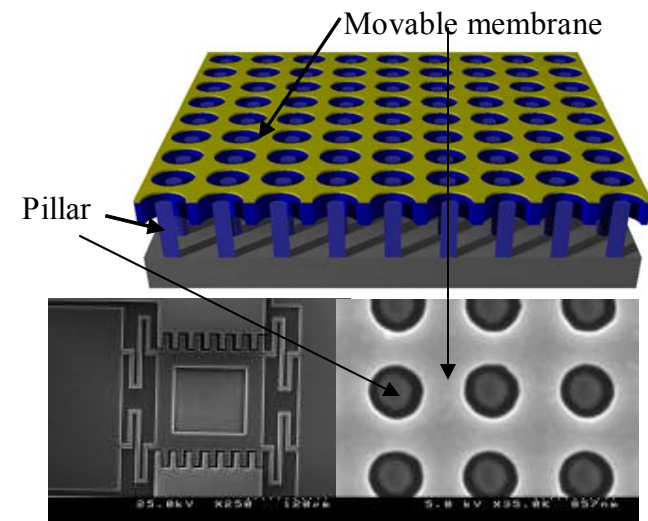
- A diffractive optical element MEMs device to align the 201 CCD elements in the Large Synoptic Survey Telescope was fabricated.
- Various prototype diffractive grids were fabricated using electron beam, laser direct-write and standard optical lithography and the best methodology was determined.



C. Kenney, M. Perl, R. Schindler & E. R. Lee, Stanford University
Work performed at SNF

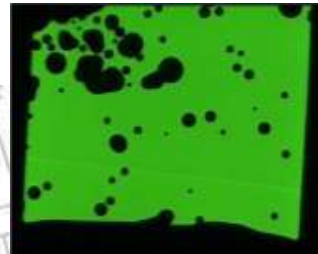
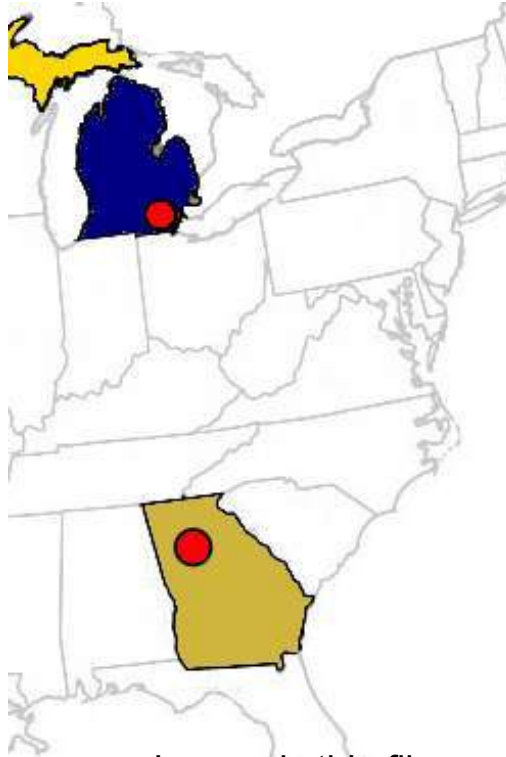
New Structures Magnify Interfacial Effects in Photonic Crystals

- Mechanically tunable photonic crystal displacement sensors have been developed.
- These devices are fabricated using SNF's epitaxial reactor.
- This is a breakthrough for fast crystal fabrication since single crystal, hydrogen anneal of these devices was possible.

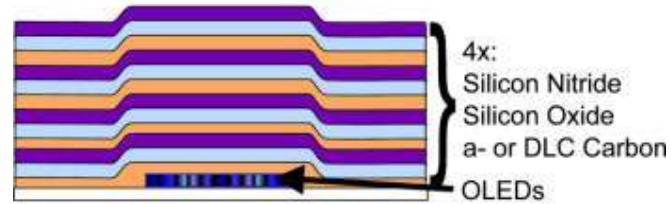


G. Yama, Robert Bosch Corporation
T. Kenny, R. Howe & J. Provine, Stanford University
Work performed at SNF

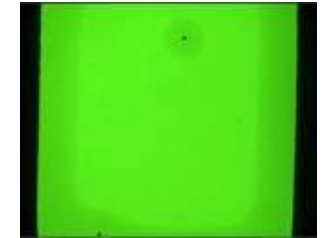
Low Temperature Encapsulation of Organic Light-Emitting Devices



OLED failure



Example of Encapsulation Scheme



Encapsulated OLED

Microelectronics Research Center:

- Electron Cyclotron Resonance (ECR) deposition of
 - Amorphous and Diamond-like Carbon
 - Silicon Nitride and Silicon Oxide

Michigan Nanofabrication Facility:

- Silicon Nitride and Oxide by PECVD and sputtering
- Parylene deposition

Organic Molecular Electronics Lab:

- OLED fabrication and characterization

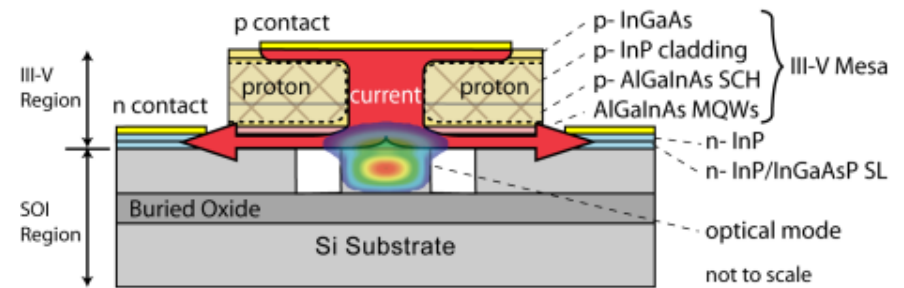
Inorganic thin films function as a barrier to oxygen and moisture, extending the lifetime of organic devices.

A. R. Johnson (UM), G. Book (GT), J. Kanicki (UM)
Work performed at Ga Tech and U. of Michigan

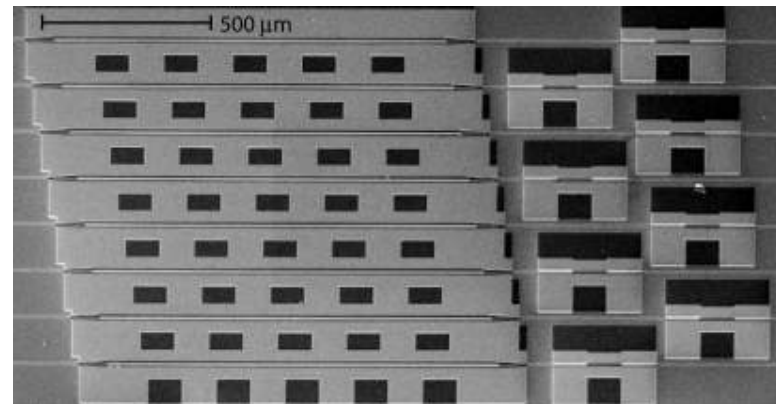
Silicon Evanescent Photonic Integrated Circuits

Silicon photonics research has gained a lot of momentum in recent years due to breakthroughs in modulator speeds and photo detection responsivity. In the recent 2 years, UCSB researchers in Professor John Bowers group, in collaboration with Intel, have developed a hybrid integration solution to achieve electrically pumped optical gain elements on silicon. The device consists of III-V active layers bonded to silicon waveguides to achieve evanescently coupled gain.

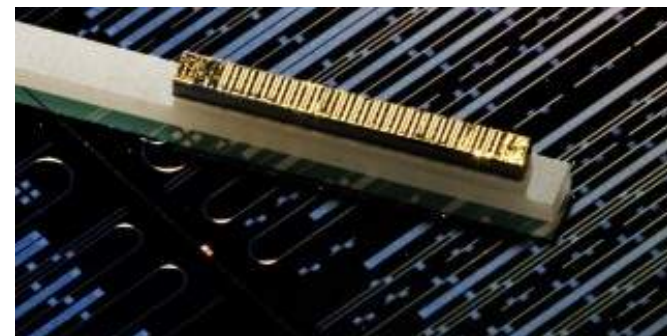
With this platform, the Bowers group have demonstrated the electrically driven lasers with output powers of 39 mW, 105 C operating temperatures, and thresholds as low as 20 mA. They have also demonstrated amplifiers capable of providing on chip gains of 13 dB and preamplified receivers with responsivities of 5.7 A/W.



A.W. Fang *et al.* Optics Express 2006



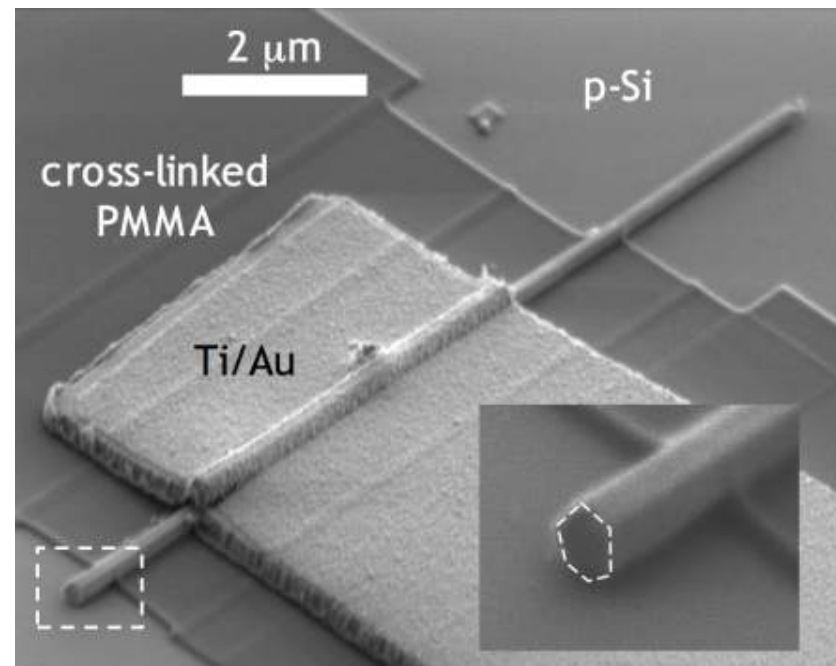
H. Park *et al.* Optics Express 2007



J. Bowers, UCSB
Work performed at UCSB

Nanowire Optoelectronics using GaN UV LED

Fabrication of an **ultraviolet (UV)** GaN single-nanowire light-emitting diode (LED): this work demonstrated that when an n-type semiconductor nanowire (GaN) is placed into contact with a p-type semiconductor substrate (Si), the resulting junction is, in general, a tunnel junction instead of a traditional p-n junction.



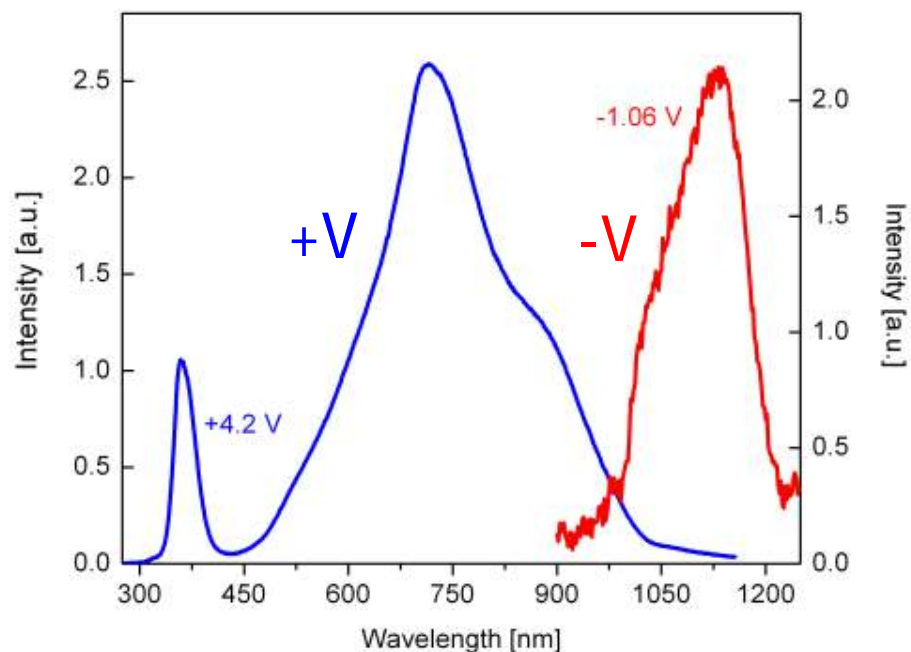
Fabrication of an **ultraviolet (UV)** GaN single-nanowire light-emitting diode (LED)

F. Capasso and V. Narayanamurti, Harvard University
Work performed at Harvard University

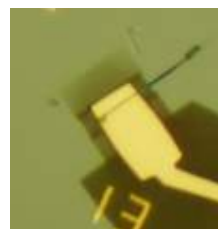
Two-color GaN-Si Nanowire LED

Two-color light emission results from the tunneling of electrons from the valence band of one semiconductor into the conduction band of the other semiconductor. For +V electrons can tunnel from the GaN valence band into the Si conduction band. The holes thus created recombine with conduction band electrons generating ultraviolet light. For -V, the opposite occurs.

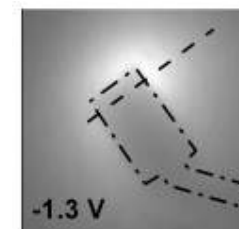
Electroluminescence spectra



F. Capasso and V. Narayanamurti, Harvard University
Work performed at Harvard University



+V --> light
from NW



-V --> light
from
substrate

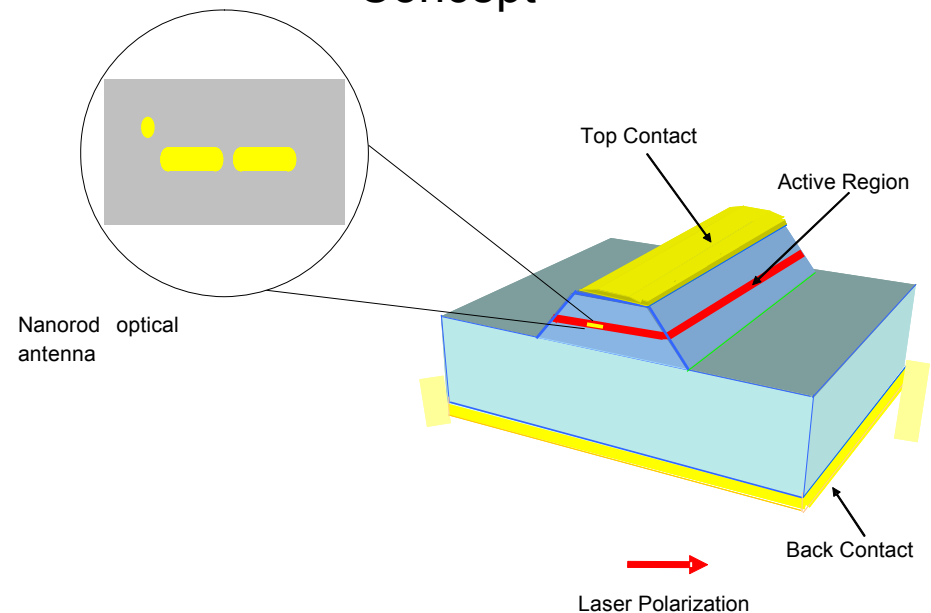
Plasmonic Laser Antenna

Using focused ion beam, a plasmonic antenna with 30 nm gap is formed on a commercial laser diode facet. The resulting peak intensity is 800x the incident intensity, in excess of 1 GW/cm². The intensity and reduced spot size have been confirmed by near-field measurement.

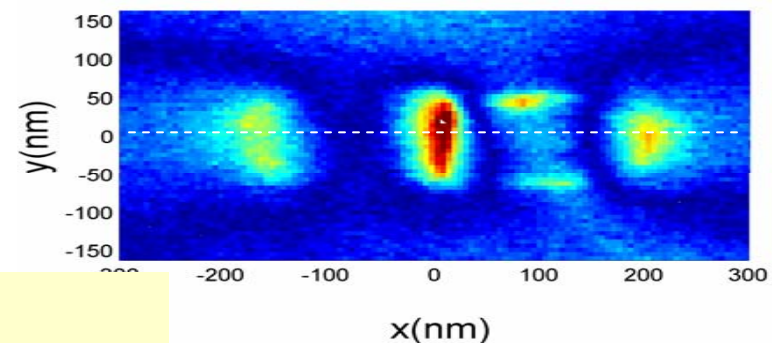
Applications include:

- High-density optical data storage (up to 1 TB/inch²)
- High-resolution spatially resolved imaging and spectroscopy
- Laser assisted processing and repair of nanoscale devices
- Nano-optical lithography
- Nano-optical tweezers

Concept



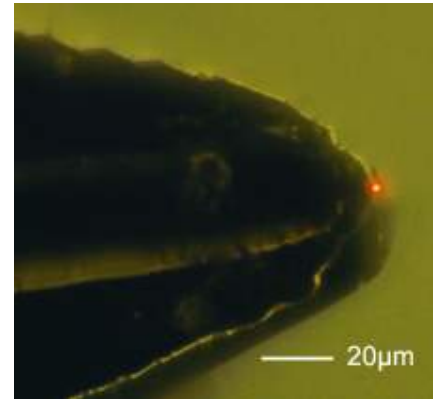
NSOM Image



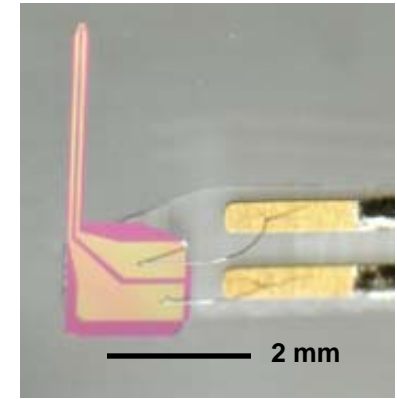
Nano-LED at Probe Tip for Near-field Imaging

We have built a nanoscale light emitting diode (LED) on a silicon MEMS probe for near-field scanning optical microscopy (NSOM). NSOM measures optical properties such as fluorescence on the nano-scale, which cannot be measured by a regular AFM and STM.

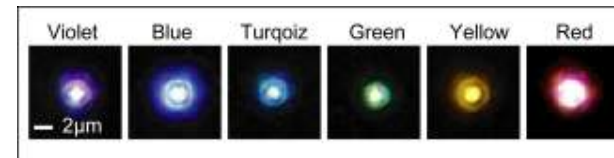
We successfully carried out optical and topographic imaging of a test chromium pattern as shown the figures. Intensity and topographic profiles indicate that optical and topographic resolutions of 400nm and 50nm, respectively, were achieved. To our knowledge, this is the world first successful NSOM image directly taken with an apertureless near-field light emitter on MEMS probe tip.



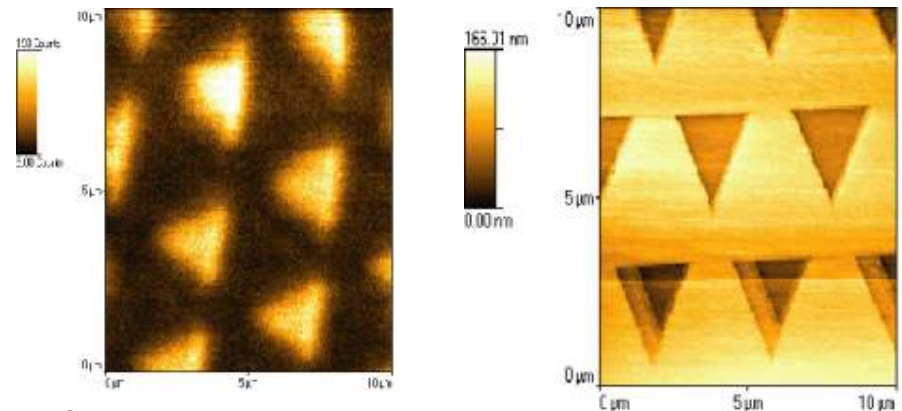
Nano-LED at probe tip



Probe



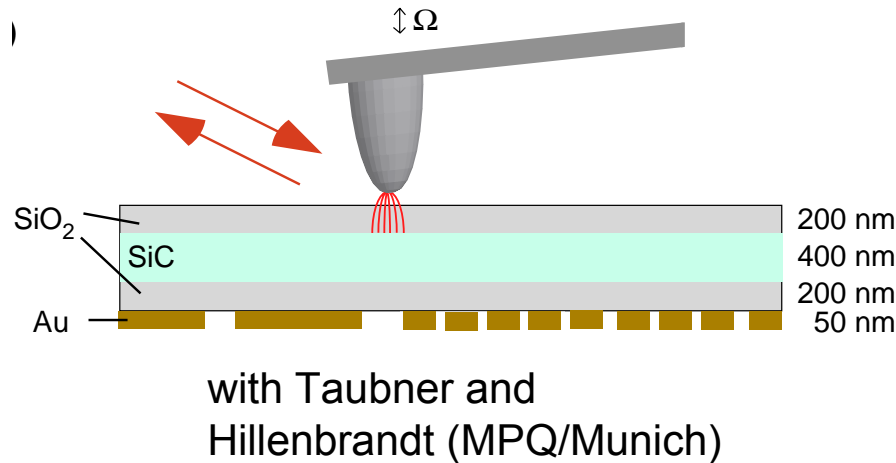
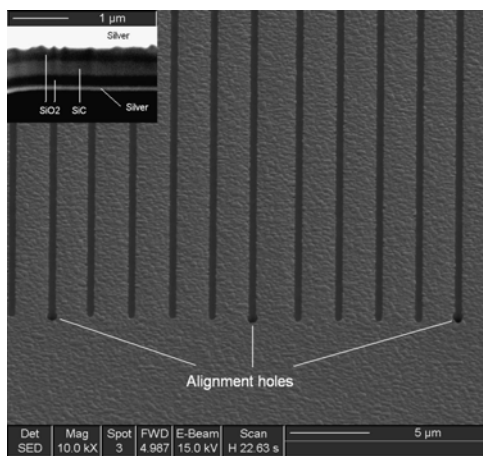
Nano-LEDs with different emission wavelengths



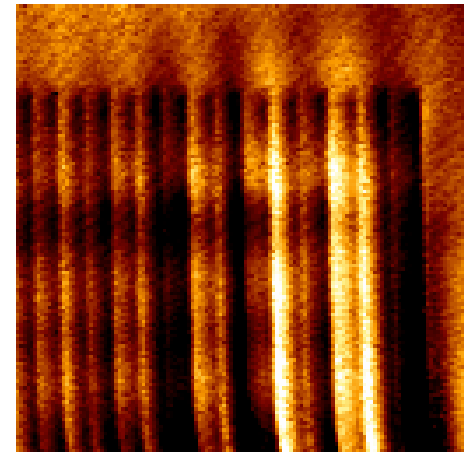
Optical and topographic imaging result with probe

Superlens in mid-IR: sub-surface imaging

pattern on bottom



NSOM image from top



- SiO₂/SiC/SiO₂ superlens with a metallic pattern (0.5 μm slits in Ag film separated by 3 μm on the bottom side) was imaged from the top using NSOM
- Sub-surface imaging of sub- λ features at 800 nm depth accomplished at 10.85 μm (CO₂ laser) using a superlens → opens the way to applications of super-lensing to sub-surface imaging of integrated circuits

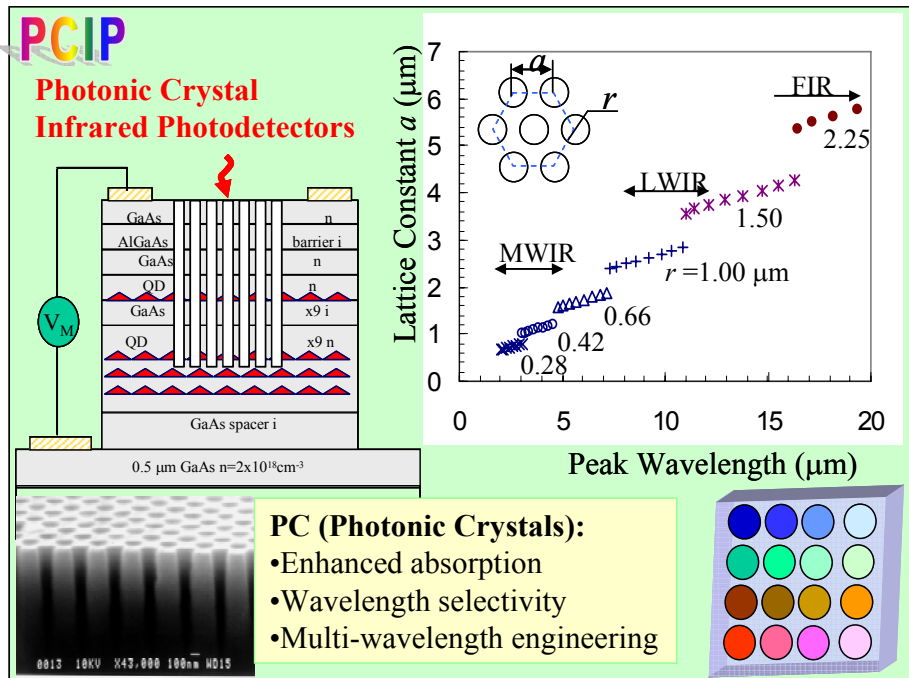
NanoPhotonic Device Research

PCIP Sensor Project:
Photonic Crystal Infrared Photodetectors

PCIP Program Objectives:

- High operation temperature (H.O.T)
- High spectral resolution
- Multi-spectral coverage

Quantum Dot Infrared Photodetectors in Photonic crystal Cavities

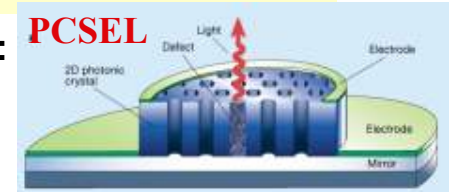


Applications: Hyper-spectral imaging; universal IR gas sensing

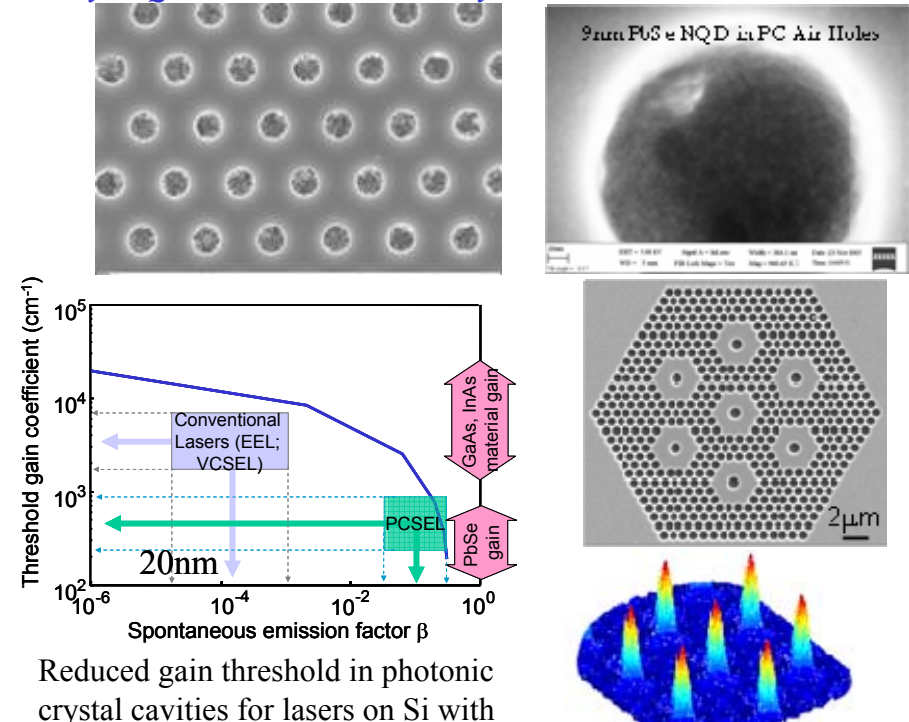
PCSEL Laser Project:
Photonic Crystal Surface Emitting Lasers

PCSEL Program Objectives:

- Nanoscale lasers on Si
- Efficient electrical injection
- Wide spectral coverage



Nanocrystal Quantum Dots in Photonic crystal Cavities on Silicon



Reduced gain threshold in photonic crystal cavities for lasers on Si with colloidal quantum dots.

Multi-wavelength laser arrays

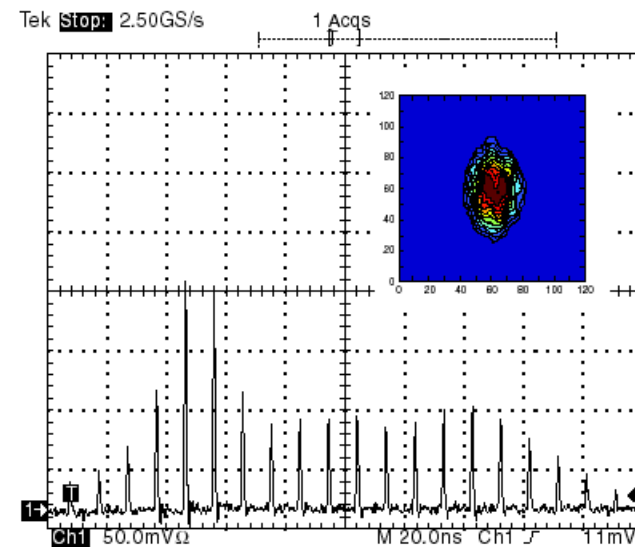
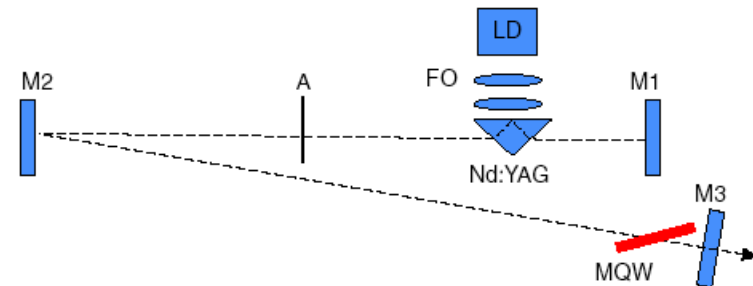
Side Pumped Nd:YAG Slab Laser Mode-Locked using Multiple Quantum Well Saturable Absorbers

Advantage: Solid-state element for mode-locking with virtually no degradation compared to existing technology

Applications: Environment sensing, laser marking, microsurgery, measurement techniques, range finding, frequency conversion

Method: Low-temperature MBE growth of switching element for ultra-fast response times

Results: Pulses down to 34 ps duration and up to 650 μJ of energy per train



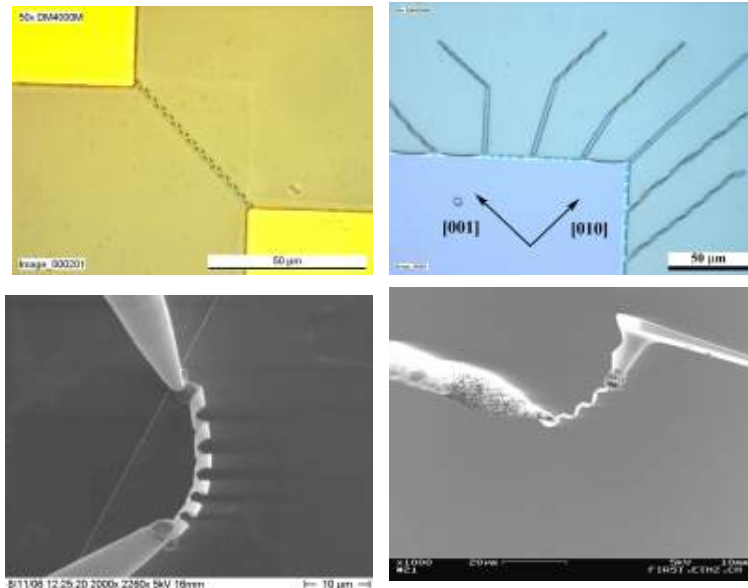
V. Kubecek, Czech Technical University
J.-C. Diels, U. of New Mexico
Work performed in part at UNM

MEMS

NEMS based on Nanocoil Structures

DESCRIPTION OF WORK

- ◆ Fabrication and integration of helical nanostructures
- ◆ Use of these structures is explored for electromechanical sensors, conductometric sensors, and for micropropulsion



MAJOR OBSERVATIONS

- ◆ A range of processes have been developed that allow for the reproducible fabrication and integration of these structures
- ◆ The structures were characterized using nanorobotic manipulation in SEM
- ◆ Devices based on these structures have been demonstrated

Publications

- ◆ D. J. Bell, S. Leutenegger, L. X. Dong, and B. J. Nelson, "Flagella-like propulsion for microrobots using a magnetic nanocoil and a rotating electromagnetic field," presented at International Conference on Robotics and Automation (ICRA '07), Rome, Italy, 2007.
- ◆ D. J. Bell, L. X. Dong, L. Zhang, M. Golling, B. J. Nelson, and D. Grützmacher, "Fabrication and characterization of three-dimensional InGaAs/GaAs nanosprings," *Nano Lett.*, vol. 6, pp. 725-729, 2006
- ◆ D. J. Bell, P. Rüst, L. X. Dong, S. Schön, and B. J. Nelson, "Conductometric sensors based on InGaAs/GaAs nanocoils," presented at IEEE MEMS, Kobe, Japan, 2007.

D. Bell, ETH Zurich, Switzerland
Work performed at U. of Minnesota

Fabrication of Cantilevers with Integrated Mesoscopic Samples

A persistent current I_p in a normal metallic ring is a mesoscopic phenomenon arising from interference of phase coherent electrons circumnavigating a ring threaded by a magnetic flux. The aim of this project is to study persistent currents in normal metal rings using a cantilever as a torsional magnetometer. High sensitivity cantilevers with integrated metal rings have been fabricated and tested. At $T = 300$ mK, the force sensitivity of the cantilevers is demonstrated to be $1.7 \text{ aN}/\sqrt{\text{Hz}}$. The phase coherence length λ_ϕ of electrons in co-deposited films is measured to be $3 \mu\text{m}$. This sensitivity should be adequate to measure persistent currents in normal metal rings.



Figure 1: SEM of fabricated silicon cantilever. Scale bar is $100 \mu\text{m}$. Inset shows a detail of the Al ring at the end of the cantilever. Inset scale bar is 400 nm .

J. Harris, Yale
Work performed at CNF

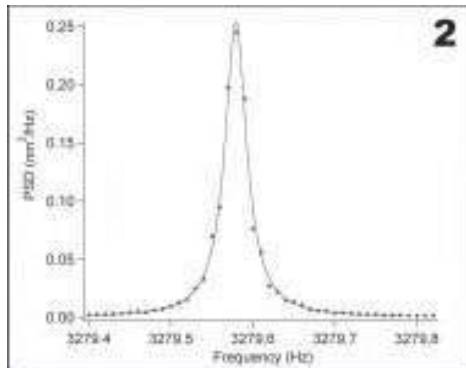


Figure 2: Vibrational spectrum of the fabricated cantilever at $T = 300$ mK.

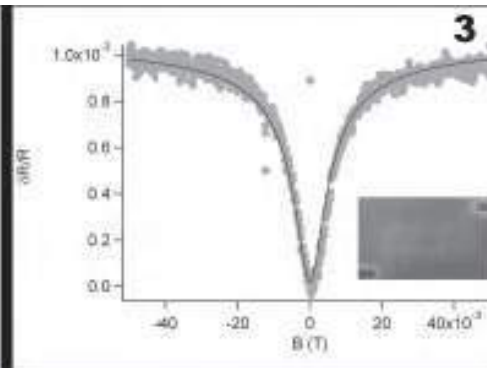


Figure 3: Resistance measurement of the meander (shown in the inset) showing weak localization.

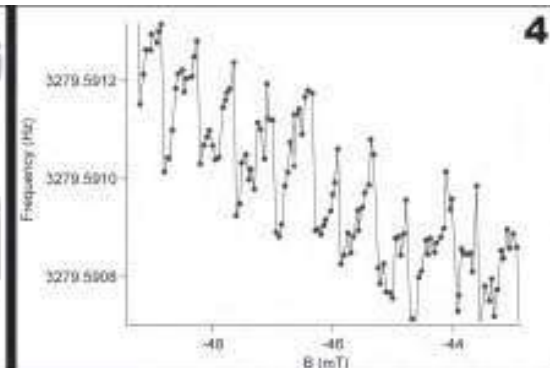
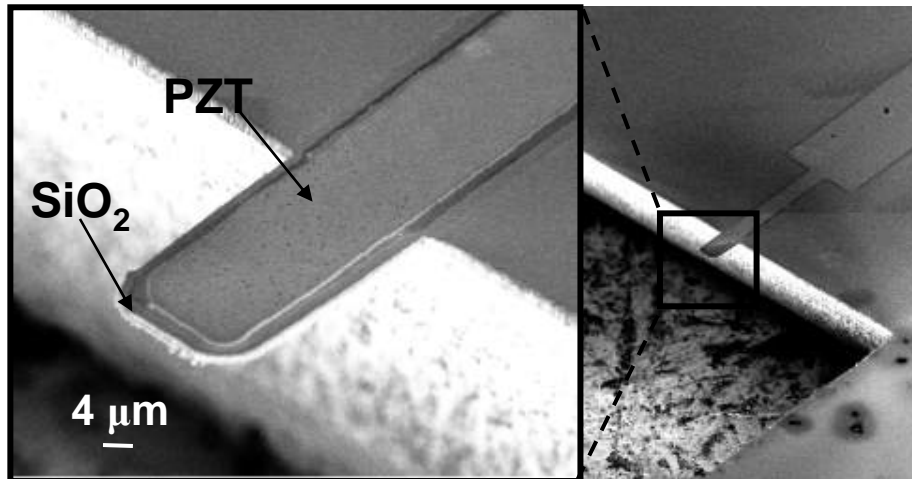
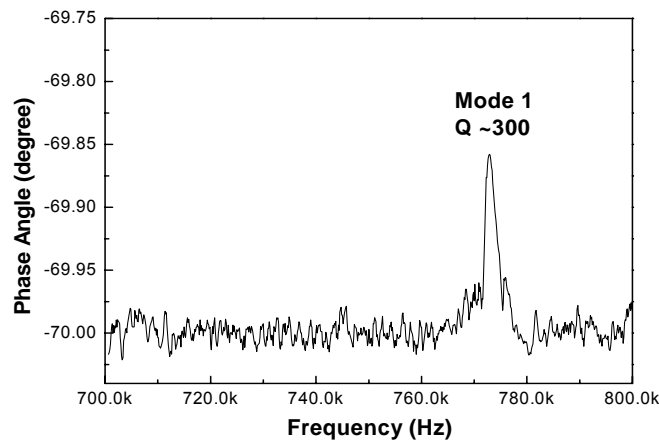


Figure 4: Cantilever's resonant frequency showing sawtooth oscillations due to flux quantization in the Al ring at the cantilever's end.

Piezoelectric Microcantilever Sensor



The piezoelectric micro-cantilever sensor (PEMS) consists of a piezoelectric layer, lead zirconium titanium (PZT), and a non-piezoelectric layer, SiO₂. The device can self-excite and self detect mechanical resonance electrically for various sensing applications.



Spectrum of 40 μm long PZT/SiO₂ micro-cantilever

The 40 μm long PEMS demonstrated 6×10^{-16} g/Hz mass detection sensitivity for humidity detection¹. It is the smallest and most sensitive PZT based PEMS in the world so far.

¹Zuyan Shen, Wan Y. Shih, and Wei-Heng Shih, *Applied Physics Letter* 89, 023506 (2006).

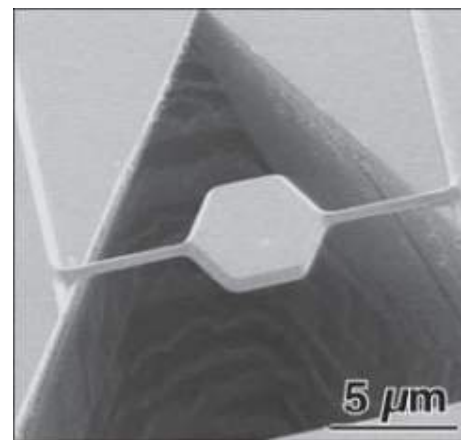
Z. Shen, W. Y. Shih and W-H Shih, Drexel University
Work performed at Penn State

Chip-based piezoelectric cantilevers for self-excite and detect with high mass detection sensitivity

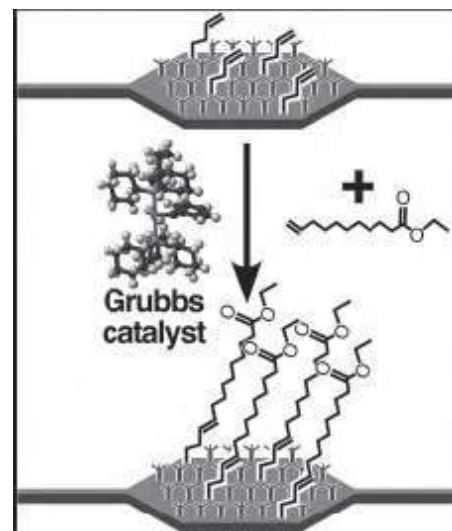
Functionalized Micromechanical Resonators with High Quality Factors

The dissipation of mechanical energy in 250-nm-thick, megahertz (MHz)-range silicon resonators is found to be strongly dependent on the chemical nature of the surface. By changing a single monolayer of molecules on the surface of a 250-nm-thick silicon resonator—less than 0.07% of the total mass—the quality factor of the resonator can be improved dramatically. In contrast, the standard commercial coating, a thin layer of silicon oxide, dissipates at least 75% of the mechanical energy in similarly sized resonators. This result shows that chemical control down to the monolayer level will be necessary for the production of high-performance nanomechanical sensors.

In related work, a robust platform chemistry for the production of high quality resonators with essentially arbitrary organic functionality has been developed. This process uses Grignard reagents to produce a partially alkene-coated surface followed by a catalyzed olefin methathesis reaction that attaches the desired functionality to the surface alkenes. This strategy is sketched in the accompanying figure. As proof of concept, ester-functionalized resonators with quality factors near those of our best performing surface coatings have been produced.



MHz-range resonator fabricated from Si(111) wafer and suspended by 450-nm-wide silicon wires.

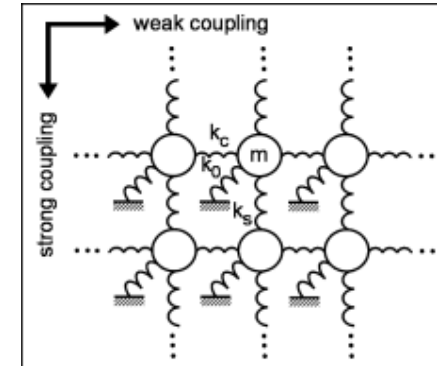


Strategy for the production of high-Q functionalized resonators.

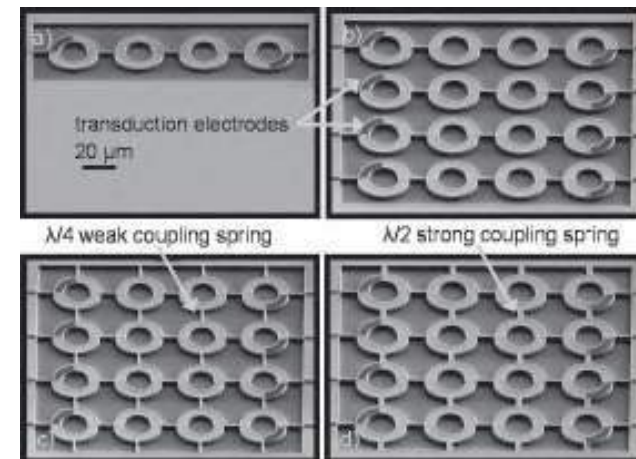
Mechanical Coupling of 2D Resonator Arrays for MEMS Filter Applications

Though two-pole filters currently dominate radio frequency microelectromechanical systems (RF MEMS) filter research, there is an impetus this to extend to multi-pole filters. In this study, four resonator coupling configurations were investigated to determine the effectiveness of the 2D strongly coupled array filter. We constructed a 1D 4-pole filter as a basis of comparison for all 2D filters in the study.

A robust coupling design for 2D array filters, comprised of weak coupling in one dimension and strong coupling in the second, is demonstrated experimentally and compared with weakly coupled and electrically summed 2D resonator array filters. Effects of inherent disorder in resonator arrays due to fabrication variations are minimized in this mechanical coupling scheme, averaging over resonator mismatch to form a smooth pass-band. The strongly-coupled 2D filter improves insertion loss and ripple without degradation in filter shape factor or stop-band rejection relative to its 1D counterpart. The filters are composed of extensional wine glass ring resonators with a fundamental resonance designed for 500 megahertz (MHz). The resonators are fabricated in a simple silicon-on-insulator (SOI) process and are driven and sensed with lateral dielectric transduction.



2D mechanical coupling configuration under investigation to reduce effective resonator variations. Here, the coupling stiffness $kC \ll kS$



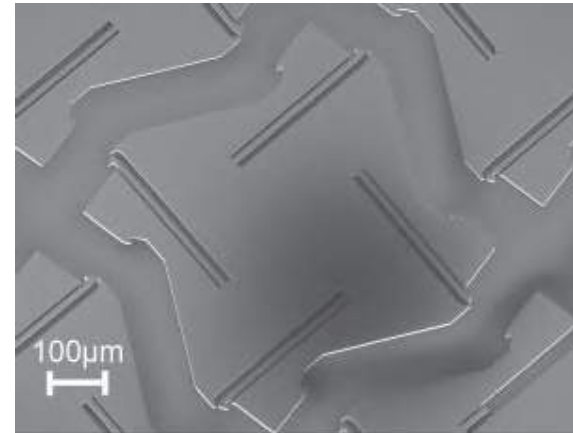
Scanning electron micrographs of: (a) a 1D 4-pole filter, (b) four electrically summed 1D 4-pole filters, (c) a 4×4 array of resonators, coupled weakly in both directions, and (d) a 4×4 array of resonators, coupled weakly in one direction and strongly in the other.

Directed Fluidic Assembly of Microscale Tiles

The aim of this project is to direct the assembly of micrometer-scale units (microtiles) into programmable, reconfigurable structures. In order to manufacture increasingly integrated devices with incompatible component fabrication processes, reliable micro-/nano-assembly techniques are required. As size scales decrease, however, traditional pick-and-place assembly with motion planning becomes increasingly intractable.

An alternative approach to assemble arbitrarily-shaped microstructures from regular components on the micro scale has been developed and tested. The difficulties of pick-and-place microassembly are circumvented by manipulating the components indirectly in a microfluidic chamber and relying on passive alignment and latching mechanisms to complete the assembly. This new microassembly approach could form the basis for an alternative microfabrication paradigm and the manufacture of complex, integrated microsystems.

D. Erickson, Cornell University
Work performed at Cornell Nanoscale Facility



Solid $500 \times 500 \times 30 \mu\text{m}$ silicon tiles with patterned sides for self-alignment and passive latches for assembly

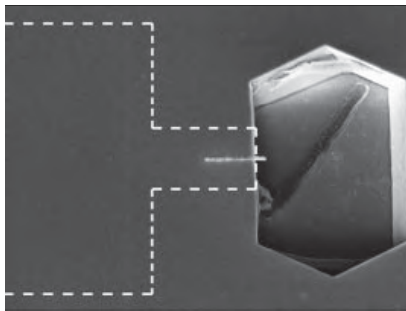


Microfluidic assembly of three tiles

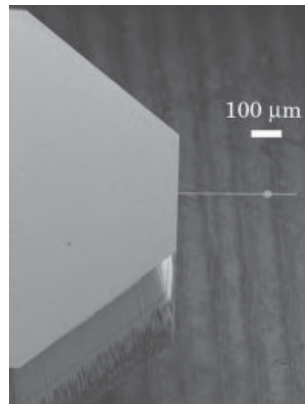
Ultrasensitive, Magnet-Tipped Cantilevers for Magnetic Resonance Force Microscopy

Magnetic resonance force microscopy (MRFM) is a developing technology in the family of force microscopy techniques. MRFM detects magnetic resonance as a force on a magnet-tipped micro-cantilever facilitating three-dimensional, chemically specific subsurface imaging at the nanoscale. If sufficiently high sensitivities can be reached, this technique could achieve atomic scale magnetic resonance imaging, and could be used, for example, to read out the structure of large biomolecules or to study buried semiconductor interfaces. An essential step in achieving the required sensitivity is the development of high sensitivity cantilevers with nanoscale magnetic tips. This project focuses on creating 50-200 nm wide cobalt magnets which extend from the tips of 5 μm wide silicon cantilevers.

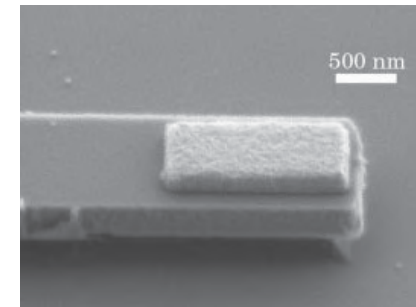
The purpose for creating overhanging nanoscale magnets is to maximize the force exerted on the cantilever by each magnetic spin, while minimizing noise in the force signal that arises from non-contact frictional forces between the cantilever and the sample. To achieve single-spin sensitivity, the front of the magnet must be within a few nanometers of the sample.



50 x 50 x 1000 nm overhanging Co magnet on a test structure.



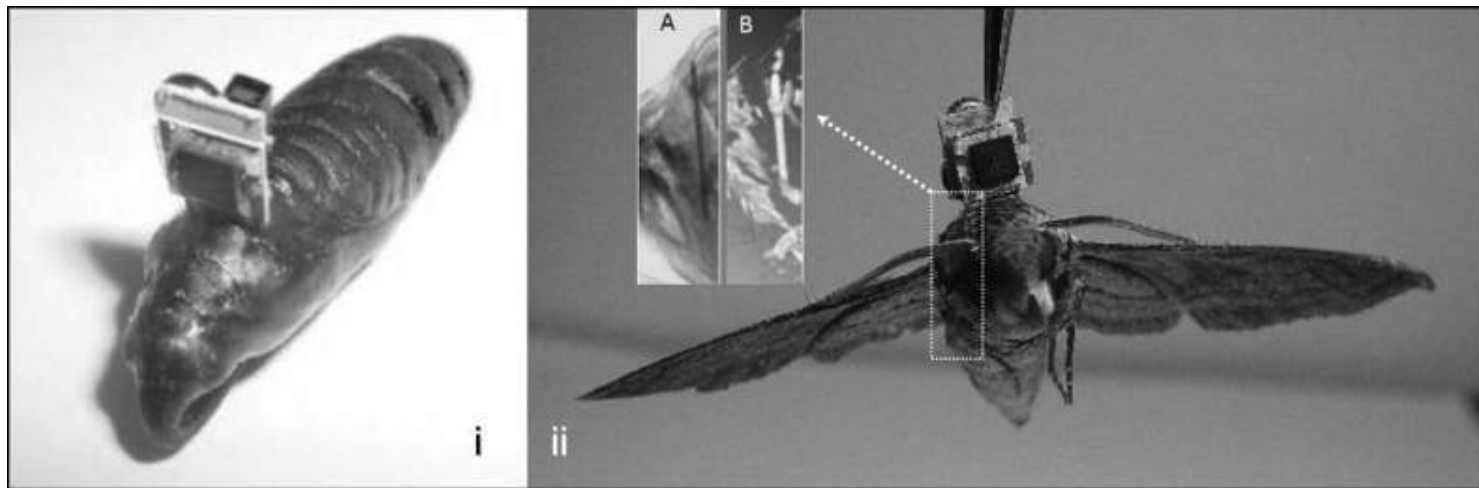
Entire cantilever and portion of base.



Close-up of cantilever tip with non-overhanging, 600 nm wide Co magnet.

MEMS-Based Interface for Insect Cyborg Control

This research demonstrated a reliable hybrid tissue-electronics interface in insects, by using silicon probes and inserting them at an early pupae stage so that the tissue grows around the probes for a highly natural implant in the insect. This work paves the way for future engineering approaches to utilize the bioelectronic interfaces and to create insect cyborgs. Preliminary flight control results indicate left and right wing control of *Manduca sexta* and full-flight control is under investigation. The insertion methodology developed here has an emergence success of 90% with our implantations. This hybrid structure enables a platform where CMOS devices and MEMS structures can be used as sensors and actuators not only for insect flight control but also for biological and environmental sensing.



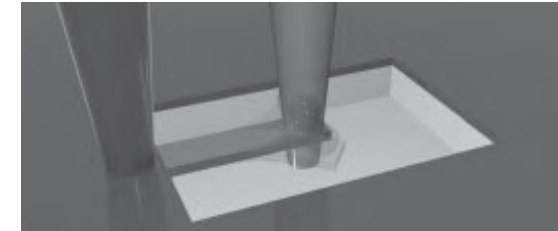
Probe microsystem inserted during pupal stage

Emerged successfully

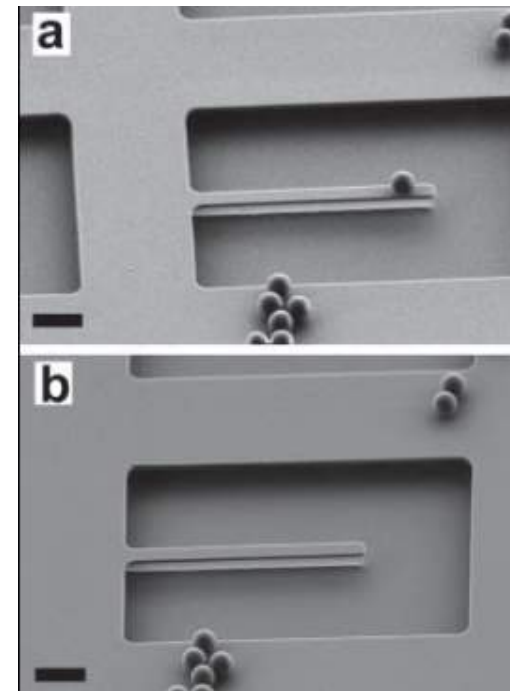
A. Lal, Cornell University
Work performed at Cornell NanoScale Facility

Manipulation of Microspheres with Optically Excited NEMS Oscillators

This work demonstrates that optical fields are extremely efficient for excitation, direct control and measurement of in-plane motion of cantilever-type nanomechanical oscillators. Using silicon cantilevers, the quality factor, Q , of a particular in-plane harmonic was consistently found to be higher than the transverse mode. The increased dissipation of the out of plane mode was attributed to material and acoustic loss mechanisms. The in-plane mode was used to demonstrate vibrational detachment of sub-micron polystyrene spheres on the oscillator surface. In contrast, the out of plane motion, even in the strong non-linear impact regime, was insufficient for the removal of bound polystyrene spheres. Our results suggest that optical excitation of in-plane mechanical modes provide a unique mechanism for controlled removal of particles bound on the surface of nanomechanical oscillators.



Schematic of optical excitation setup

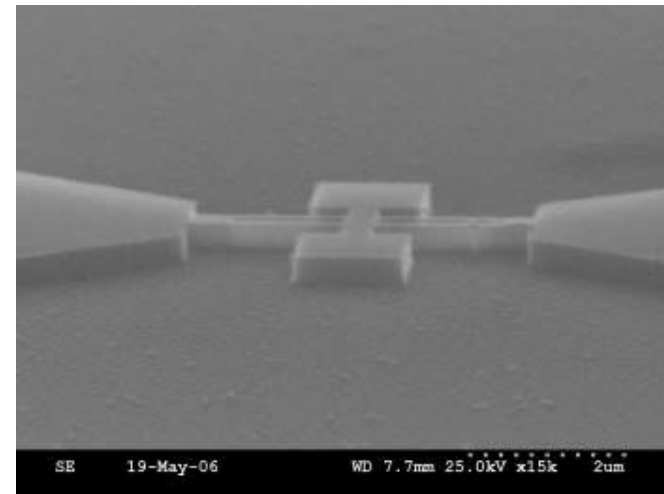
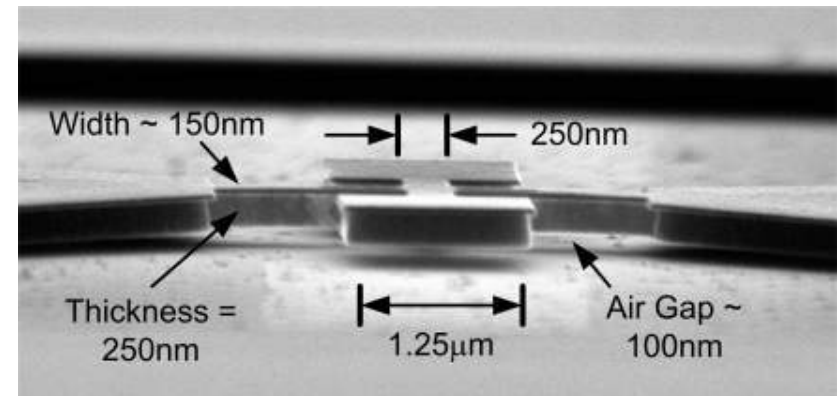


SEM of cantilever (a) with a sphere and (b) following its removal.

H. Craighead, Cornell University
Work performed at Cornell NanoScale Facility

High Frequency Inertial Instruments

- Objective
 - ◆ Develop arrays of nanomechanical structures to perform spectral analysis of ultrasonic signals
- Significance of MiRC
 - ◆ This work requires the lithographic precision of the JEOL Electron Beam Lithography system. The rest of the device processing is performed in partnership with the cleanroom at the U.S. Army AMRDEC facility in Huntsville, AL

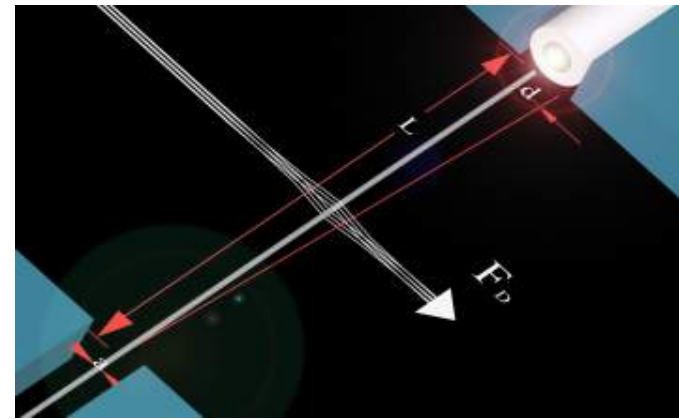


M. Kranz, Ga Tech
Work performed at Ga Tech

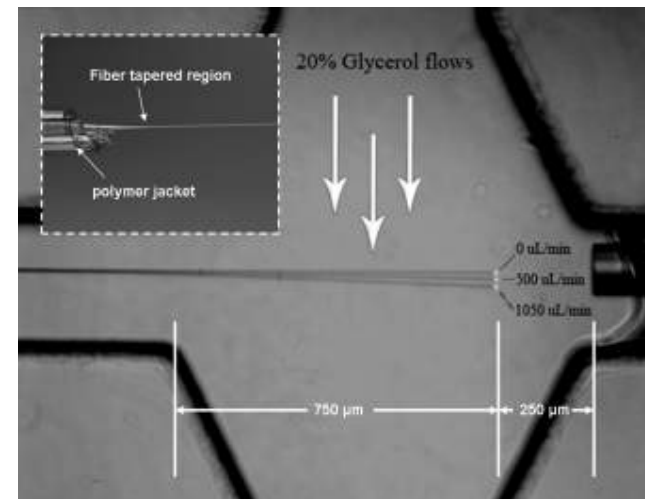
Cantilever-based integrated microfluidic flow sensor

Fiber cantilever fabricated by etching single mode fiber to a diameter of 9 micrometers. Channel made of PDMS using soft lithography. PDMS structure containing microfluidic channel bonded to glass substrate using oxygen plasma treatment forming permanently sealed channel-network.

F. Vollmer, Rowland Institute of Harvard University
Work performed at Harvard University

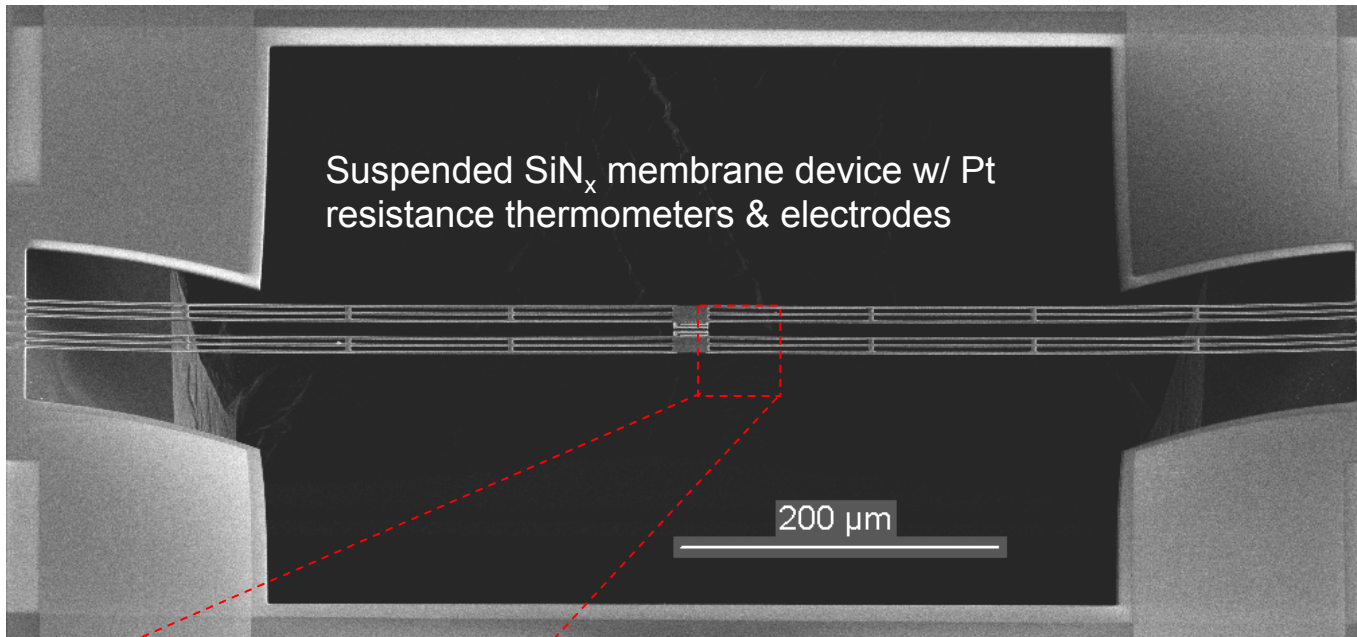


Illustration

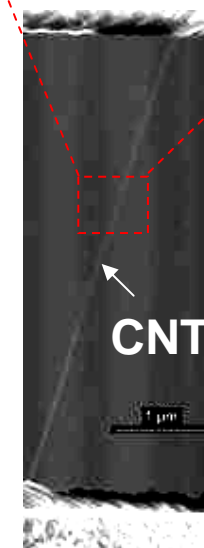
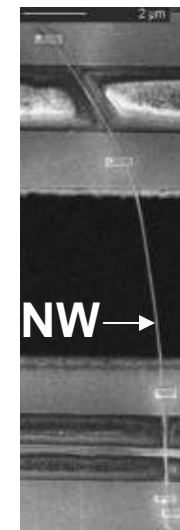
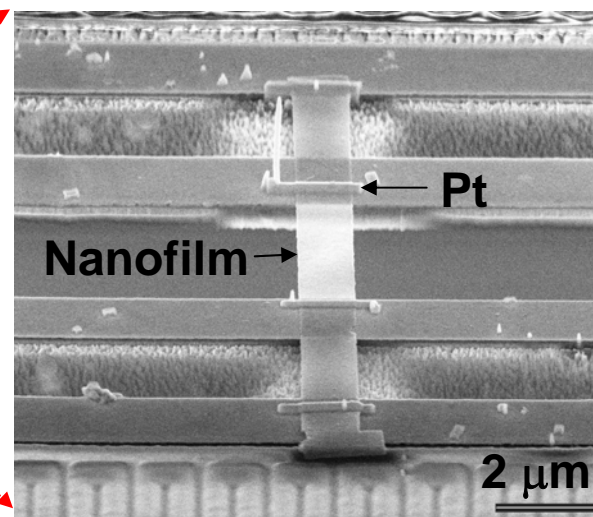
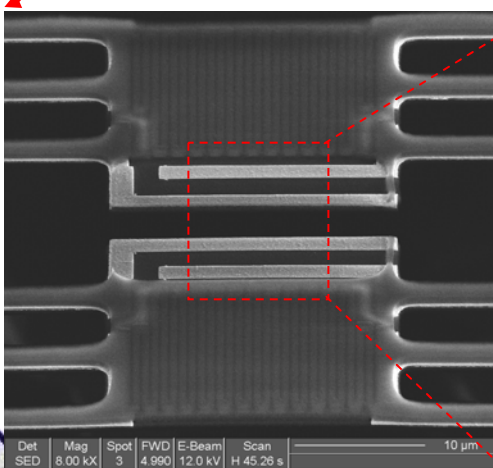
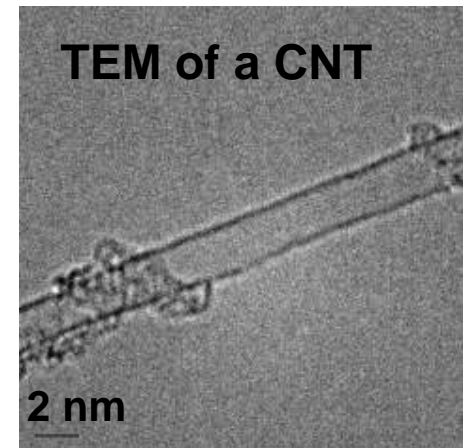


Micrograph

Microdevice for Individual Nanostructure Measurements

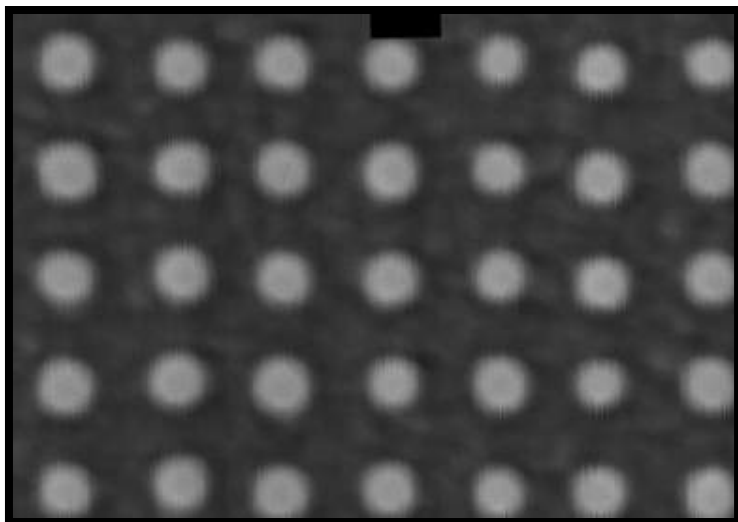


L. Shi, U. Texas
Work performed at U Texas



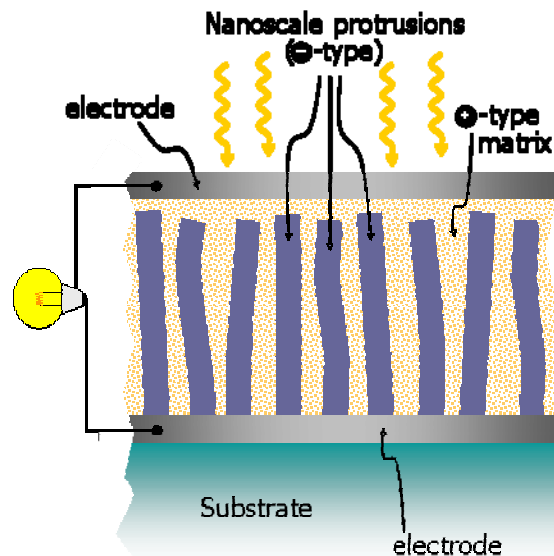
Nanophysics

Lateral Collection Nanostructured Solar Cell



Scanning electron microscope image (top view) of nanostructured solar cell fabricated at the PSU NNIN site. An illustration of the device cross-section and operation is shown (right).

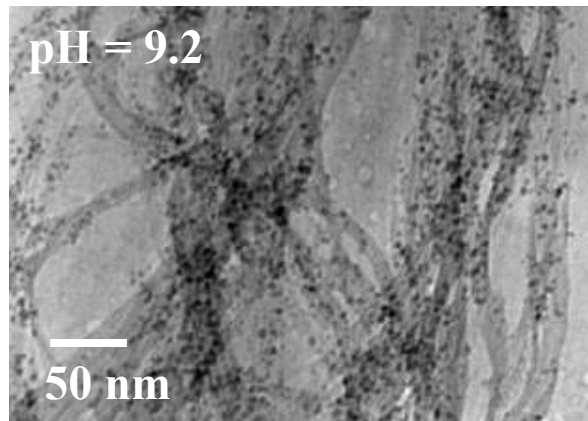
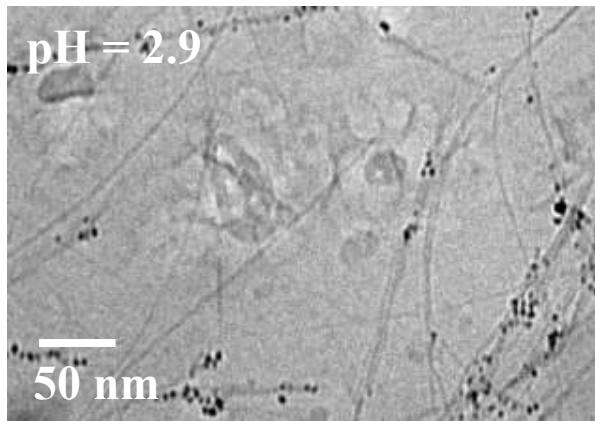
In a joint venture, Solarity *Inc.* and NanoHorizons are developing a prototype of lateral collection solar cell based on infiltration of nanoscale protrusions that will yield high performance at low cost.



H. Li and D. Stone, Solarity Inc and NanoHorizons
Work performed at Penn State

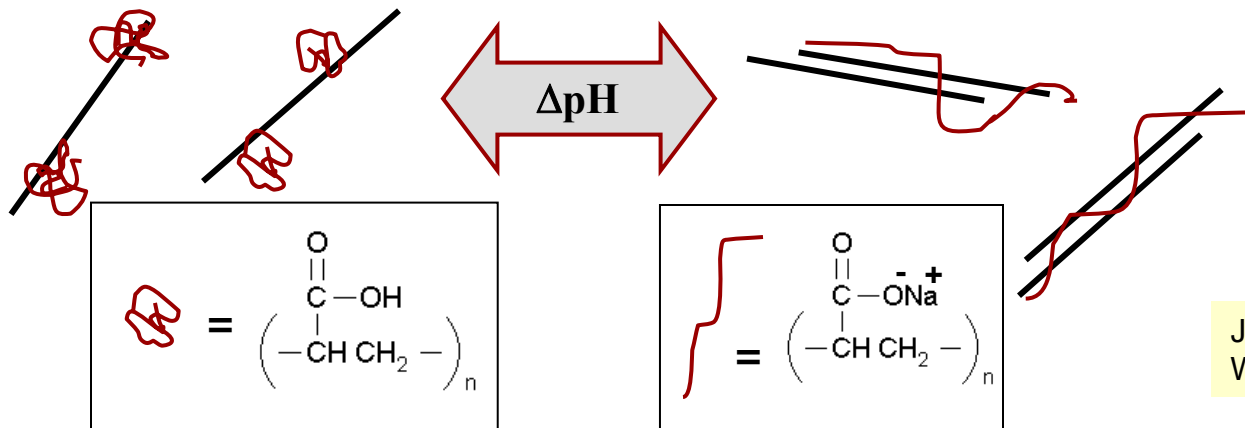
PSU NNIN site being used to develop prototype nanostructured lateral collection solar cell

Tailoring Nanotube Dispersion Using Poly(acrylic acid)



Dispersion of single-walled carbon nanotubes (SWNT) in water with PAA allows precise tailoring of the nanoparticle dispersion state as a function of pH, ranging from highly dispersed at low pH to highly aggregated at high pH. These micro-structural variations alter aqueous suspension viscosity and dry nanocomposite properties such as electrical conductivity. This work is expected to lead to new classes of lightweight engineering composites for applications like antenna substrates; sensing and actuation transducers; and flexible microelectronics.

J. C. Grunlan, Texas A&M University
Work performed at U. of Minnesota

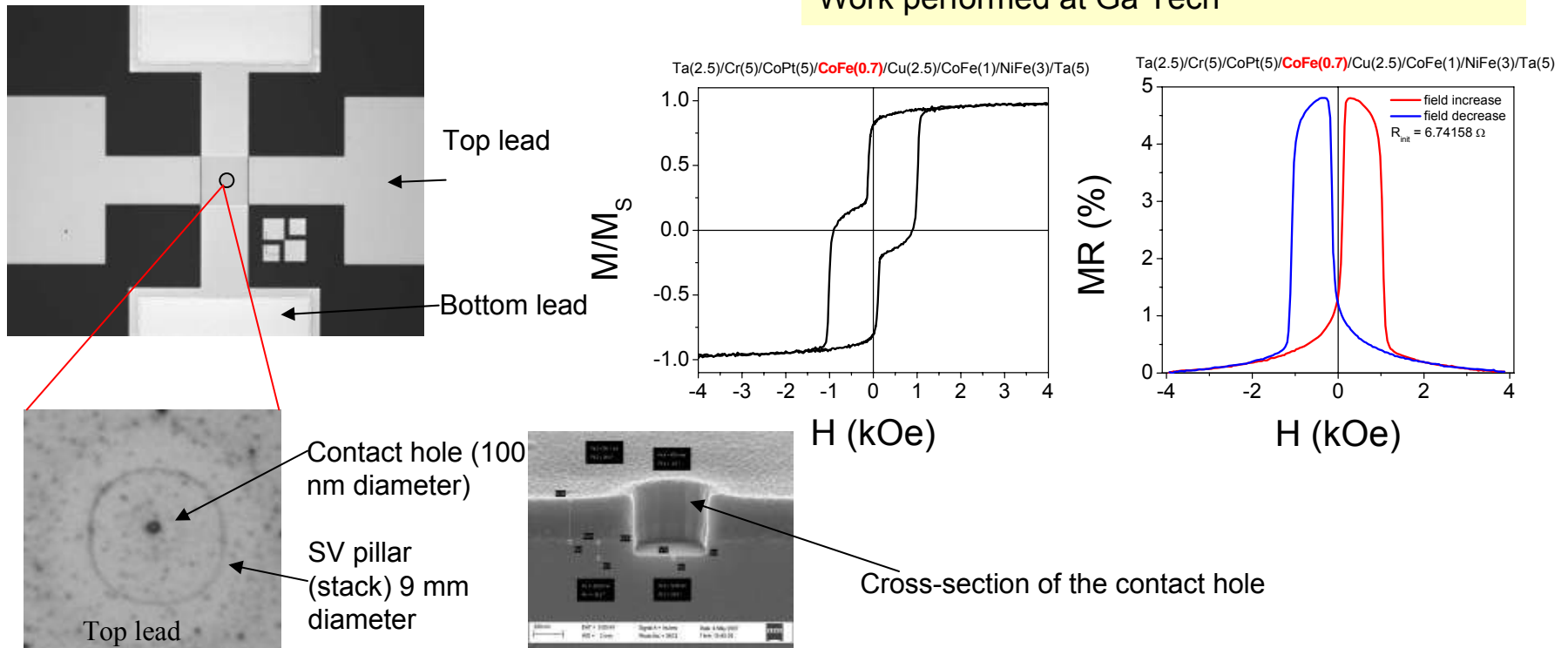


Materials currently being made with carbon nanotubes and other useful nanoparticles are limited by a lack of microstructural control (i.e., how the particles are dispersed/organized within the material). We have recently discovered a way to overcome this challenge using poly(acrylic acid) [PAA], whose molecular shape changes with pH.

Grunlan, J. C.; Liu, L.; Regev, O. *J. Coll. Interf. Sci.* **2007**, 316, in press (available online).

Fabrication of GMR Spin Valve Sensors

C.Papusoi, S.Gupta, Z.Tadisina, U of Alabama
Work performed at Ga Tech



The Current Perpendicular to the Plane (CPP) geometry, when the current is flowing perpendicular to the film plane, is expected to deliver the maximum sensitivity (GMR ratio). The challenge is to increase the output signal by creating a Current Confined Path (CCP) within the magnetic stack. The goal is to reduce the contact area between the top electrical lead and the magnetic stack through an insulating layer.

Regular Ag Nanorod Arrays as a Uniform and Reproducible Substrate for Surface enhanced Raman Spectroscopy

Objective

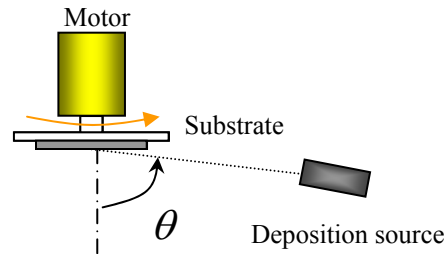
Combining nanolithography techniques and oblique angle deposition technique to produce uniform and reproducible SERS substrates.

Method

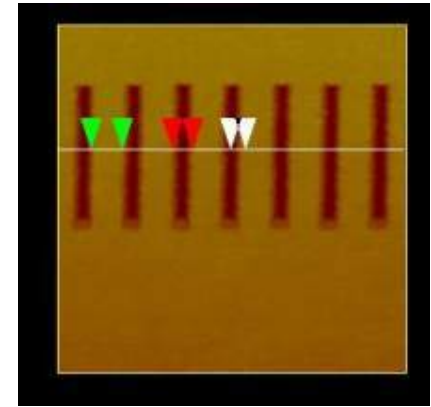
- (1) E-beam lithography to make regular nano-post array pattern on Si
- (2) Nanoimprinting to transfer the replica of the pattern to a substrate
- (3) Lift-off to fabricate Ag nano-post array
- (4) Oblique angle deposition to generate Ag nanorod array



Regular patterned array



Oblique angle deposition



Varying the dosage from $180\mu\text{C}/\text{cm}^2$ to $220\mu\text{C}/\text{cm}^2$, and obtain similar results from AFM. The nano-groove is about 120 nm.

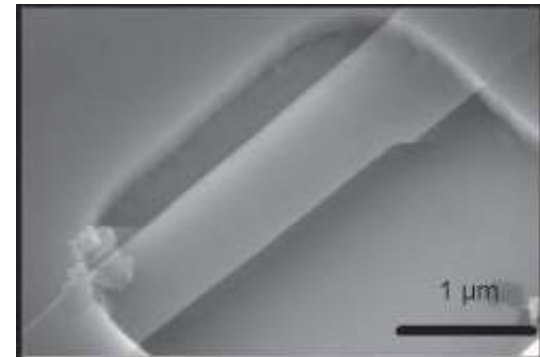


Regular nanorod array

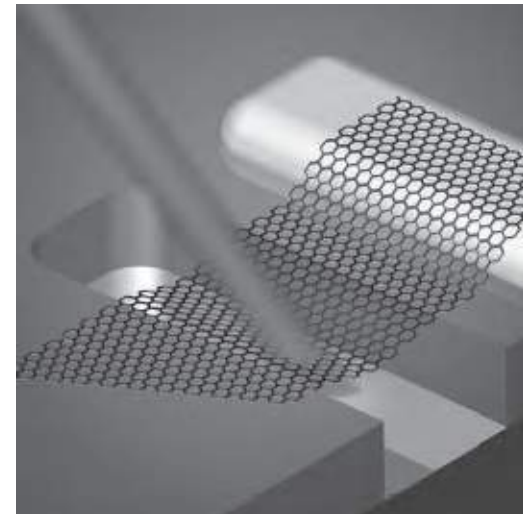
Y. Zhao, University of Georgia
Work Performed at Ga Tech

Electromechanical Resonators from Graphene Sheets

Nanoelectromechanical systems were fabricated from single and multilayer graphene sheets by mechanically exfoliating thin sheets from graphite over trenches in SiO_2 . Vibrations with fundamental resonant frequencies in the MHz range are actuated either optically or electrically and detected optically by interferometry. A Young's modulus of 1 TPa was measured. Most suspended sheets were under tension. The quality factors of the suspended graphene sheets are in the range of 20-850 and show no dependence on the thickness. ***The thinnest resonator consists of a single suspended layer of atoms and represents the ultimate limit of two dimensional nanoelectromechanical systems.*** The application of graphene NEMS extends far beyond just mechanical resonators. This robust, conducting, membrane can act as a nanoscale supporting structure or atomically thin membrane separating two disparate environments.



SEM image of suspended Graphene sheet.



Graphic of measurement technique.

D. Tannenbaum, Pomona College, P. McEuen, H. Craighead, J. Parpia, Cornell University
Work performed at Cornell Nanoscale Facility

Spin-Torque Excitations in Magnetic Nanopillars with an Exchange-Biased Fixed Layer

When current passes perpendicularly through the layers of a spin-valve structure (ferromagnet / metal / ferromagnet), electrons polarized by one magnetic layer (the “fixed layer”) can transfer their spin angular momenta to the other magnetic layer (the “free layer”) and hence exert a torque on the free layer. This effect provides a new way to manipulate small magnets by electrical current rather than magnetic field, and has potential applications in developing non-volatile magnetic memories.

Iridium manganese (IrMn) / permalloy (Py) / Cu / Py spin-valve nanopillars have been fabricated. Electron-beam lithography and ion milling are used to define pillars with elliptical cross sections having an aspect ratio $\sim 3:1$ and a short axis diameter between 30 nm and 100 nm.

These samples were used to measure the bias dependence of the spin transfer torque vector using spin-transfer-driven ferromagnetic resonance (ST-FMR), showing that the torque stays in the plane defined by the two magnetic moments in the bias range $|I| < 2$ mA. Resonant magnetic switching using the spin-transfer torque from microwave-frequency pulses was also studied.

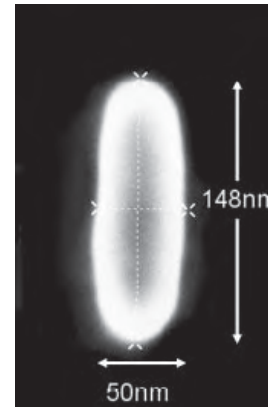


Figure 1: SEM image; cross section of the nanopillar device.

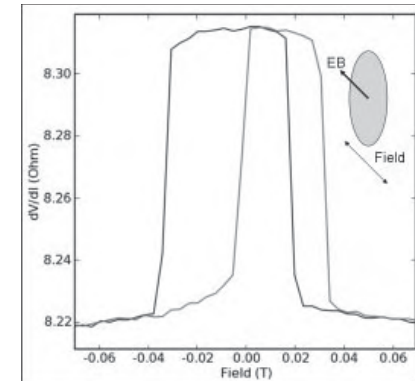


Figure 2: dV/dI vs. applied magnetic field, with a field along direction 45° from the easy axis.

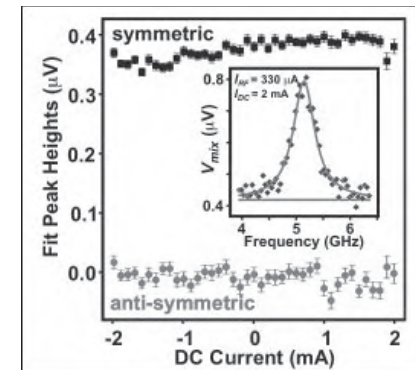
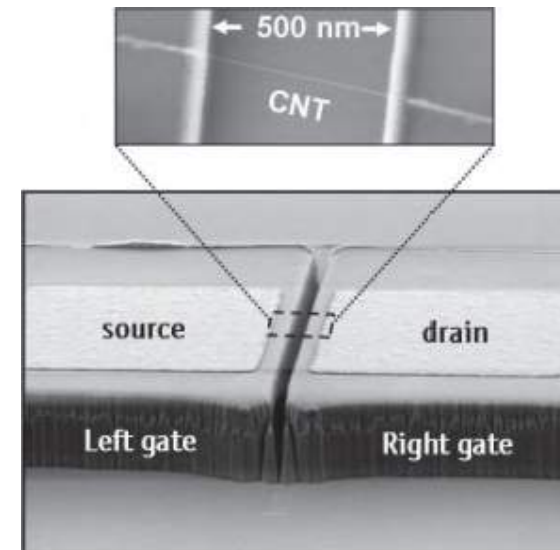


Figure 3: Bias dependence of the frequency-symmetric and antisymmetric components of ST-FMR resonance peak shape

Polarizability of Quantum-Dot States within a Suspended Carbon Nanotube

Single-electron-transistor devices made from an individual carbon nanotube suspended between two independent side gates have been fabricated. The nanotube acts as a clean quantum dot, isolated from the disordered substrate. By applying gate voltages, the dot can be populated controllably with any number of electrons, from zero to many tens. By applying different voltages to the two side gates, the electric polarizability of individual few-electron quantum states in a nanotube has been measured for the first time.

When measured at zero bias, the curvature of the n th Coulomb oscillation is a measure of the electric polarizability of the n th electron ground state. Unlike single particle levels in a harmonic potential (which all shift in space by an equal amount when applying a constant electric field), the energy levels in our quantum dot are less polarizable if other electrons are present on the dot. This indicates the importance of electron-electron interactions in suspended carbon nanotubes, and that screening takes place despite the one-dimensional confinement.



Schematic of a carbon nanotube single electron transistor. The nanotube is suspended between two independent, isolated gate electrodes spaced 500 nm apart, and contacted by source and drain electrodes.

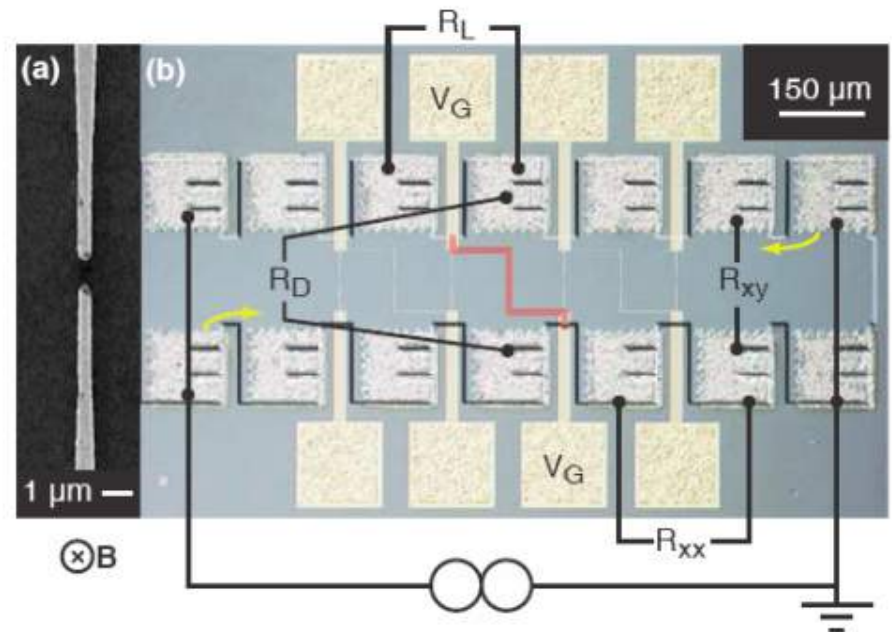
P. McEuen & D. Ralph, Cornell.
Work performed at CNF

Fractional quantum Hall effect in a quantum point contact at filling fraction 5/2

We study the transport properties of quantum point contacts (qpc) fabricated on a GaAs/AlGaAs two dimensional electron gas that exhibits well-developed fractional quantum Hall effect

We find that a plateau at effective filling factor $QPC = 5/2$ is identifiable in point contacts with lithographic widths of $1.2 \mu\text{m}$ and $0.8 \mu\text{m}$, but not $0.5 \mu\text{m}$.

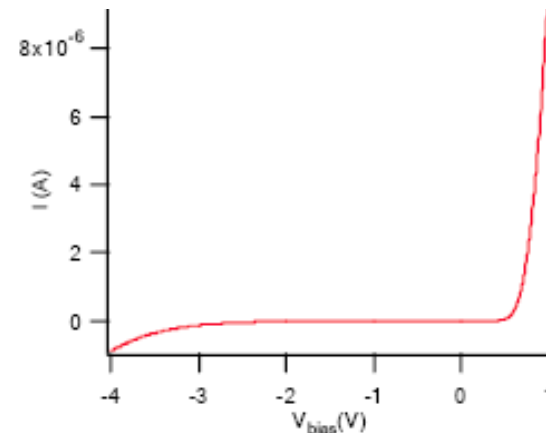
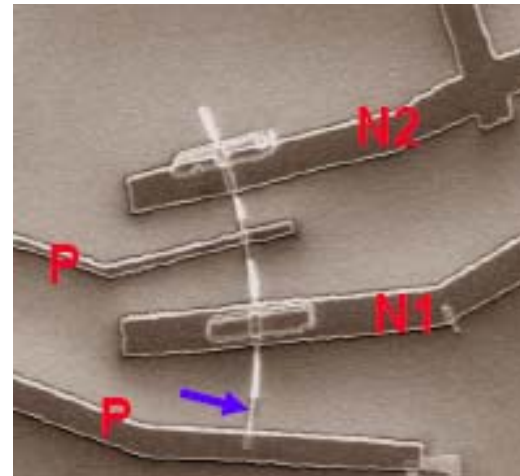
C. Marcus, Harvard University
Work performed at Harvard University



SEM micrograph of the $0.5 \mu\text{m}$ qpc (the outline of the wet-etched Hall bar has been enhanced for clarity).

Design of Small *p-i-n* Radial Core/Shell Nanowire Structures

The nanowires consist of a single-crystalline *p*-Si nanowire core and controlled thickness, conformal *i*- and *n*-shells. Scanning and transmission electron microscopy analyses demonstrate that the two shells are uniform but polycrystalline with thicknesses determined growth time. These new *p-i-n* nanowire structures open up unique opportunities as building blocks for the creation of novel photovoltaics and integrated electronic logic gates.

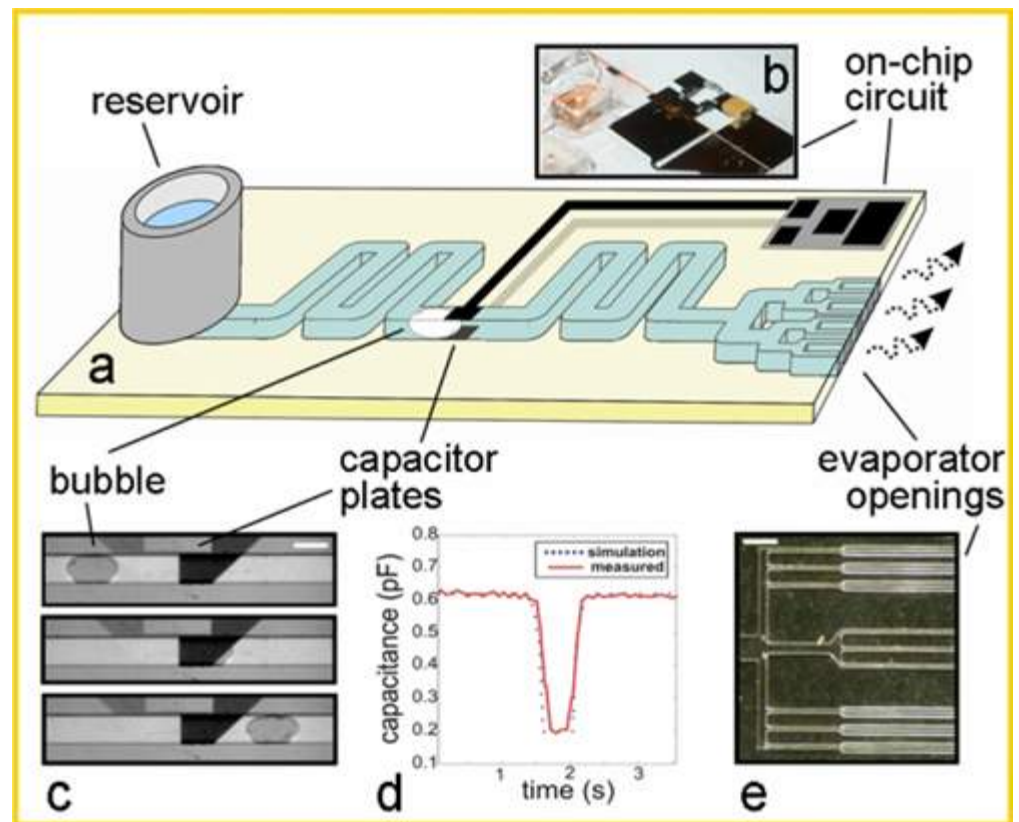


C. Lieber, Harvard University
Work performed at Harvard University

Scavenging Power: A leaf-Inspired Charge Pump Scavenger

Plants routinely pump water hundreds of feet into the air without active pumping. Can we design a 'synthetic leaf' with an electrical energy scavenger?

In this device, evaporation-induced flows within leaf-like microvasculature networks drive the movement of gas bubbles through capacitor plates (right). The alternating dielectric of gas and liquid allows the charge pumping of an on-chip circuit (Figure 1b), from which voltage and current are used to provide electrical power. This method of power scavenging has unique properties: (1) volumetric power density is high and scales favorably with miniaturization of evaporative feature sizes, (2) devices are robust and easy to fabricate, and (3) any humidity gradient can provide energy.



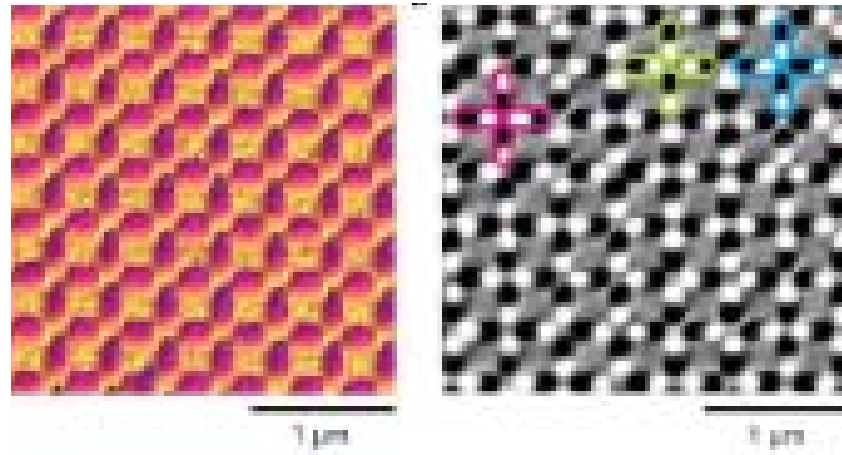
M. Maharbiz, University of Michigan
Work performed at Michigan Nanofabrication Facility

Artificial 'Spin Ice'

N. Samarth, C. Leighton, V. H. Crespi, and P. Schiffer, Penn State University and University of Minnesota
Work performed at Penn State



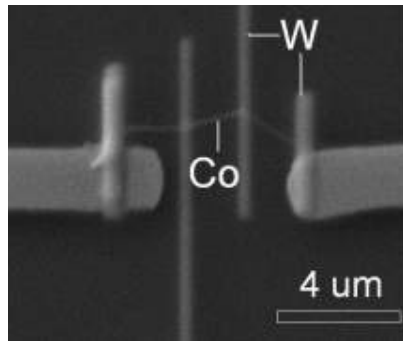
Nature 439, 2006



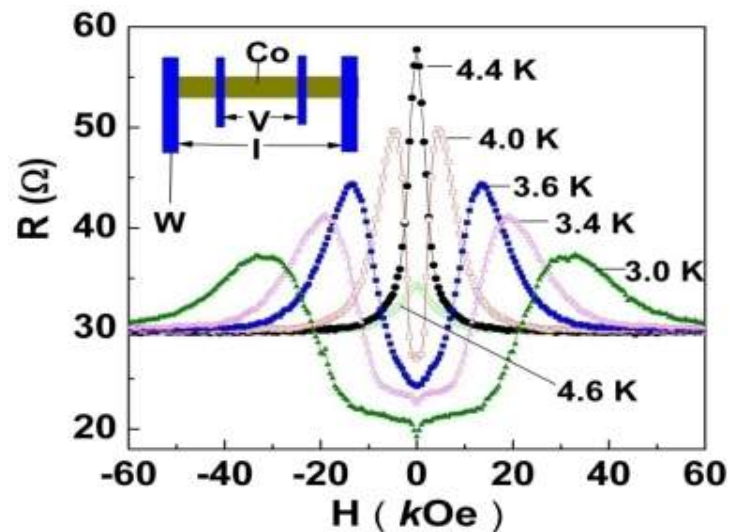
AFM (left) and MFM (right) of permalloy array with lattice spacing of 400 nm showing single-domain ferromagnetic character of islands and distribution of lattice moments

Lattice of nanoscale ferromagnetic islands can be used to study the physics of frustration

Long-range proximity effect of Co nanowires with FIB deposited superconducting W-electrodes



SEM image of four-terminal probe on single-crystal Co nanowire by FIB technique. W is superconducting at 4.8 K.



R v.s. H at different temperatures. The peak corresponds to the H_c of W electrodes.

Superconductivity (S) and ferromagnetism (F) require long range ordering with different spin alignments. When a superconductor is in contact with a ferromagnetic material, the S-wave superconducting order parameter is expected to decay rapidly to zero within a few nanometers inside the ferromagnet. We made four-terminal transport measurements on an individual single-crystal Co nanowire with superconducting tungsten electrodes deposited by FIB. The low temperature resistance (R) has two sharp peaks near the critical field $\pm H_c$ of W and a very substantial (40%) drop in R at low field. Only one sharp peak in R near $H=0$ kOe is observed below 4.8K. These data indicate that superconducting electron pairs survive over a length scale of at least 500 nm.

M. Chan, Penn State University
Work performed at Penn State

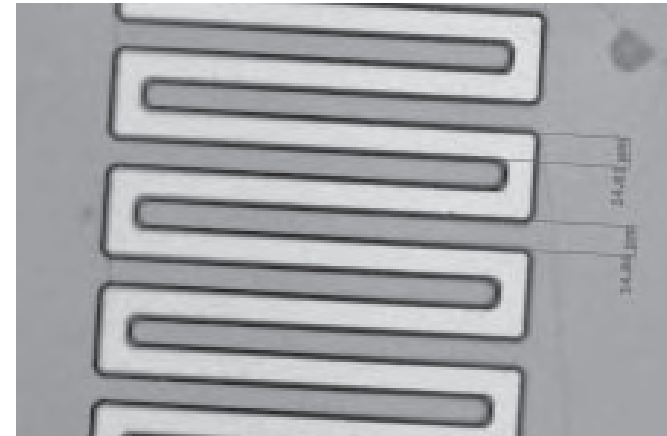
Four terminal electrical transport measurements on individual crystalline Co nanowire shows long range proximity effect

Chemistry

Microfabrication of Flexible Sensing Arrays

The goal of the Center of Advanced Microelectronic Manufacturing (CAMM) is to develop tooling and processes to use unsupported flexible polymeric substrates. Researchers at CAMM have fabricated gold microelectrode devices on glass substrates to explore the use of thin film coatings of monolayer-capped nanoparticles for chemical sensors (volatile organic compound sensing), medical diagnostics and other microelectronic applications. Here we attempt to fabricate copper microelectrode devices using unsupported poly(ethyleneterephthalate) (PET) substrates for use in low-cost, disposable sensor applications.

This research demonstrates the feasibility of fabricating the flexible copper microelectrodes on flexible unsupported PET substrates using the microfabrication facilities at CNF. Parameters such as etchant concentration, etching time and temperature need to be further improved to prevent overetching the copper layer. PET substrate surface flatness will be improved by use of tooling and a more carefully controlled Cu sputtering process.

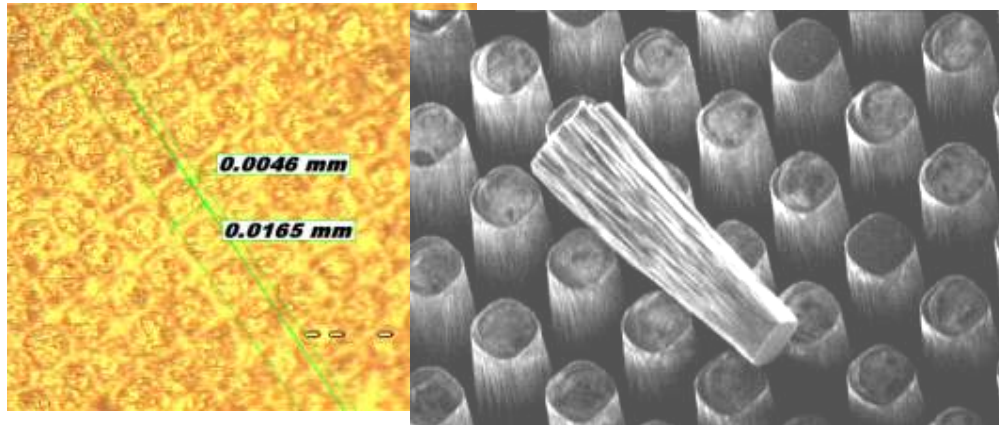


15/15 μm line/space resist features after development.

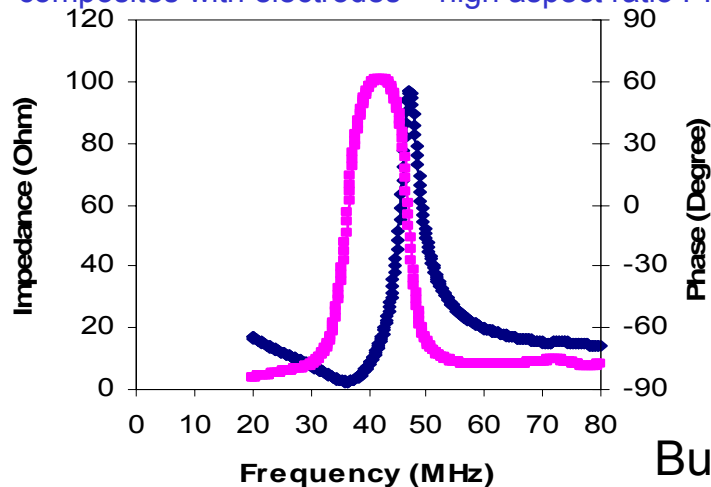


Flexible PET "mock-wafer" showing largest (1.5 mm) copper features of the microelectrodes patterns.

Micromachined Piezoelectrics for High Frequency Ultrasound



composites with electrodes high aspect ratio PMN-PT micro-posts



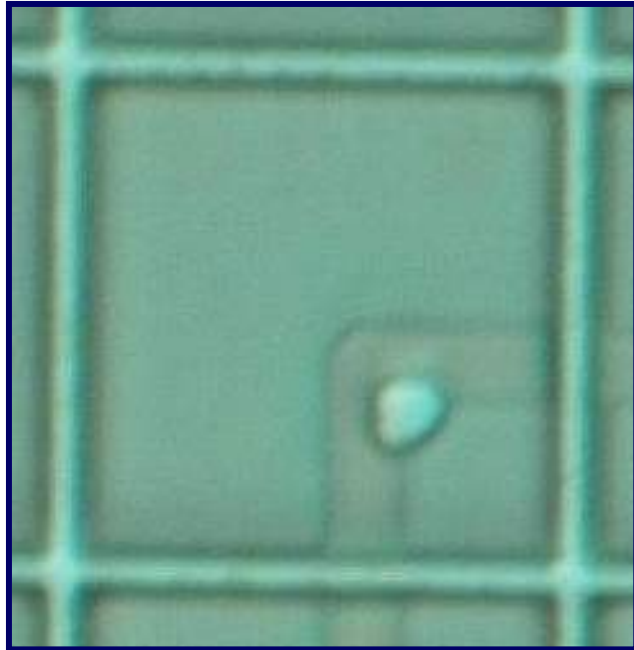
Impedance-phase spectrum of 40 MHz 1-3 composite transducer

High frequency (HF) ultrasound is used for medical imaging and industrial non-destructive evaluation (NDE) because of its high resolution. A deep reactive ion etching process was developed at the PSU NNIN site for micromachining bulk piezoelectrics to fabricate 2-2 and 1-3 PMN-PT single crystal/epoxy composites for HF ultrasound transducers. The electromechanical coupling coefficients of the micromachined composites are > 0.7 , and the frequency range is about 20-60 MHz. Transducers fabricated using these composites have unprecedented performance for IV ultrasound imaging.

X. Jiang and W. Hackenberger, TRS Technologies
Work performed at Penn State

Bulk ceramics are being micromachined into 2-2 and 1-3 composites for high resolution ultrasound

Pyroelectric Materials for Thermal Imaging



Optical microscope image of a $48 \mu\text{m}^2$ PZT infrared sensor element integrated on a silicon substrate



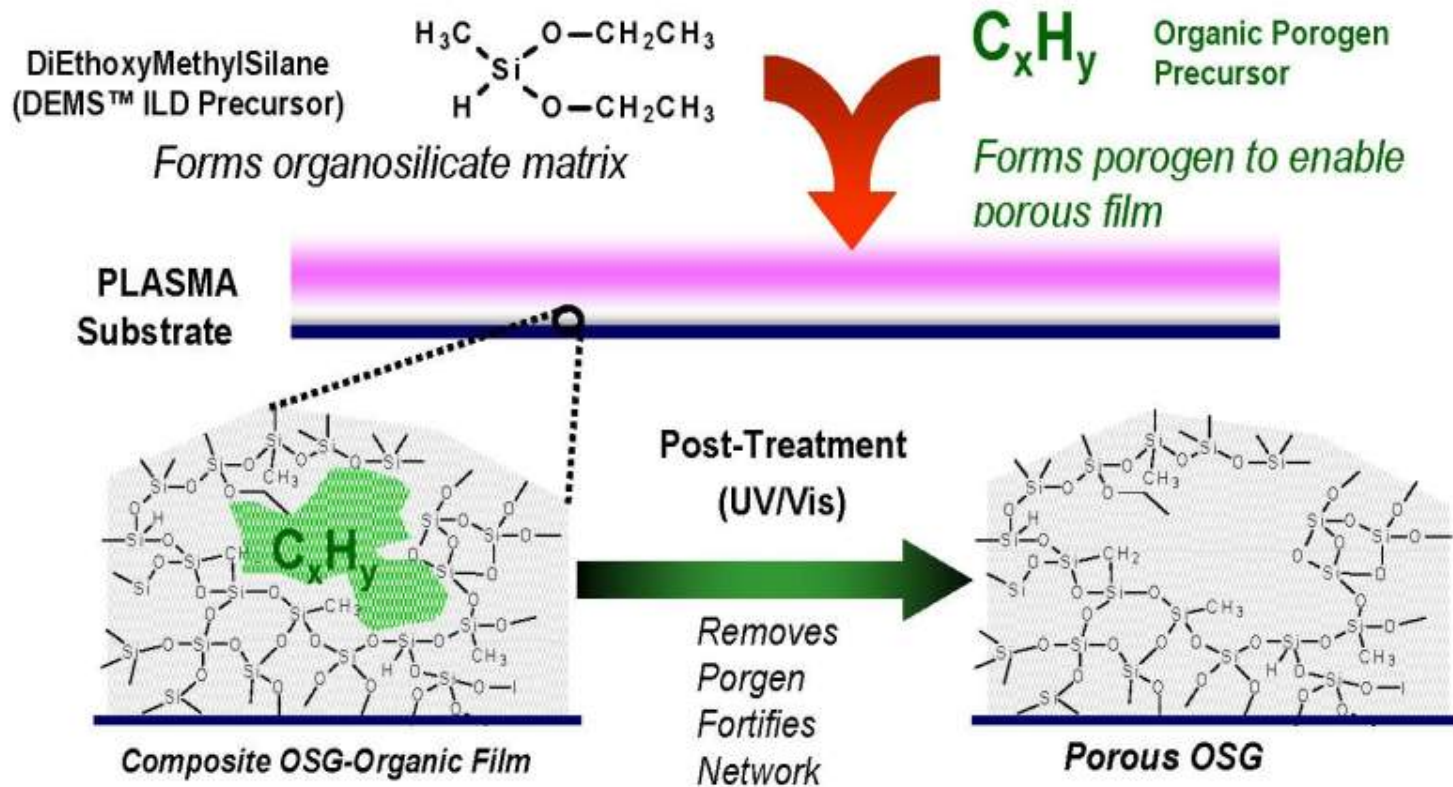
Prototype complex oxide based infrared sensor arrays are being fabricated using PZT materials and fabrication processes developed at the PSU NNIN site. The sensor arrays have been integrated into infrared cameras and show great promise for low-cost thermal imaging systems.

E. Hong and J. Richards, Bridge Semiconductor Corporation
Work performed at Penn State

Complex oxide PZT materials are being integrated into low-cost thermal imaging systems

Porous OSG Films by PECVD

PSU NNIN site used to deposit porous organosilicate films by plasma enhanced chemical vapor deposition using alternative precursors developed at Air Products



Results on this PDEMS™ ILD process included in an APCI presentation at the 2006 Advanced Metallization Conference

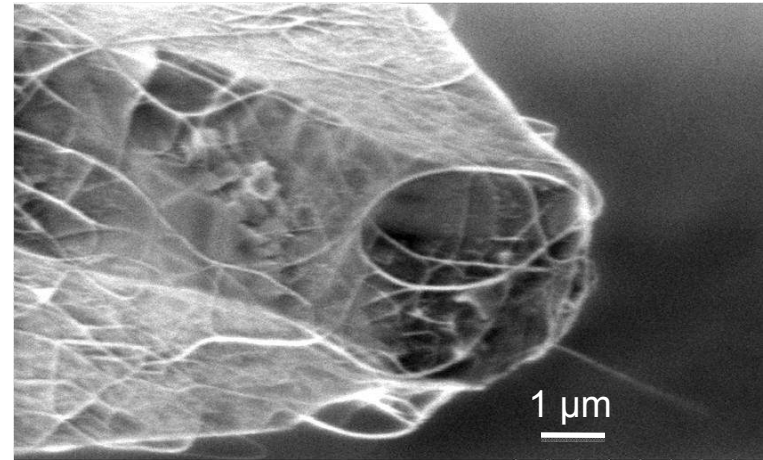
R. Vrtis, Air Products and Chemicals
Work performed at Penn State

New OSG films developed using PECVD with alternative liquid source precursors

Carbon Nanotube AFM Tip

Atomic Force Microscopy (AFM) has been a workhorse of nanoscale research and development. Because it not only allows imaging at the nanoscale, but also permits manipulation and physical interactions with samples, AFM could become an enabling tool in drug discovery if its resolution could be increased to allow rapid determination of protein structure in coordination with protein folding algorithms.

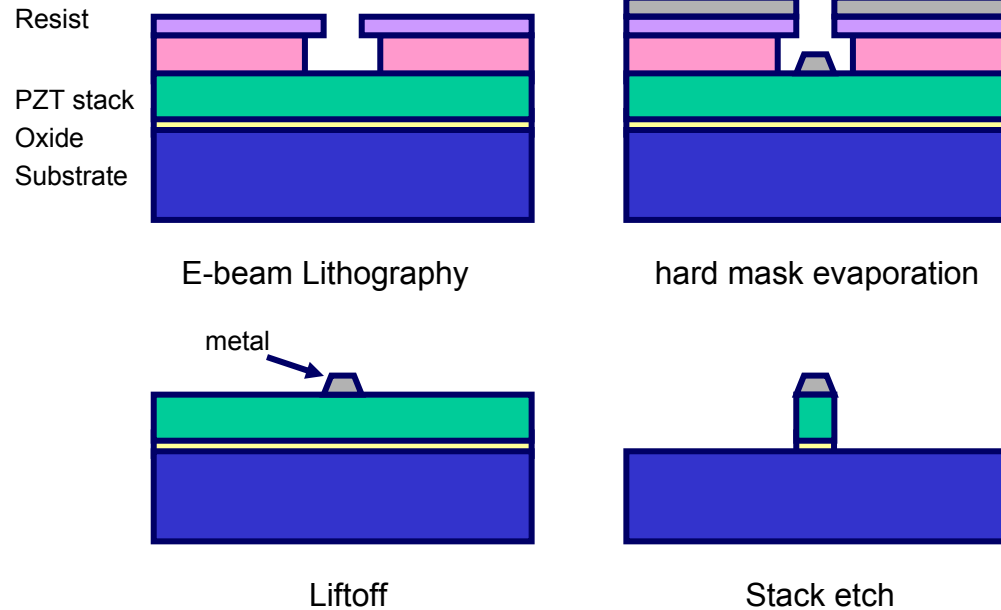
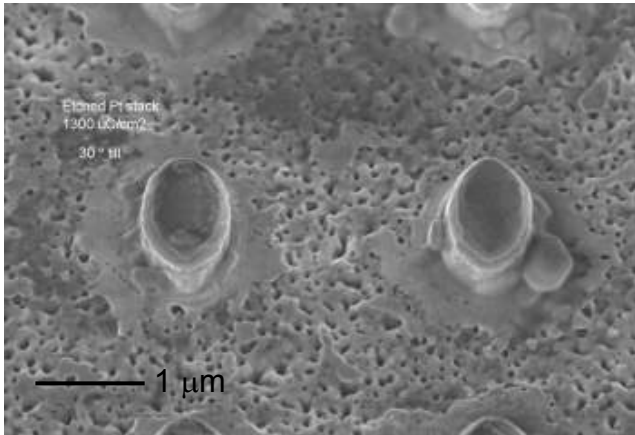
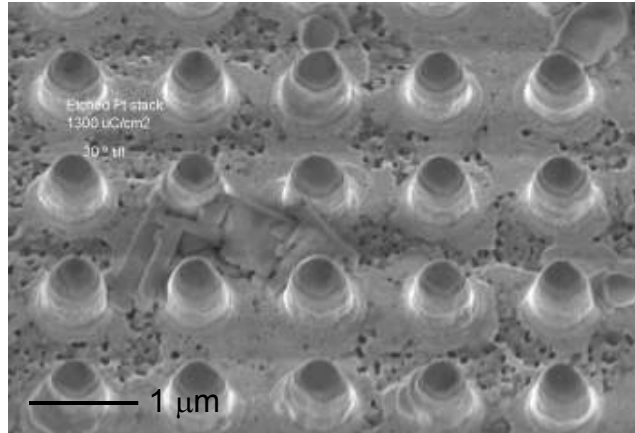
One approach to increase AFM resolution is to use single-walled carbon nanotubes (SWNTs). SWNTs make the world's sharpest AFM probes and will hopefully open up a world of rapid protein structural analysis. Such a technology advance will have tremendous impact in structure-based drug design. Carbon Nanoprobes relies on the UW Nanotech User Facility to characterize and test its SWNT probes.



SEM image of a single-walled carbon nanotube on an AFM tip.

Carbon Nanoprobes, Inc.
Work performed at UW Nanotech User Facility

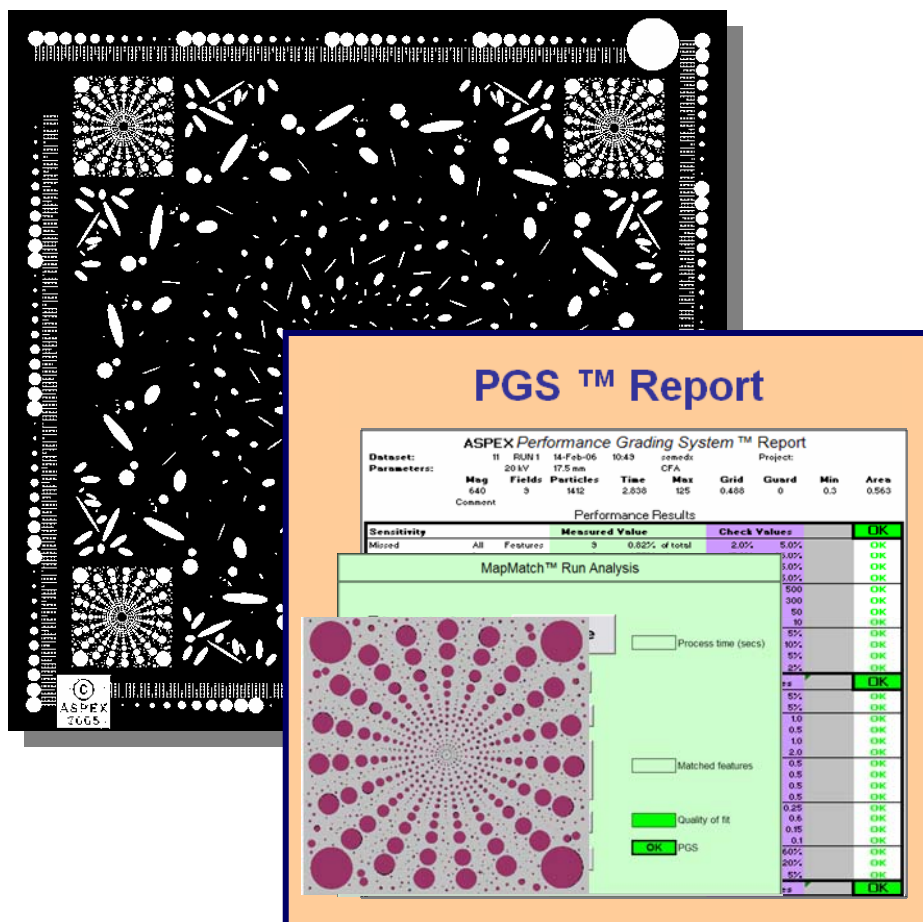
PZT Nanopillar Arrays



Scanning electron microscope images (left) of circular and oval PZT nanopillars. The process (top) uses e-beam lithography to pattern a metal hard mask followed by high-aspect ratio etching of a PZT thin film.

PZT nanopillar arrays are fabricated using e-beam lithography and reactive ion etching

Performance Grading System™

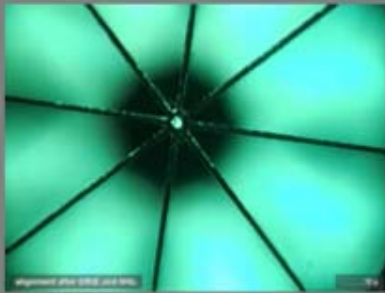


The Aspex PGS™ (Performance Grading System*) is the first practical method for routine checking of particle analyzer performance in the submicron particle range. A process was developed at the PSU NNIN to fabricate PGS specimens with thousands of precisely known micron- and nanometer-scale features. The PGS system is very easy to use, and within minutes produces detailed and precise metrics that summarize virtually every significant aspect of instrument performance. A key metric is its insensitivity to foreign material that might otherwise skew the results.

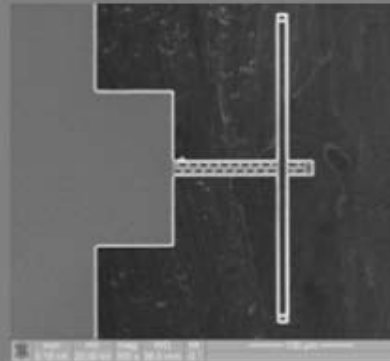
F. Schamber, Aspex Corporation
Work performed at Penn State

Nanofabrication techniques developed for a performance grading system used for particle analysis

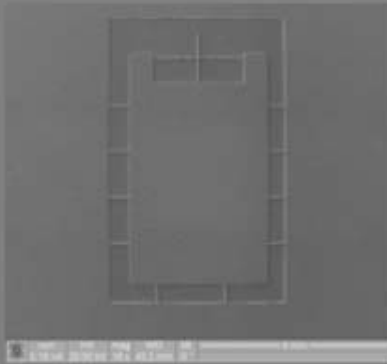
Three Degrees of Freedom Atomic Force Microscope



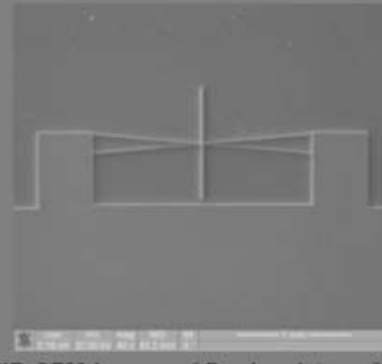
Alignment marker from backside mask after DRIE



FIB SEM image of a free standing Two Degree of Freedom AFM fabricated using this process



FIB SEM Image of Device 3 (two 2µm thick beams, 4° angle) etched 10µm into a Si wafer



FIB SEM image of Device 4 (two 3µm thick beams, 10° angle) etched 10µm into a Si wafer.

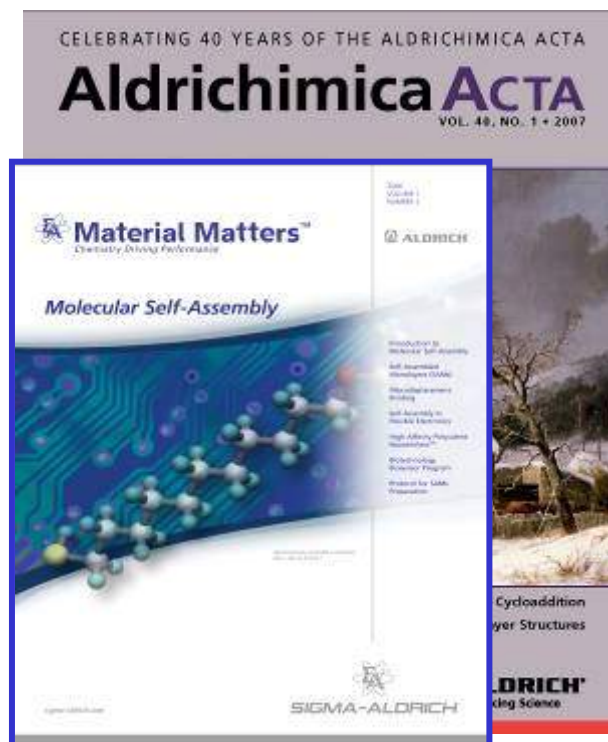
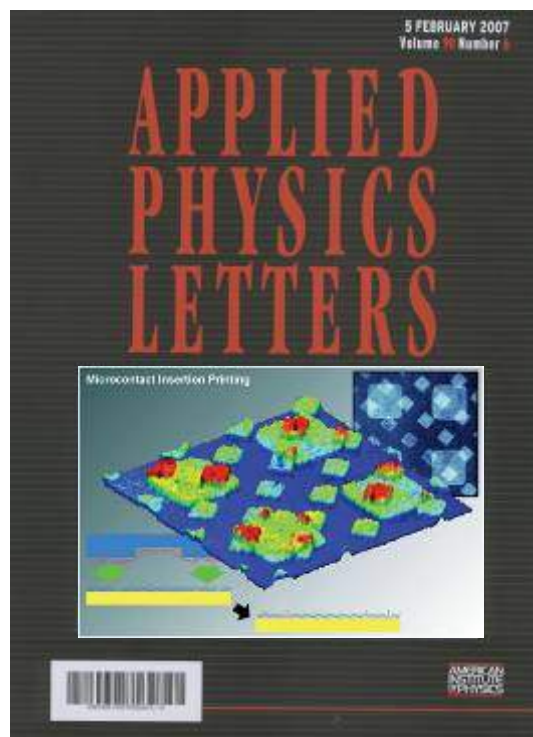
Atomic Force Microscopes are typically used to measure forces in one direction. They can be adapted to measure forces in other directions, but it is time intensive and challenging. Here we show a *Three Degrees of Freedom Atomic Force Microscope* design.

Microfabrication techniques were used to design, fabricate, and test a miniature system that can measure forces in three directions with high resolution. Typical applications for the 3DOF AFM are probing nanostructures and studying hard disk drive interactions with the reading head.

C. Bergstein, Carlow University,
A. Haque and A. Desai, Penn State University,
Work performed at Penn State

Silicon micromaching techniques are being used to develop a 3DOF AFM for probing nanostructures and disk drives

Advances in Chemical Patterning



Enables patterning of isolated molecules in controlled matrices – the inserted molecules can be further functionalized

Chemical patterns have immediate applications in biospecific capture surfaces for functional proteomics, neuroscience, and homeland security

Developing and commercializing new molecules for patterning with Sigma-Aldrich

P. S. Weiss, Penn State and S. Jasty, Sigma-Aldrich
Work performed at Penn State

Joint molecular design and commercial syntheses are opening new ideas and possibilities in chemical patterning for devices

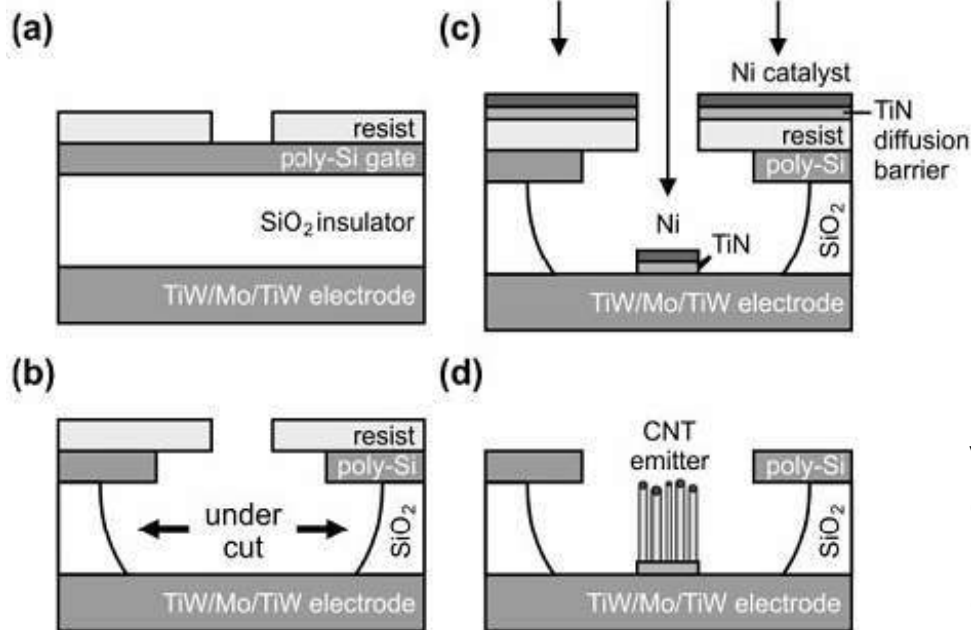
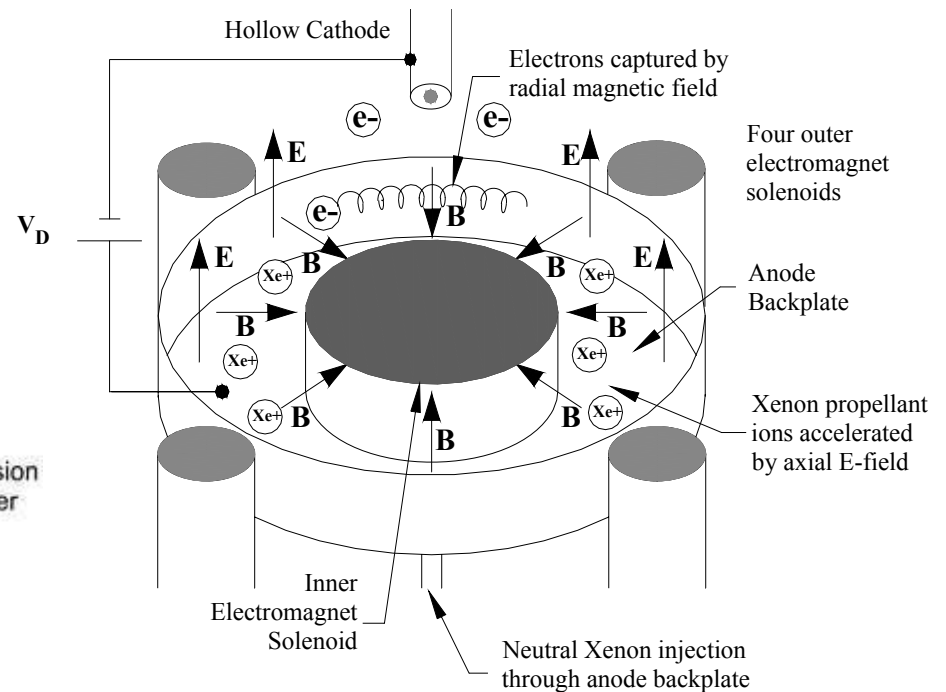
Electron Field Emission from Carbon Nanotubes (CNTs)



Early model of a 200W Busek Hall Thruster

Substituting conventional emitters with CNTs for field emission has the potential for substantially increased current densities; $>40 \text{ mA/cm}^2$

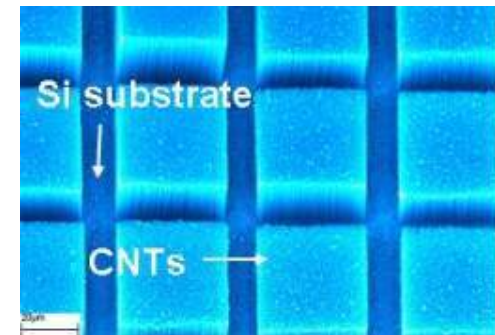
Hall Thruster Schematic



Process steps for CNT Field Emitters

- poly Si is the gate (positive bias)
- TiW/Mo/TiW is the cathode

Vertically aligned CNT arrays by the Ready Group at GTRI



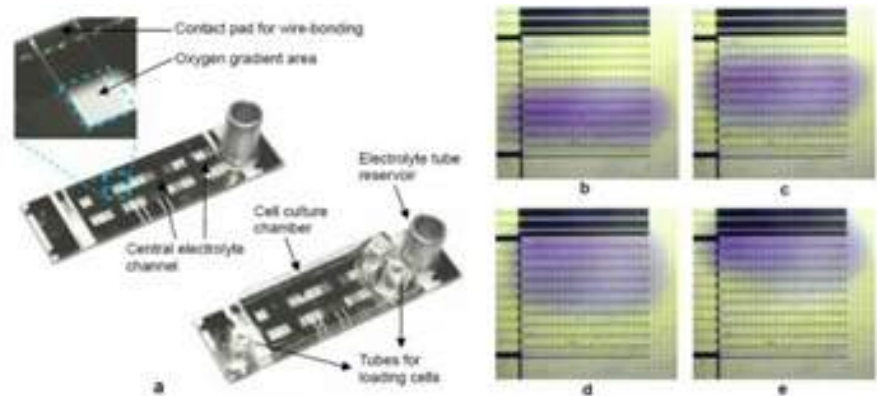
J. Ready, GT
Work performed at Ga Tech

An Oxygen Microgradient Chip

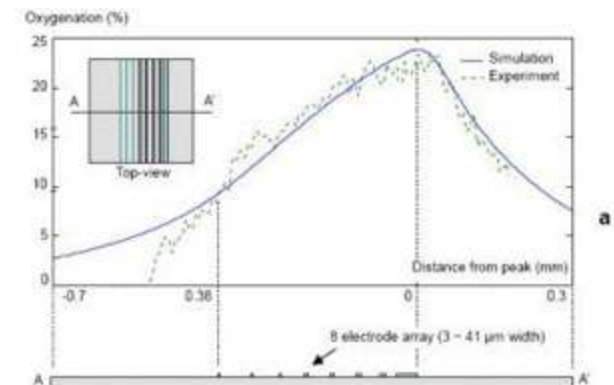
The oxygen microenvironment within tissue plays a crucial role in many biological processes and diseases.

No technology currently exists that allows the researcher to control localized oxygen doses and impose arbitrary oxygen gradients within tissue with microscale resolution. We have developed an oxygen microgradient chip that allows control of the oxygen environment in a tissue sample or microbial culture with microscale spatio-temporal resolution. Our fabricated device generates 1D and 2D dissolved oxygen gradients across several millimeters with microscale precision and has the potential to test the effect of localized oxygen delivery on a wide range of tiny animals, tissues, and cell samples. Importantly, user-defined microgradient profile is generated at the time of the experiment, adjustable during the course of an experiment, and actively responsive to transient experimental conditions.

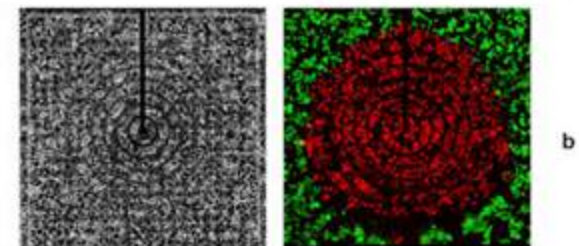
M. Maharbiz, University of Michigan
Work performed at Michigan Nanofabrication Facility



top (a) Fabricated oxygen microgradient chip, (b)-(e) Visualization of temporarily generated oxygen dissolved into solution with redox indicator that changes its color to purple in the presence of oxygen. Video images are 40 seconds apart.

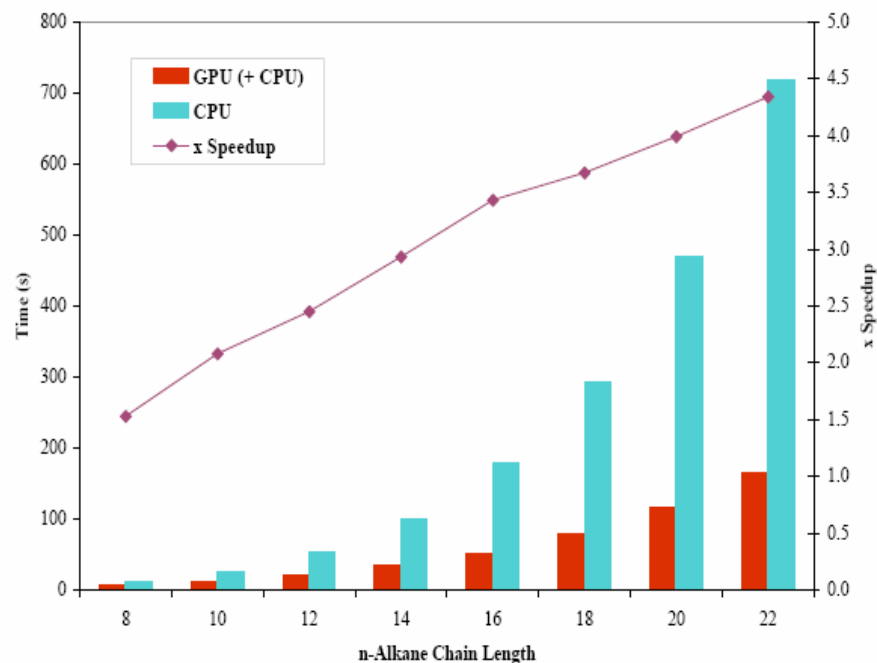


right (a) Simulated and measured linear oxygen microgradients with an eight electrode array; (b) Initial hyperoxic test of C2C12 myoblasts.



Accelerating Resolution-of-the-Identity Second Order Møller-Plesset Calculations with Graphical Processing Units

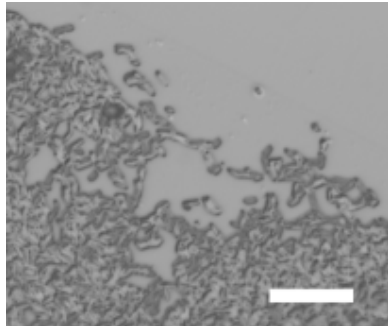
The modification of a general purpose code for quantum mechanical calculations of molecular properties (Q-Chem) to use a graphical processing unit (GPU) is reported. A 4.3x speedup of the resolution-of-the-identity second order Møller-Plesset perturbation theory (RI-MP2) execution time is observed in single point energy calculations of linear alkanes. Furthermore, speedups of other matrix algebra based electronic structure calculations are anticipated as a result of using a similar approach.



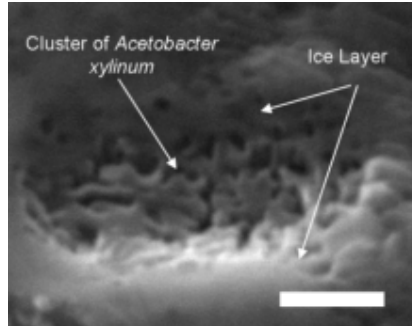
Total processing times for the calculation single point energies for a series of linear alkanes. Speedups of 1.5x to 4.3x are achieved throughout the series.

Focused Ion Beam (FIB) Sectioning of Frozen Samples

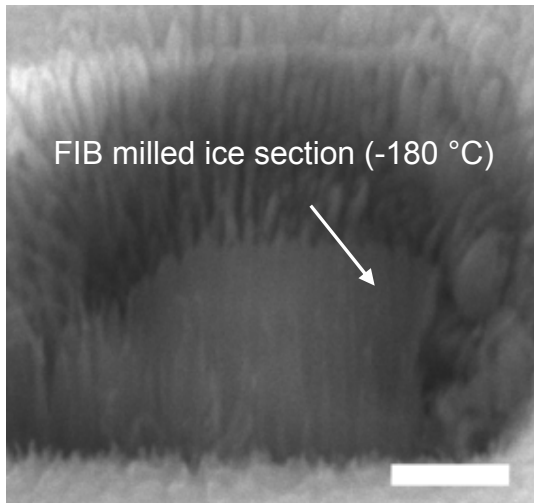
FIB milled frozen *Acetobacter xylinum*



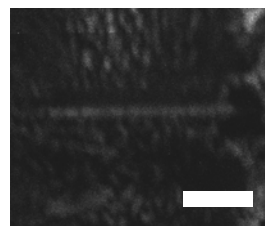
Optical (scale: 20 μm)



SEM (scale: 3 μm)



FIB milled ice section (-180 °C)



Thin section of ice (400nm) ready for TEM lift out (scale: 5 μm)

Cryo-electron microscopy has become a promising tool to study cellular assemblies in their native state by immobilizing biological cells instantly in a cryogenic environment. Although FIB has become an invaluable tool for materials science, the lack of milling processes for biological materials has prevented this capability from being used to any extent in the biological sciences. Here we demonstrate using a dual beam FIB to section frozen samples, which facilitates automatic data acquisition of cellular structures. Two applications are being investigated: FIB of *Acetobacter xylinum* bacteria after plunge freezing and interfaces between artificial surfaces and biological cells.

J. Catchmark, Penn State University
Work performed at Penn State

Acid Degradable Crosslinkers

Motivation: Maximize template lifetime.

- Templates are expensive to fabricate/inspect/repair
- Imprint resist is difficult to strip and may contain silicon

Solution: Change resist chemistry

- Replace crosslinking monomer
- Add new crosslinkers which degrades into soluble polymers

Materials: Degrade in the presence of acid and heat



- **Tertiary Ester Diacrylate (TEDA)**

- Viscosity: 21.1 cP
- Dose to cure: 13.5 mW/cm²

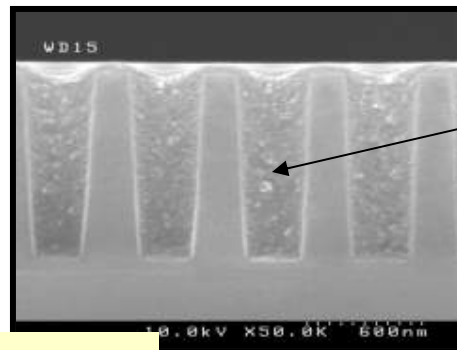


- **Acetal Diacrylate (ADA)**

- Viscosity: 12.3 cP
- Dose to cure: 58.3 mW/cm²

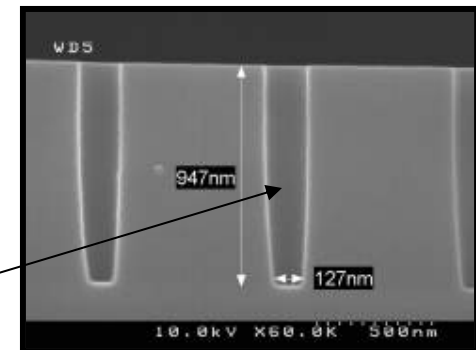
Results:

Simulated cleaning of deep template holes.



Polymer filled cavities

Clean cavities



Directly Patternable Dielectrics (DPD)

Motivation: Simplify circuit fabrication

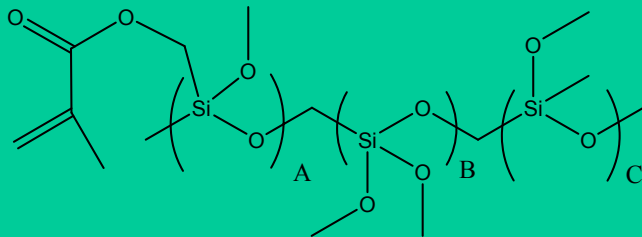
- Back end of line wiring is difficult and costly to fabricate
- Multi-level templates allow for broad selections of imprint materials

Solution: Use a DPD

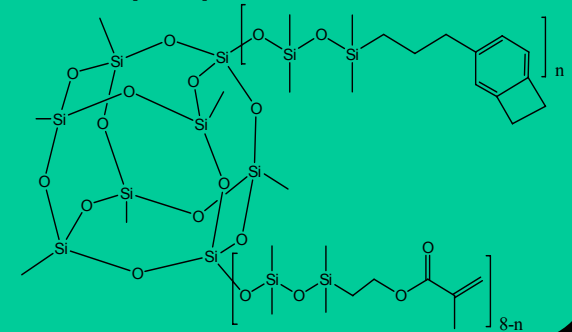
- Print wire structures directly into insulator, not a sacrificial resist.
- Reduce wire fabrication steps by more than half

Materials: UV cure to pattern / heat cure to achieve dielectric properties.

Sol-gel

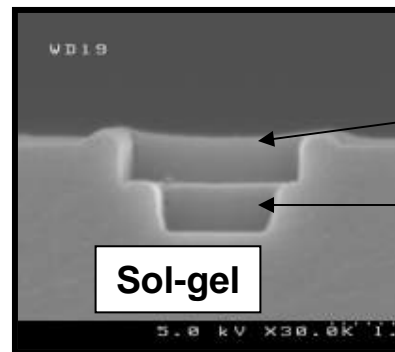


POSS +
BCB +
acrylate



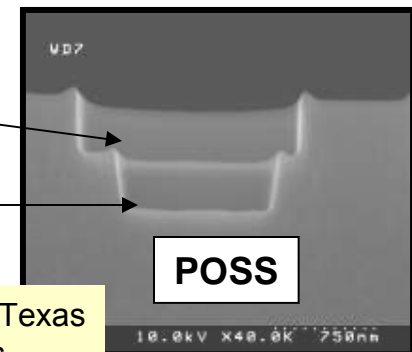
Results:

UV and bake cured multi-level imprinted structures



Trench

Via



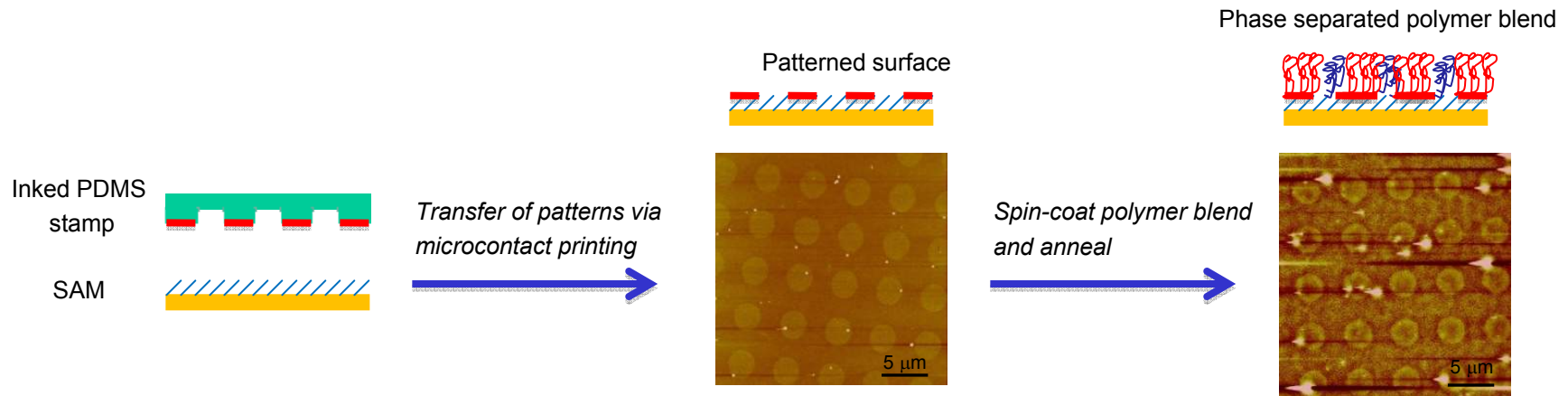
Willson research group, U. Texas
Work performed at U Texas

Materials

Guiding Polymer Phase Separation

Microcontact printing offers a means to control phase separation in surface-cast polymer blends. As illustrated in the figure, printing a self-assembled monolayer with a reactive ink, allows one to pattern the surface with specific chemical functionalities. After a polymer blend has been spin-coated onto the surface and annealed, the influence of the printed islands on the phase separation of the polymer blend can be clearly observed in the AFM. These and related methods are being studied for the fabrication of organic electronic devices.

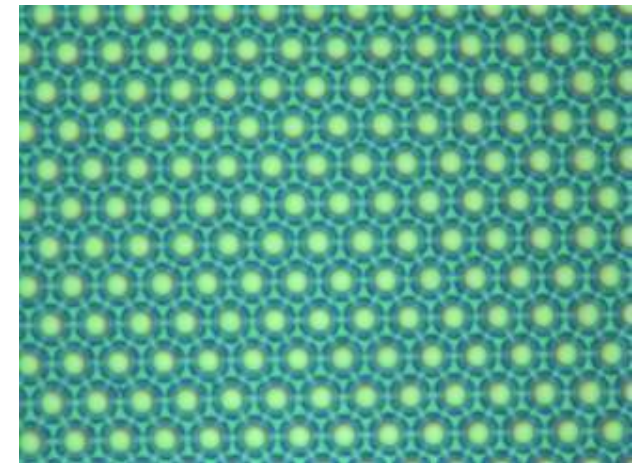
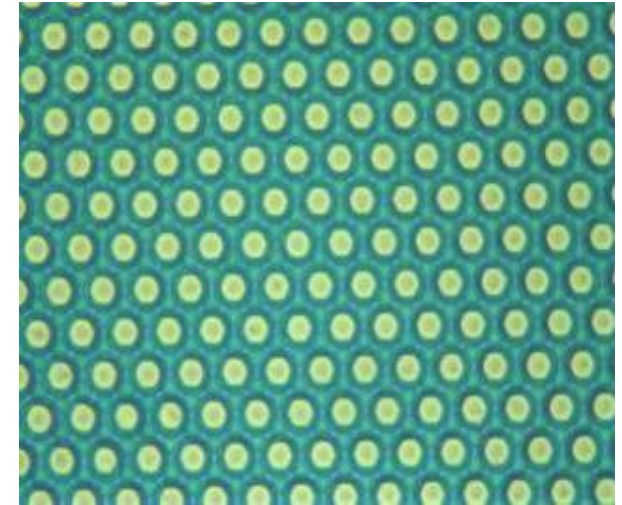
Much of this work has been carried out using the soft lithography shop, SPM resources and staff assistance at the UW Washington Nanotech User Facility.



L. Park, Williams College
Work performed at UW Nanotech User Facility

Color Variation based on Structure Beneath Multilayer

The research involves investigating nature and implementing observations made through fabrication. The thickness of SiN_3 and SiO_2 using the Woollam Elipsometer was first characterized. Then the STS PECVD tool was used to create a multilayer on top of a micro-lens structure which made progress a little further in comparing with nature. Demonstration of the results obtained from the usage of the STS PECVD tool at GT-MiRC



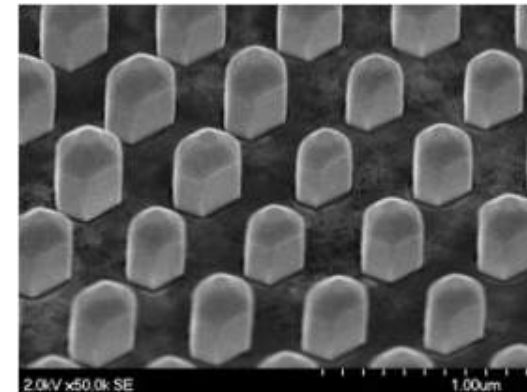
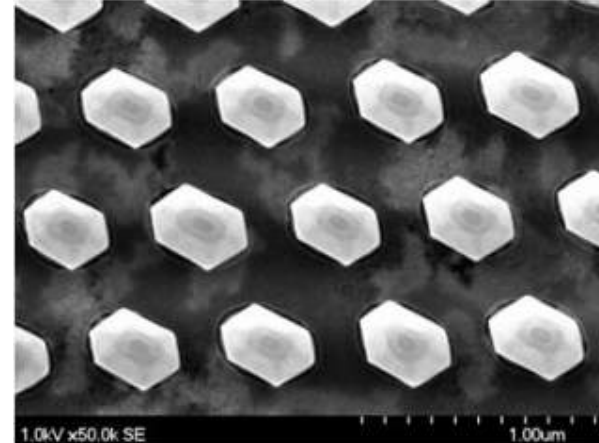
K. Buhl, A. Mehta, E. Johnson, U. of North Carolina at Charlotte
CREOL – U. of Central Florida
Work Performed at Ga Tech

Microscope Images at 100x

Low Defect Density Gallium Nitride Wafers

The semiconductor market for Gallium Nitride (GaN) is the most important next to silicon and includes visible and ultra-violet LEDs for general illumination and displays, visible lasers for high density optical storage and high power, high speed microelectronics. Currently the poor quality and high cost of GaN wafers is the most significant factor that prevents the full development of the market for high performance microelectronic devices.

The objective of Nanocrystal Corp is to develop a GaN wafer technology which will address real market need for high quality (i.e., very low defect density) and cost efficient GaN wafers needed for high performance LEDs, lasers and transistors. The foundation of its approach is the technology developed at the Center for High Technology Materials of the University of New Mexico related to the ordered growth of uniform defect-free GaN nanowires.



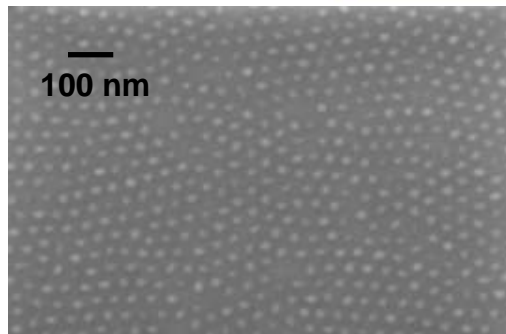
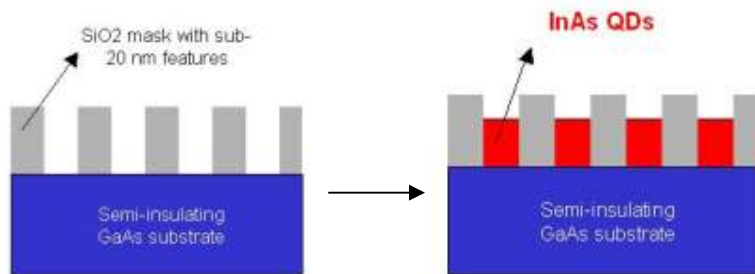
Gallium Nitride nanowires

Nanocrystal Corp
Work performed at UNM

Nano-Patterned Growth of sub-20 nm In(Ga)As Quantum Dots

Templated growth process:

- Fabrication of a sacrificial template
- Selective area growth of nanostructures compatible with most growth techniques

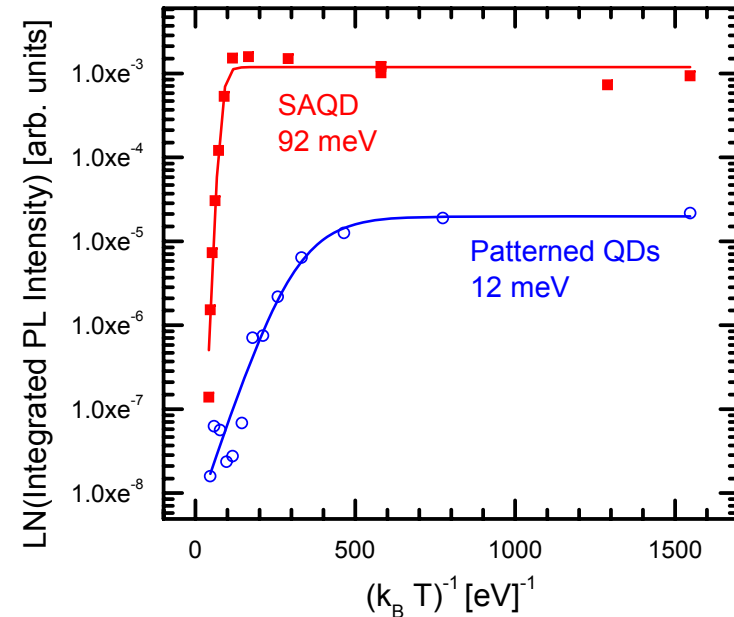


20.6 ± 2.1 nm
Dot density: 7 × 10¹⁰ dot/cm²

Advantages

- Uniform size and spacing (narrow emission)
- No wetting layer
- High nucleation density
- Arbitrary heights
- Arbitrary dot-substrate combinations

Optical Performance of sub-20 InAs Quantum Dots



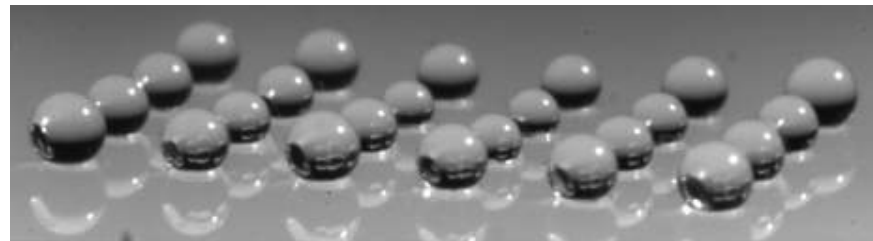
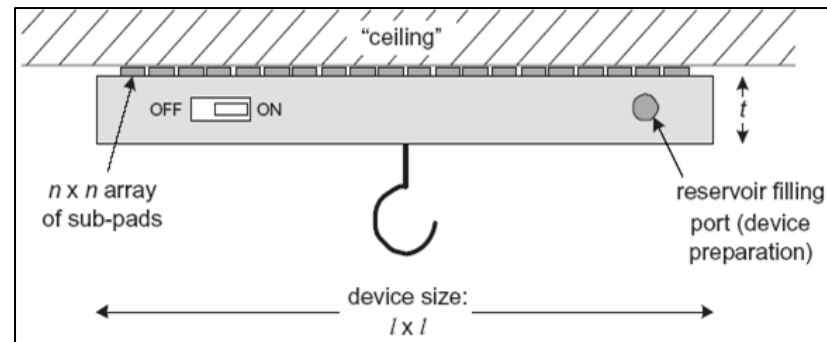
The nano-patterned InAs quantum dots show a significantly lower activation energy as compared to the SK dots. This behavior is consistent with the presence of defects and compromised interface integrity in patterned QDs

A. Alizadeh, GE

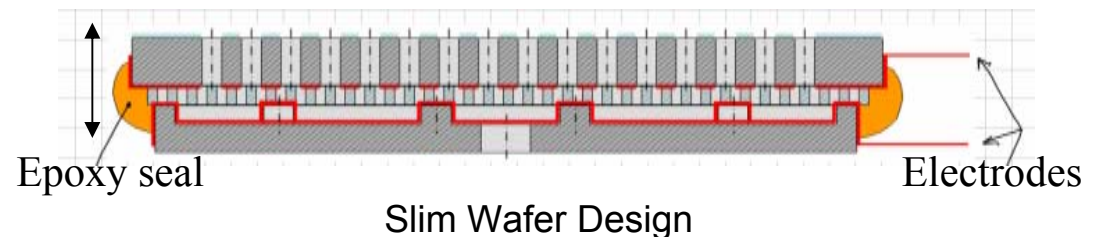
Work performed in part at UNM node of NNIN.

Reversible Super-Adhesion

Inspired by the incredible adhesive forces exhibited by the palm beetle insect, this research seeks to demonstrate reversible super adhesion using arrays of electro-osmotic pumps. The technology goal is to demonstrate 1 atm adhesion strength using liquid surface tension with many parallel small scale actions.



4x6 array of droplets pumped from reservoir using electro-osmosis



P. Steen & M.J. Vogel, Cornell University
Work performed at Cornell NanoScale Facility

Lithographically-Designed Colloidal Particles

A method to produce well-defined, lithographically-designed, non-spherical colloidal particles was developed. The work demonstrates that formation of a highly anisotropic structure in a model system of Brownian cylindrical particles can be achieved by precisely controlling electrostatic, van der Waals and depletion interactions, as well as the surface properties of the particles. The method can also be used to produce a diversity of particles of more complex shape, and thus opens the road to the formation of a broad diversity of structures at the colloidal scale.

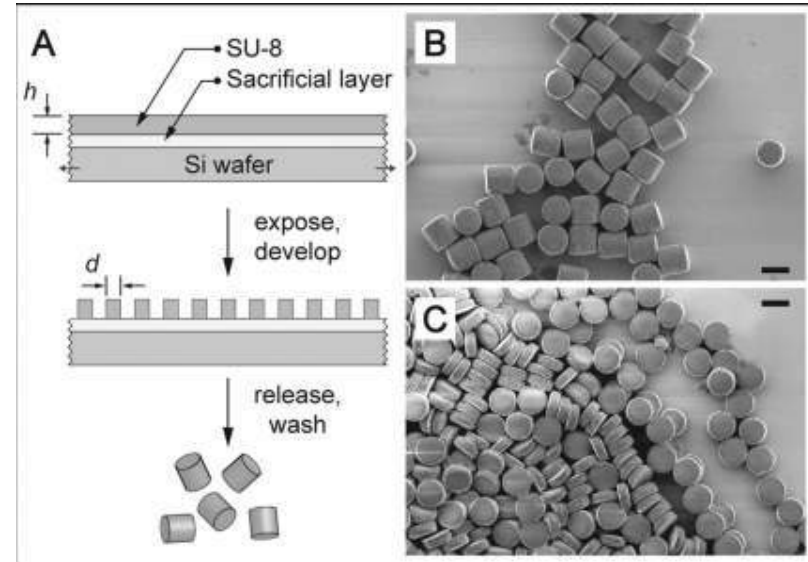


Figure 1: (A) Schematic diagram of formation of cylindrical particles in an epoxy-based negative photoresist (SU-8) via projection photolithography. (B and C) SEMs of SU-8 particles produced by this process and redeposited on a silicon wafer from water.

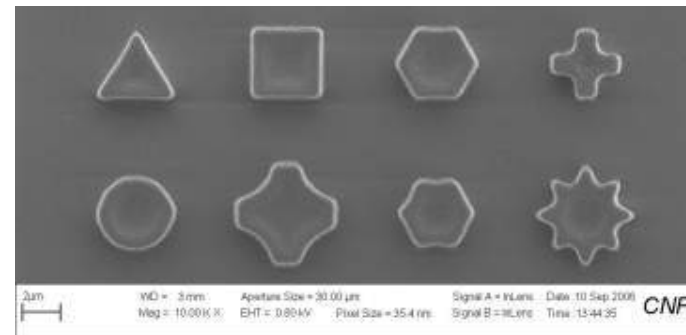


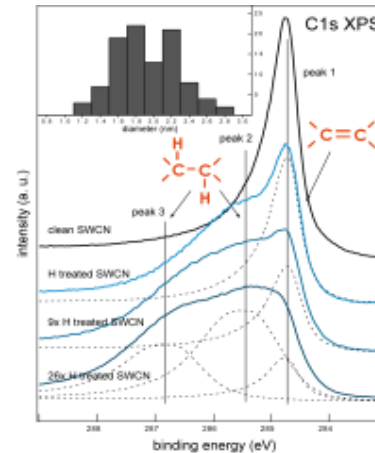
Fig. 2. Process and Shapes of Lithographically designed colloids

A. Stroock, Cornell University
Work performed at Cornell NanoScale Facility

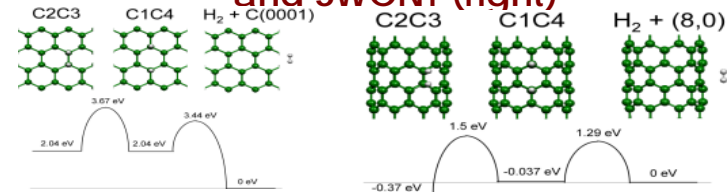
Hydrogen Storage in Carbon Nanotube Composite Material

- Carbon nanotubes can be hydrogenised to store up to 7% by weight of hydrogen, meeting the Department of Energy requirement.
- Computational studies have determined the optimal hydrogenation/dehydrogenation pathways.
- This explains the experimentally observed optimal carbon nanotube diameter ranges for maximum hydrogen storage.

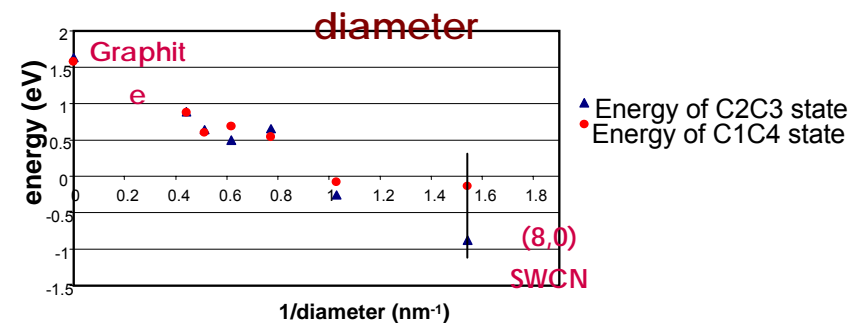
H.J. Dai, A. Nilsson, K.J. Cho, Z. Zhang & A. Nikitin, Stanford University
Work performed at SNF



H desorption pathways on graphite (left) and SWCNT (right)



Dependence of energies on SWCNT diameter



Pd/Ag Alloy Nano-Membranes for Hydrogen Separation

L. McLeod, Ga Tech
Work performed at Ga Tech

KEY IDEAS

- Pd alloys absorb large amounts of H₂ with virtually infinite selectivity to all other gases
- H₂ pressure gradient across membrane drives solid-state diffusion resulting in hydrogen separation
- On-demand and on-site purification of hydrogen is enabling technology for utilization of liquid fuels

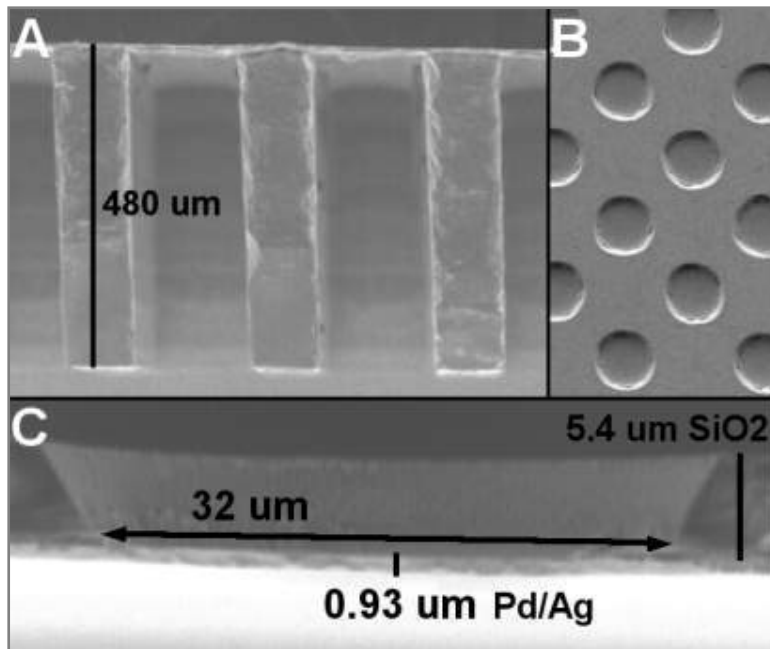
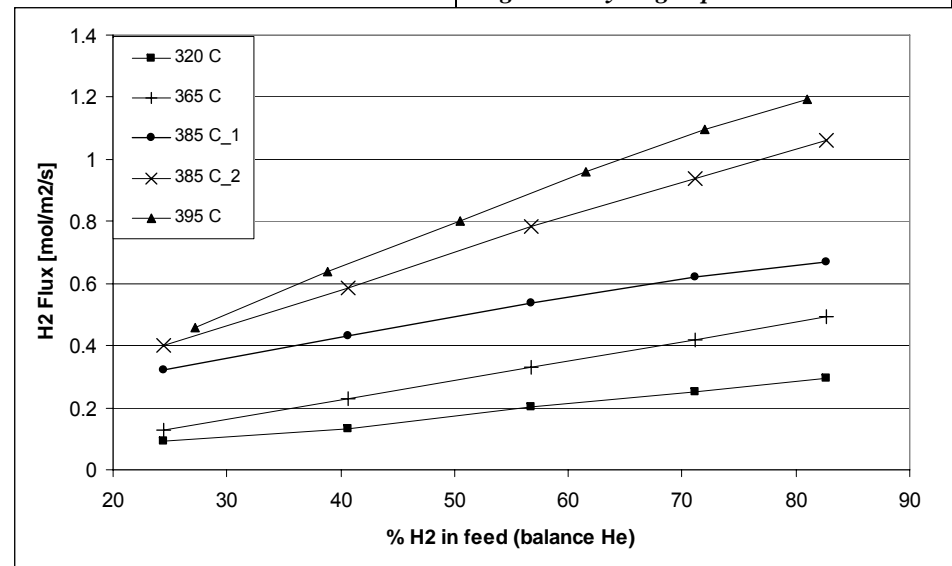


Figure 1: Fabricated composite membrane. (A) Membrane x-section showing vertical sidewalls from DRIE etch and thin SiO₂-Pd/Ag membrane (top surface) (B) Array of 30 μm pores which constitutes the support superstructure. (C) Single pore cross-section showing 930nm thick Pd/Ag membrane

TECHNOLOGY DEVELOPMENT DRIVERS

- Permeation rate is typically diffusion-limited calling for robust sub-μm thick membranes
- Presence of CO and H₂S in the product stream inhibits permeation of hydrogen

Figure 2: Hydrogen permeation results

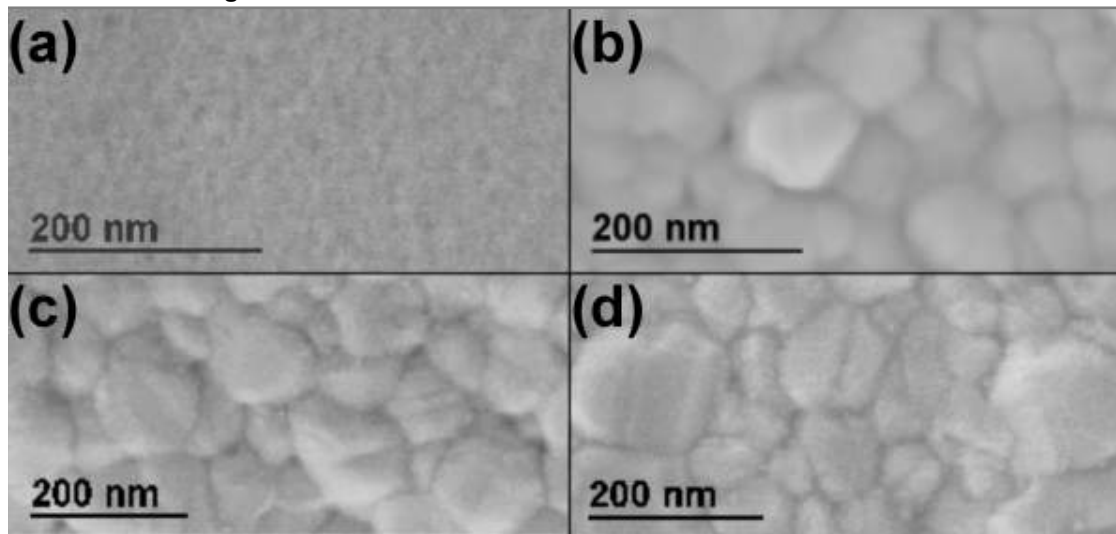


Microstructure Effects on H₂ Permeation Rate through Pd-Alloy Membranes

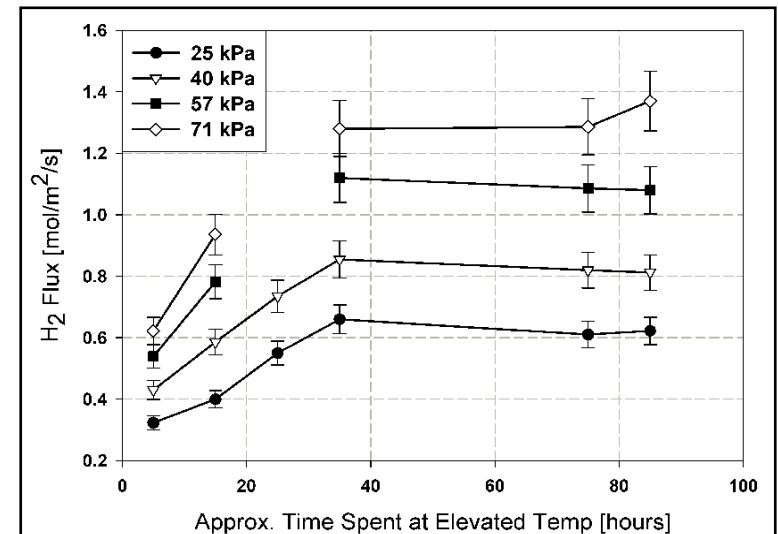
- Thin film deposition methods result in highly non-equilibrium film microstructure with nanometer grain size.
- Film release and subsequent annealing causes coalescence and growth of grains to minimize surface area associated with grain boundaries.
- Since grain boundaries act as hydrogen “traps” during diffusion, increasing grain size results in enhanced hydrogen permeation.

L. McLeod, Ga Tech
Work performed at Ga Tech

(a) Bottom surface of as-deposited Pd/Ag thin film. (b) Top Surface of as-deposited Pd/Ag thin film. (c) Bottom surface of annealed Pd/Ag thin film. (d) Top surface of annealed Pd/Ag thin film.



Long-term transient response of Pd/Ag membrane illustrating increase in permeation rate due to annealing.

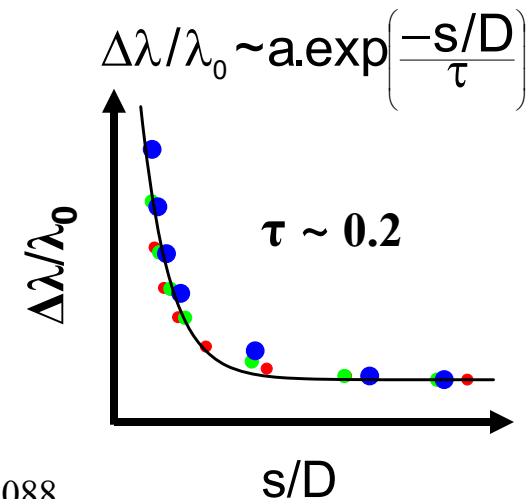
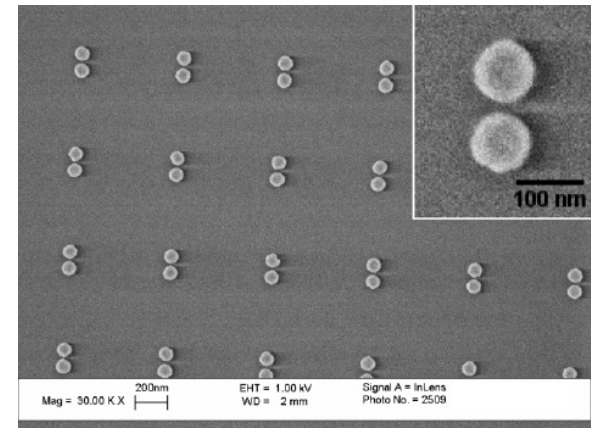


Universal Distance Scaling of Plasmon Coupling in Noble Metal Nanoparticle Pairs: Application to Plasmon Ruler

M. A. El-Sayed, Georgia Tech
Work performed at Ga Tech

The optical properties of an individual noble metal nanocrystal depend on its particle plasmon resonance, i.e. the collective oscillation of free electrons of the particle in resonance with light. In the case of a nanoparticle pair, when the light is polarized along the inter-particle axis, we observe the favorable coupling or “bonding” of the plasmons on the pair partners resulting in the red-shift of the plasmon resonance with respect to the single particle case. Optical microabsorption spectroscopy of electron-beam lithography-fabricated Au particle pairs shows that the strength of this inter-plasmon bonding interaction, as measured by the fractional plasmon resonance shift ($\Delta\lambda/\lambda_0$), decays near-exponentially ($\tau \sim 0.2$) with the inter-particle separation gap s scaled by the particle size D . Electrodynamics simulations show that this distance scaling is universal over different nanoparticle size, shape, metal, or surrounding medium.

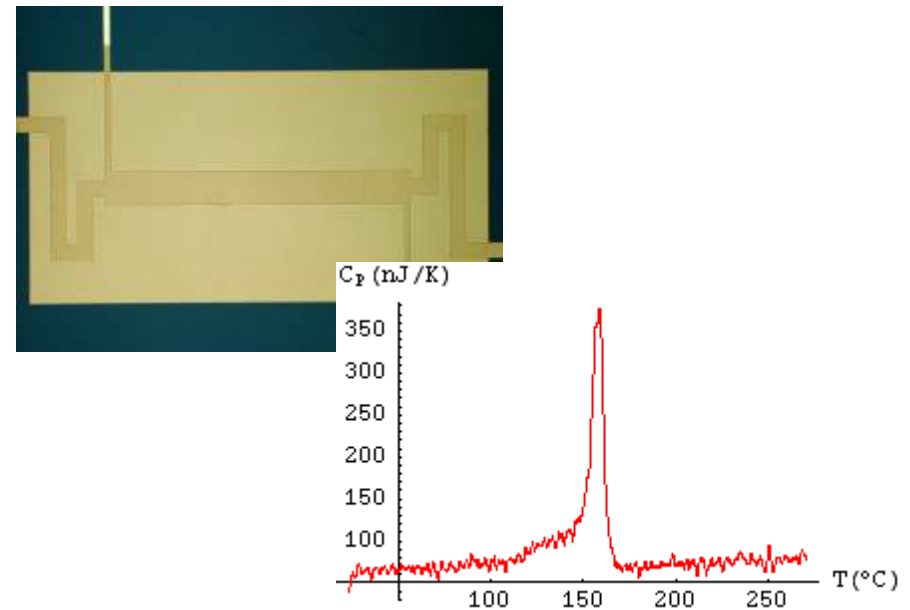
Recently, Alivisatos and Liphardt groups at Berkeley have designed the plasmon ruler which is used to measure nanoscale distances in macro- and biomolecules from the shift in the plasmon resonance of a metal particle-pair, observed by dark-field scattering spectroscopy. From our universal scaled-distance dependence of the inter-particle plasmon coupling in the metal nanoparticle pair, we are able to provide a simple expression $\Delta\lambda/\lambda_0 \sim 0.18 \exp^{-s/0.23D}$ to predict with reasonable accuracy the inter-particle separation from the measured plasmon shift of the particle-pair in biological media.



P.K. Jain, W. Huang, M. A. El-Sayed, *Nano Lett.* 7(7), 2007, 2080-2088.

The P-nDSC: A combinatorial approach to thermal analysis of materials

The Parallel nano-Differential Scanning Calorimeter (P-nDSC) is a measurement system for studying the thermal properties of complex nano-scale material systems. It consists of an array of micromachined calorimeter cells, each one of which can measure the heat capacity of a sample with nJ/K sensitivity in just a few tens of milliseconds. The graph on the right shows the heat capacity of a 25 nm indium film. The signal shows a distinct peak at 157°C corresponding to the melting point of indium. The system is ideal for the combinatorial analysis of materials that can be deposited in thin film form.



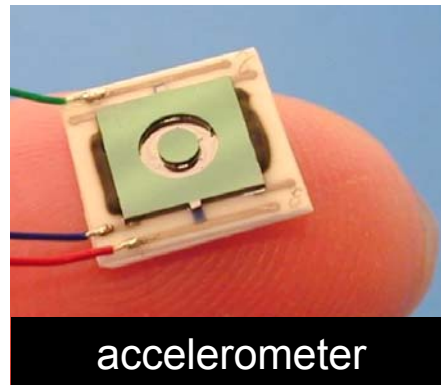
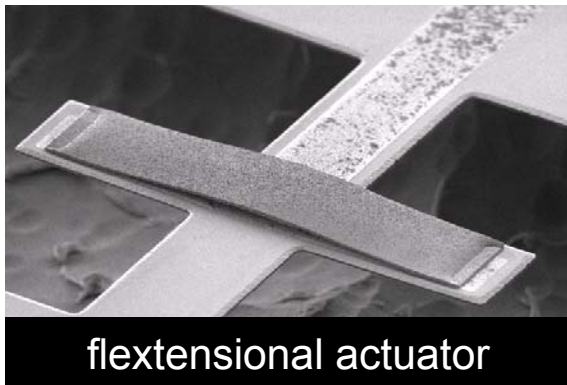
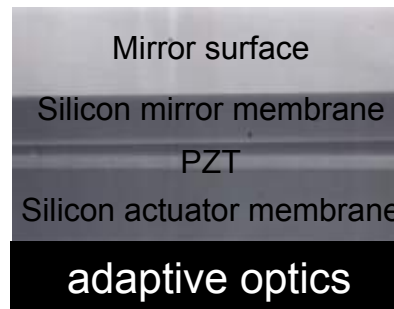
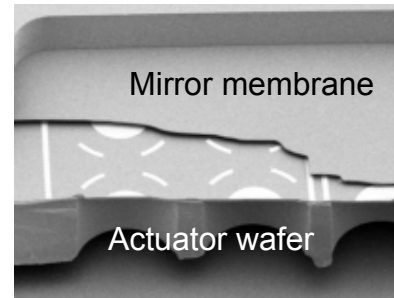
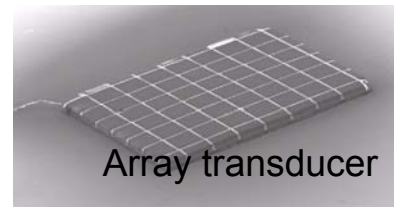
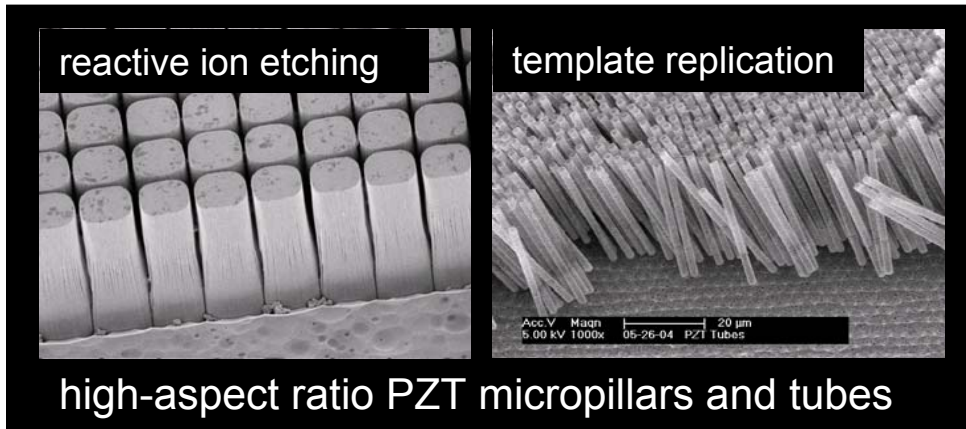
(a) Single calorimetric sensor micromachined out of a 80 nm SiN_x membrane with W and Al metallization;
(b) Heat capacity of a 25 nm thick evaporated indium coating as a function of temperature

J.J. Vlassak, Harvard University
Work performed at Harvard University

Examples of Complex Oxide Device Integration

S. Trolier-McKinstry, Penn State University
Work performed at Penn State

Fabricated devices in collaboration with Northrop Grumman, Geospace Research, Wilcoxon Research, Jet Propulsion Lab, and Army Research Lab



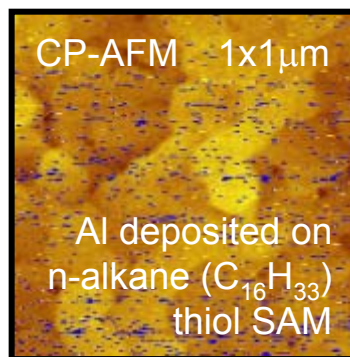
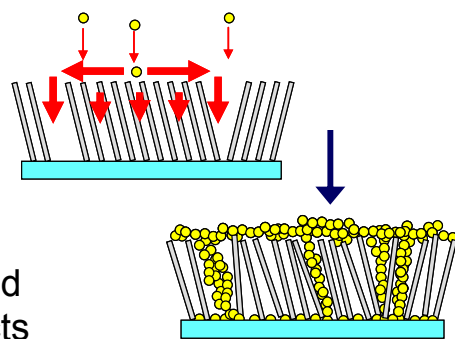
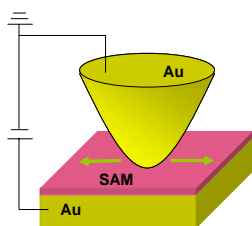
e.g., Bharadwaja *et al.*, *J. Am. Ceramic Soc.* 89(9) 2695 (2006), Yang *et al.*, *J. MEMS* 15(5) 1214 (2006), Hong *et al.*, *J. MEMS* 15(4) 832 (2006).

Examples of integrating piezoelectric and pyroelectric thin films into microelectromechanical systems and electro-optic devices

SAM Contacts and Nanoscale Junctions

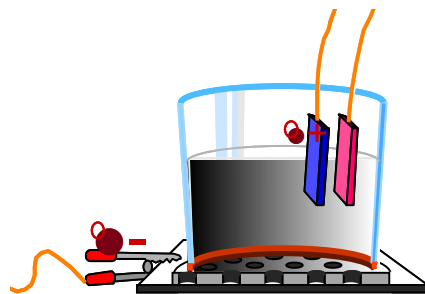
T. Mallouk, T. Mayer, C. Keating, and D. Allara, Penn State University
Work performed at Penn State

FTIR & CP-AFM used to study SAM contacts

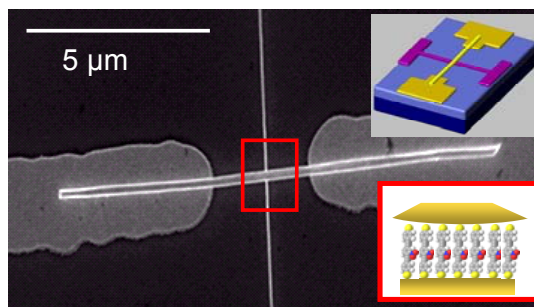
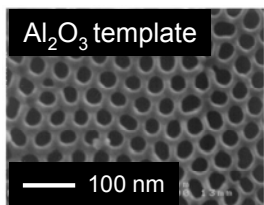
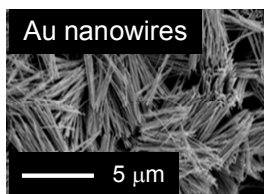


FTIR and scanning probe techniques used to study interface between vapor deposited metal and hydrocarbon SAMs

e.g., Z. Zhu, *et al.*, *J. Am. Chem. Soc.* 128(42) 13710 (2006), T. B. Tighe, *et al.*, *J. Phys. Chem. B*, 109(44) 21006 (2005).



Template-based metal nanowire synthesis



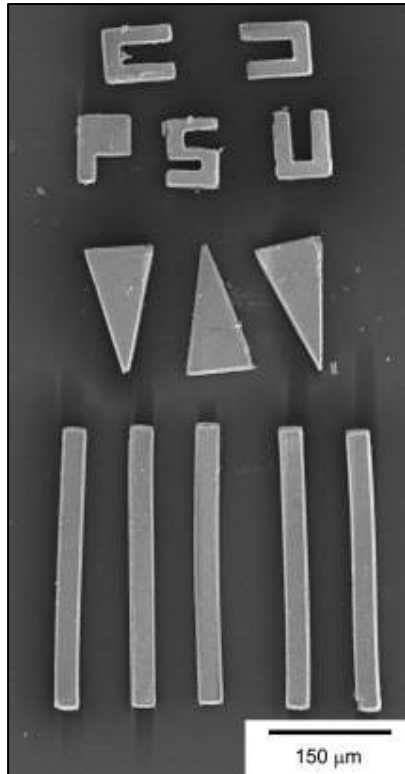
nanoscale metal-SAM-metal junction assembly

Template-based nanowire synthesis permits bottom-up fabrication of nanoscale molecular junctions for basic electrical transport studies in SAMs

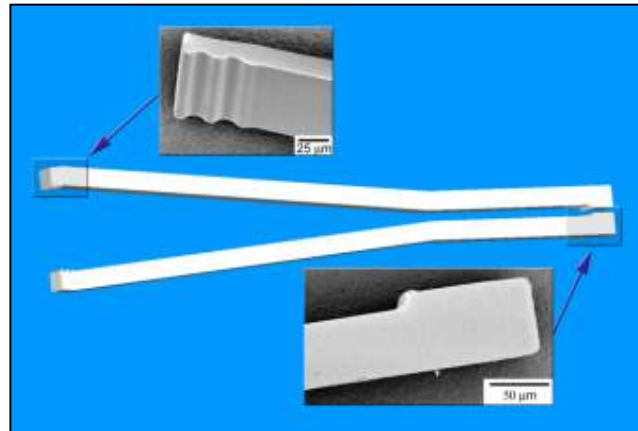
e.g., Cai, *et al.*, *Nanoletters* 5(12) 2365 (2005), Selzer, *et al.*, *Nanoletters* 5(1) 61 (2005).

Micron-scale Ceramic Instruments

G. Hayes, N. Antolino, J. Adair, M. Frecker, Penn State University
Work performed at Penn State



sintered mechanical test bars and triangle parts



Generation 1 ceramic tweezers with SEM of the gripping and foot ends



Next generation surgical tweezing/cutting instruments using multilayer molds

Micron-scale ceramic parts were fabricated by infiltrating high aspect ratio SU8 photoresist molds patterned on refractory substrates with vitra stabilized zirconia particles. The infiltrated structures are fired to remove the mold and sinter the ceramic, which leaves free standing parts that have mechanical properties comparable to bulk ceramics.

These ceramic parts are being investigated for use in a variety of applications including surgical instruments.

Combining microfabriation and oxide processing techniques yields new micron-scale surgical instruments

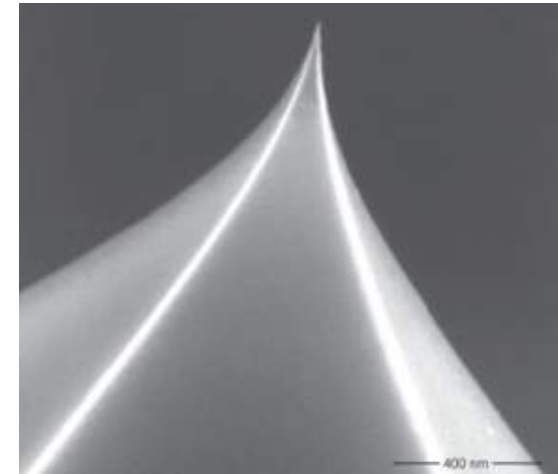
Processes and Characterization

Fabrication of Ultra-Sharp Diamond AFM Probes

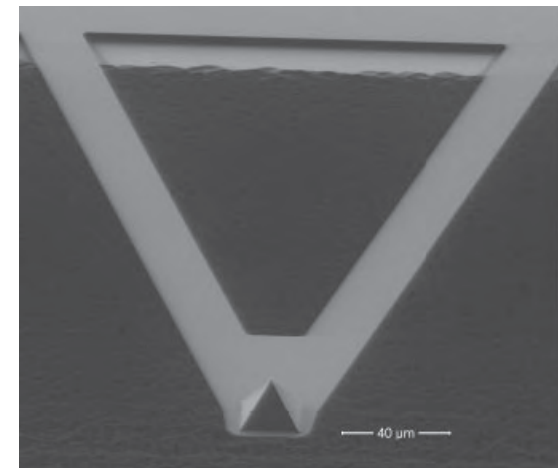
Monolithic, ultra-sharp ($R < 10$ nm) diamond probes were fabricated from ultra-nanocrystalline diamond (UNCD®). UNCD® has desirable properties for diamond AFM probes: high hardness, low wear, low stiction to particles, low roughness (7 nm Ra), low differential stress, and good conformity.

The fabrication sequence developed uses optimized diamond processing with precision lithography, selective etching, anisotropic etching, and precision dicing. The probes showed low wear and stiction as expected, based on the physical properties of diamond, outperforming standard silicon nitride probes in these aspects.

These all-diamond probes should open up new avenues of research to explore nanoscale friction and adhesion at the nanoscale, as well as nanofabrication.



Ultra-sharp UNCD® tip. Tip radius ~ 5 nm.

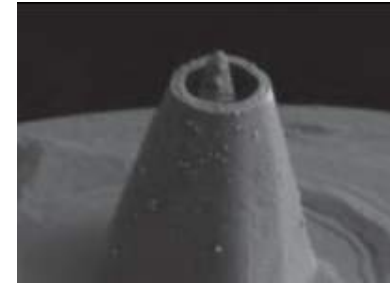


Monolithic UNCD® AFM probe – general view.

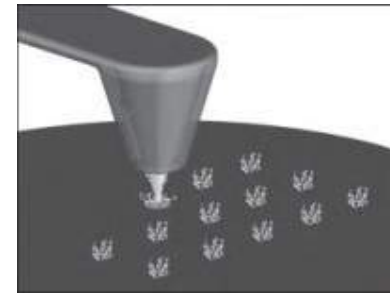
Advanced Diamond Technologies, Inc.
Work performed at Cornell Nanoscale Facility

Nanofountain Probes for the Delivery of Molecular Inks

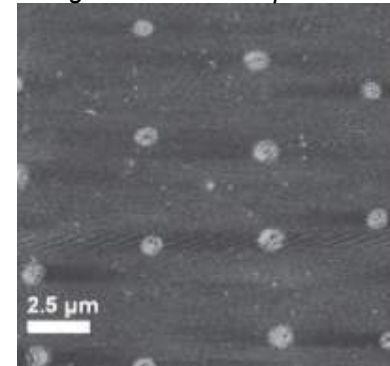
Nanofountain probes (NFPs) are atomic force microscopy (AFM) probes designed to pattern planar substrates with molecular inks in the 50 nm - 1 μm range. They extend the “dip-pen nanolithography” mode of patterning, by increasing the writing speed and eliminating the need for disruptive re-inking and subsequent probe realignment. This is accomplished by supplying fluid ink from on-chip reservoirs through microchannels to the probe tips. A volcano-shaped aperture keeps the fluid ink as close as possible to the probe-substrate contact point, without allowing a real flow over the substrate. This is essential to achieving sub-100 nm lines and avoids the formation of outer menisci (droplets) being dragged over the surface, as is the case with nano-pipette and apertured probe writing devices.



a) Nanofountain probe



b) Schematic of DNA deposition using a nanofountain probe.



c) AFM image of nanoparticle spots patterned by the nanofountain probe.

H. D. Espinosa, Northwestern University
Work performed at Cornell Nanoscale Facility

Nanoparticle Contamination Control in Extreme Ultraviolet Lithography (EUVL) Systems

Protection schemes against nanoparticle contamination of EUVL photomasks are studied.

- Particles generated in mask carriers are measured and analyzed.
- Deposition of particles with known size and speed is studied under vacuum conditions.
- Protection schemes including cover plate, thermophoresis and electrophoresis.

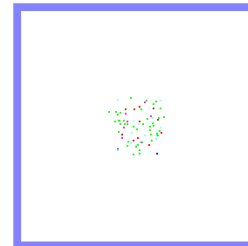


D.Y.H.Pui, J. Wang and S.J. Yook, Univ of Minnesota;
H. Fissan and C. Asbach, U. of Duisburg-Essen;
K. Orvek and P. Yan, Intel Corporation
Work performed at U. of Minnesota

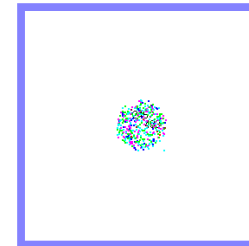
• MAJOR OBSERVATIONS

- ◆ Relative motion between the mask and pins is the major reason for particles inside carriers.
- ◆ Thermophoresis is most helpful to protect against particles driven by diffusion.
- ◆ Drag force is the main factor to protect against particles with large inertia.

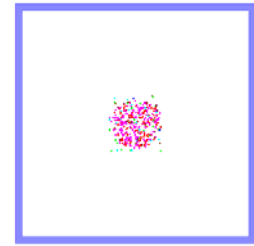
SiO₂ 50 nm



SiO₂ 60 nm



SiO₂ 70 nm



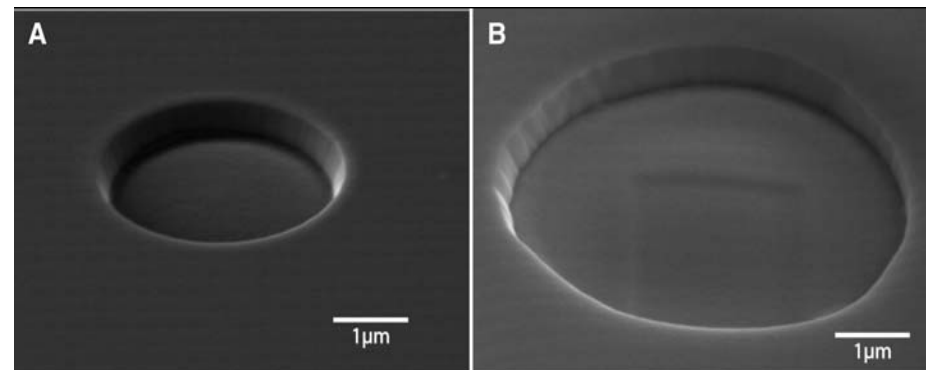
SiO₂ Deposition on Qz Mask Blanks

• Publications

- ◆ Asbach, C., Fissan, H., Kim, J. H., Yook, S. J., and Pui, D. Y. H. *J. Nanopart. Res.* **8**, 705 – 708, 2007.
- ◆ Kim, J. H., Fissan, H., Asbach, C., Yook, S. J., Wang, J., Pui, D. Y. H., and Orvek, K. J. *J. Vacuum Science & Technology B* **24**(4):1844-1849, 2006.
- ◆ Yook, S. J., H. Fissan, C. Asbach, J. H. Kim, J. Wang, P. Y. Yan, and D. Y. H. Pui. *J. Aerosol Sci.* **38**, 211 – 227, 2007.

Shocks in Ion Sputtering Sharpen Steep Surface Features

We report a regime of ion beam sputtering that occurs for sufficiently steep slopes. High slopes propagate over large distances without dissipating the steepest features. The ability to propagate sharp features without dissipation leads to the intriguing possibility of pre patterning a surface (by lithography or some other means) and then uniformly irradiating it to develop predetermined structures on an even smaller length scale. Directing two fronts toward each other might be exploited as a method of sublithographic patterning and may lead to new phenomena as well.

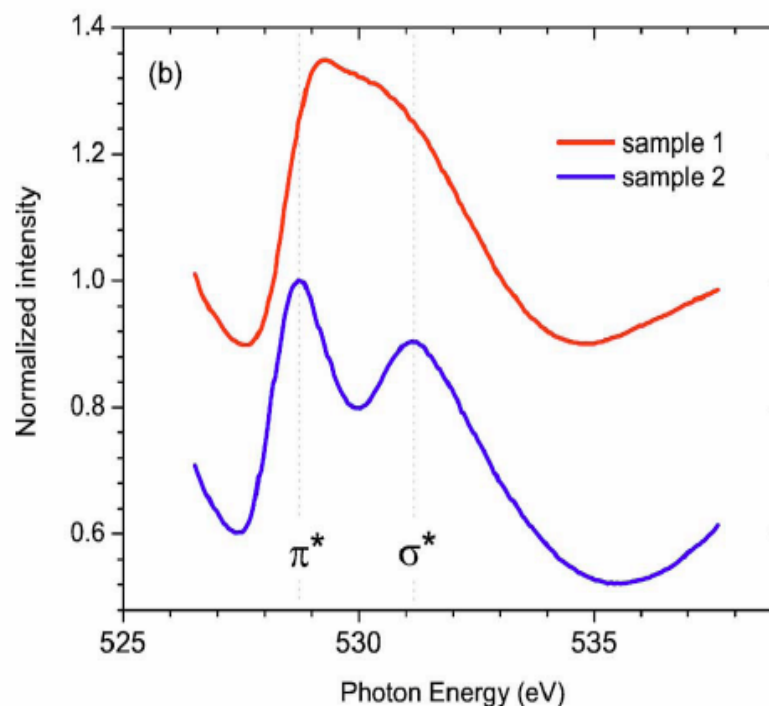


Enlarged pit shows continued sharp sidewalls.

M. J. Aziz, Harvard University
Work performed at Harvard University

X-ray absorption spectroscopy of vanadium dioxide thin films across the phase-transition boundary

X-ray absorption spectroscopy XAS and x-ray photoemission spectroscopy of the V L edge and O K edge were performed on VO₂ thin films rf sputtered at various conditions. The spectra give evidence of the changes in the electronic structure depending on the film quality. The observed variation of the spectra in films of different morphologies may reflect the changes of the density of states responsible for the considerable variation of the metal-insulator transition T_{MIT} properties reported for VO₂ thin films synthesized at different conditions.



Room-temperature XAS data for samples sputtered at (1) 300 °C and (2) 500 °C.